

**DYNAMICS AND DAMPING OF THIN RIVETED BEAM
COMPOSITE STRUCTURES OF VARIOUS
CONFIGURATIONS**

Binit Kavi



**DEPARTMENT OF MECHANICAL ENGINEERING
NATIONAL INSTITUTE OF TECHNOLOGY
ROURKELA – 769008, ORISSA, INDIA
DECEMBER 2014**

**DYNAMICS AND DAMPING OF THIN RIVETED BEAM
COMPOSITE STRUCTURES OF VARIOUS
CONFIGURATIONS**

A THESIS SUBMITTED TO NATIONAL INSTITUTE OF TECHNOLOGY,
ROURKELA IN PARTIAL FULFILMENT OF THE REQUIREMENTS FOR THE
DEGREE OF

DOCTOR OF PHILOSOPHY

IN

MECHANICAL ENGINEERING

BY

**Binit Kavi
(Roll : 509ME304)**

UNDER THE GUIDANCE OF

Prof. Bijoy Kumar Nanda



**DEPARTMENT OF MECHANICAL ENGINEERING
NATIONAL INSTITUTE OF TECHNOLOGY
ROURKELA – 769008, ORISSA, INDIA
DECEMBER 2014**

Acknowledgement

I would like to express my deep sense of gratitude and sincere thanks to Dr. B. K. Nanda, Professor, Mechanical Engineering Department for his constant guidance and valuable suggestions at the various levels of progress of my thesis work.

I take this opportunity of thanking Prof. R. K. Sahoo, Prof. K. P. Maity, ex Heads of department and Prof. S. S. Mahapatra, present Head of Department for providing me facilities for computational and experimental work. I am grateful to Prof. S. C. Mohanty, Prof. S. K. Sahoo of our department for providing experimental and instrumental facilities and Prof. D. R. K. Parhi for his encouraging remarks for my research work. I thank Dr. M. Panda and Dr. B. K. Ojha members of D. S. C. for their invaluable suggestions for my work.

I take this opportunity to express my gratefulness to our honorable director Prof. S. K. Sarangi for his inspiring advices.

I extend my thanks to Mr. Kunal Nayak for his assistance in conducting experimental work.

I also thank my friends Dr. B. K. Chaudhary, Mr. S. C. Chaini and Mr. Abhishek Tiwari who helped me in various matters related to my work.

Lastly, I thank every individual of the department and my family members who helped me in successful completion of the present work.

(Mr. Binit Kavi)



Department of Mechanical Engineering
National Institute Technology
Rourkela-769008, Odisha, India

Certificate

This is to certify that the thesis entitled “Dynamics and damping of thin riveted beam composite structures of various configurations” being submitted to the National Institute of Technology, Rourkela by Mr. Binit Kavi for the award of the degree of Doctor of Philosophy (Mechanical Engineering) is a record of bonafide research work carried out by him under my supervision and guidance. Mr. Kavi has worked for five years on the above problem and the work has reached the standard fulfilling the requirements and regulations for the degree. To the best of my knowledge, the work incorporated in this thesis has not been submitted in part or full to any other University or Institute for the award of any degree or diploma.

Rourkela

(Prof. Bijoy Kumar Nanda)

Date:

Supervisor

ABSTRACT

Composite structures built up of two or more layers of thin beams connected by an array of rivets or weldments have extensive industrial and structural applications because of their low vibration, high damping, reduced fatigue and low weight properties. In the present investigation dynamic and damping analysis of such structures of various configurations, have been made by classical energy and finite element methods.

In the first case, a continuous model is represented by a partial differential equation with respect to spatial and time coordinates. An analytical exact solution for the motion of composite beam with fixed fixed, fixed simply supported and simply supported simply supported boundary conditions has been obtained. Natural frequencies and normal modes of such structures have been determined by solving the frequency equations. Damping characteristics are evaluated by considering energy dissipation due to friction at the interfaces.

In the later case, the structure is represented by one dimensional beam elements with each element having two nodes, each with two degrees of freedom, i.e. transverse displacement and rotation. The equation of motion involving reduced mass and stiffness matrices has been derived and solved to determine natural frequencies and mode shapes. Energy of dissipation and stored energy has been determined in terms of nodal displacements and used to determine damping factor of beams.

An experimental set up has been developed to measure the dynamic and damping characteristics of prepared beam specimens with various configurations. There has been close agreement between theoretical and experimental results. Effect of geometrical and material parameters of beam, on its dynamic and damping properties have been reported.

CONTENTS

Nomenclature.....	10
English symbols.....	10
List of figures.....	13
List of tables.....	16
1. Introduction to dynamics and damping of jointed structures	17
1.1 Genesis	17
1.2 Motivational aspects.....	19
1.3 Problem formulation	20
1.4 Structure Modeling	21
1.5 Outline of the present work	22
1.6 Theoretical Assumptions	23
1.7 Layout of the thesis	24
2. Literature Survey	26
2.1 Introduction.....	26
2.2 Vibration and damping	26
2.2.1 Material Damping	27
2.2.2 Structural Damping	28
2.3 Measurement of structural damping	29
2.3.1 Logarithmic decrement	29

2.3.2	Quality factor (R)	30
2.3.3	Specific damping Capacity (Ψ)	31
2.3.4	Loss factor (η).....	31
2.4	Methods to improve damping capacity	32
2.4.1	Unconstrained and sandwich construction	32
2.4.2	Use of high damping inserts	33
2.4.3	Use of layered and jointed structures	33
2.5	Review of literature on joint damping	34
2.6	Concluding Remarks	40
3.	Theoretical Formulation Using Classical Energy Method	41
3.1	Introduction.....	41
3.2	Classification of beam model	41
3.3	Governing equations for free transverse vibration.....	41
3.3.1	Determination of constants C_1, C_2, C_3, C_4, C_5 and C_6 for a beam fixed at both ends	44
3.3.2	Determination of constants C_1, \dots, C_6 for a beam simply supported at both ends	46
3.3.3	Determination of constants C_1, \dots, C_6 and mode shape of a beam fixed at one end and simply supported at the other end	48
3.4	Evaluation of micro slip at the interfaces of jointed beams	49

3.5	Normal force under each rivet	51
3.6	Determination of damping factor	55
3.8	Chapter Summary	57
4.	Finite Element Analysis of Jointed Structures	57
4.1	Introduction.....	57
4.2	Finite Element Concept	58
4.3	Governing equations of motion.....	59
4.4	Global and reduced mass and stiffness matrices	61
4.5	Determination of natural frequencies & mode shapes.....	64
4.6	Determination of damping factor	65
5.	Experimental Study	67
5.1	Introduction.....	67
5.2	Preparation of test specimens	67
5.3	Description of the Experimental Set-up	71
5.4	Testing procedure	79
5.4.1	Measurement of elasticity modulus (E).....	79
5.4.2	Measurement of Static bending stiffness (K)	79
5.4.3	Measurement of modal frequencies	80
5.4.4	Measurement of logarithmic decrement ‘ δ ’	80

5.4.5	Measurement of damping factor ‘ ζ ’	80
5.5	Experimental determination of α ’ μ	81
5.6	Comparative study of experimental and theoretical results.....	82
5.6.1	Experimental and theoretical comparison of damping factor for aluminium specimens	82
5.6.2	Experimental and theoretical comparison of damping factor for mild steel specimens	82
5.6.3	Experimental and theoretical comparison of modal frequencies and mode shapes for aluminium specimens	83
5.6.4	Experimental and theoretical comparison of modal frequencies and mode shapes for mild steel specimens	83
6.	Results and discussion	110
7	Conclusion and scope for further work	116
7.1	Conclusion	116
7.2	Scope for further work.....	120
8.	Bibliography	121

Nomenclature

English symbols

A : Cross sectional area of beam

A_0 : Cross sectional area of rivet

A'_c : Area under rivet head

d : Diameter of rivet

$\{d\}$: Global displacement matrix

C_1, C_2, \dots, C_4 : Constants defining spatial function $W(x)$

C_5, C_6 : Constants defining time function of displacement

$[D]$: Dynamic matrix

E : Elasticity modulus

E_f : Energy of dissipation per cycle

E_{loss} : Total energy loss per cycle

E_0 : Energy loss due to beam deformation

E_n : Energy stored per cycle

F_r : Frictional force at the interface

F_{rM} : Maximum frictional force at the interface

h_1 : Half the thickness of layer 1

h_2 : Half the thickness of layer 2

I : Moment of inertia of the beam

$[I]$: Identity matrix

K, K' : Flexural stiffness of composite beam and solid beam respectively

$[k_i^e]$: Element stiffness matrix of ' i 'th element

$[K_0]$: Global stiffness matrix

$[K]$: Reduced stiffness matrix

l : Length of beam finite element
 L : Total length of beam
 m : Mass per unit length of beam
 $[m_{ij}]$: Element mass matrix of ' i 'th element
 $[M_0]$: Global mass matrix
 $[M]$: Reduced mass matrix
 n : Total number of finite elements
 N : Normal force under each rivet
 N_{ix} : Shape functions associated with ' i 'th degree of freedom
 p : Interfacial pressure
 P : Preload on a rivet
 q : Total number of connecting rivets
 R : Any radius within influencing zone
 R_m : Limiting radius of influence zone
 R_v : Radius of connecting rivet
 $[S]$: Shape function matrix
 t : Time coordinate
 $T(t)$: Kinetic energy of beam element
 $u_0(x,t)$: Relative dynamic slip at the interfaces without friction
 $u_r(x,t)$: Relative dynamic slip at the interfaces with friction
 u_{rM} : Relative dynamic slip at the interfaces at maximum amplitude of vibration
 $v(t)$: Strain energy of beam element
 $\{w\}$: Element nodal displacement vector
 $w(x,t)$: Time and space dependent displacement
 $\{w(t)\}$: Time dependent element nodal displacement vector

$w_i(t)$: Time varying i^{th} degree of freedom, ($i = 1, 2, 3, 4$)

$\{w^{(j)}(t)\}$: Nodal displacement vector for element 'j'

$\{w_0(t)\}$: Reduced time dependent nodal displacement vector

$\{W_0\}$: Reduced nodal displacement vector

$V(t)$: Time function of displacement

$v(t)$: Kinetic energy of beam element

$W(x)$: Spatial displacement function

$W_i(t)$: Time varying displacement at ' i^{th} ' node

Greek symbols

α : $(\omega_n/c)^{1/2}$

α' : Dynamic slip ratio (u_r/u_0)

δ : Logarithmic decrement

δ_f : Log. decrement due to interface friction

ζ : Damping factor

ω_n : Natural frequency of vibration

ρ : Mass density

σ_0 : Initial stress on rivet

σ_s : Surface stress on jointed structure

Superscripts

e : element

Operators

'.' : d/dt

'\prime' : d/dx

T : Transpose of matrix

List of figures

Figure 1.1 Mechanism of microslip at the jointed interface	19
Figure 1.2 Comparison of Linear and Nonlinear systems . Error! Bookmark not defined.	
Figure 2.1 A typical hysteresis loop for material damping.....	27
Figure 2.2 R-factor method of measuring ‘ ζ ’	30
Figure 3.1 Differential Analysis of Fixed Fixed beam	42
Figure 3.2 Mechanism of microslip at the interface	50
Figure 3.3 (a) Plates clamped by a rivet	Error! Bookmark not defined.
Figure 3.3 (b) Surface stress and interfacial pressure distribution around rivet	Error! Bookmark not defined.
Table 3.1 – Polynomial Constants for varying thickness ratios.....	53
Figure 3.4 – Circular zone of influence of interfacial pressure	54
Figure 3.5 F_r vs u_r during one cycle.....	55
Figure 4.1 Discretization of beam.....	59
Figure 4.2 A typical beam element showing nodal and intermediate displacements	59
Figure 5.1 Photograph of the thin riveted mild steel specimens.....	69
Figure 5.2 Photograph of the thin riveted aluminium specimens	69
Figure 5.3 Photograph of the thin riveted aluminium specimens	70
.....	70
Figure 5.4 Photograph of the riveted mild steel specimens	70
Figure 5.5 Schematic layout of the specimen in the set-up	Error! Bookmark not defined.
Figure 5.6 Schematic diagram of experimental setup.....	Error! Bookmark not defined.
Figure 5.7 Amplifier	Error! Bookmark not defined.
Figure 5.8 Exciter.....	73
Figure 5.9 Oscillator	73
Figure 5.10 Ometron LASER vibrometer back view	74
Figure 5.11 Ometron LASER vibrometer with tripod.....	74
Figure 5.12 Dial gauge.....	75
Figure 5.13 Setup view for clamping beams at both ends	75
Figure 5.14 DPO 4000 series oscilloscope.	76
Fig 5.15 Ometron Laser vibrometer lens view	78
Figure 5.17 Effect of length on damping factor for Aluminium specimen using Finite Element method.	84
Figure 5.16 Effect of length on damping factor for aluminium specimen using classical method.....	84

Figure 5.18 Effect of length on damping factor for alumunium specimen using experimental method.....	85
Figure 5.19 Comparison of effect of length parameter on damping factor for Alumunium specimen using all methods.	85
Figure 5.20 Effect of length on damping factor for Mild steel specimen using classical method.....	86
Figure 5.21 Effect of length on damping factor for Mild steel specimen using Finite Element method.	86
Figure 5.22 Effect of length on damping factor for Mild steel specimen using Experimental method.....	87
Figure 5.23 Comparison of effect of length parameter on damping factor for Mild steel specimen.	87
Figure 5.24 Effect of diameter of rivets on damping factor for Alumunium specimen using classical method.	88
Figure 5.25 Effect of diameter of rivets on damping factor for Alumunium specimen using Finite Element method.	88
Figure 5.26 Effect of diameter of rivets on damping factor for Alumunium specimen using Experimental method.	89
Figure 5.27 Comparison of effect of diameter of rivets on damping factor for Alumunium specimen using all methods.....	89
Figure 5.28 Effect of diameter of rivets on damping factor for Mild steel specimen using classical method.	90
Figure 5.29 Effect of diameter of rivets on damping factor for Mild steel specimen using Finite element method.....	90
Figure 5.30 Effect of diameter of rivets on damping factor for Mild steel specimen using experimental method.....	91
Figure 5.31 Comparison of effect of diameter of rivets on damping factor for Mild steel specimen using all methods.	91
Figure 5.32 Effect of thickness ratio of beams on damping factor for Alumunium specimen using classical method.	92
Figure 5.33 Effect of thickness ratio of beams on damping factor for alumunium specimen using Finite element method.	92
Figure 5.34 Effect of thickness ratio of beams on damping factor for alumunium specimen using experimental method.	93
Figure 5.35 Comparison of effect of thickness ratio of beams on damping factor for alumunium specimen using all methods.	93
Figure 5.36 Effect of thickness ratio of beams on damping factor for mild steel specimen using classical method.	94
Figure 5.37 Effect of thickness ratio of beams on damping factor for mild steel specimen using finite element method.....	94

Figure 5.38 Effect of thickness ratio of beams on damping factor for mild steel specimen using classical method.	95
Figure 5.39 Comparison of effect of thickness ratio of beams on damping factor for mild steel specimen using all methods.	95
Figure 5.40 Effect of number of layers in composite beam on damping factor for alumunium specimen.	96
Figure 5.41 Effect of number of layers in composite beam on damping factor for mild steel specimen.	96
Figure 5.42 Variation of 1 st modal frequency with length for alumunium specimen using classical method.	97
Figure 5.43 Variation of 2 nd modal frequency with length for alumunium specimen using classical method.	97
Figure 5.44 Variation of 3 rd modal frequency with length for alumunium specimen using classical method.	98
Figure 5.45 Variation of 1 st modal frequency with length for mild steel specimen using classical method.	98
Figure 5.46 Variation of 2 nd modal frequency with length for alumunium specimen using classical method.	99
Figure 5.47 Variation of 3 rd modal frequency with length for mild steel specimen using classical method.	99
Figure 5.48 Effect of number of rivets on damping factor for alumunium specimen using classical method.	100
Figure 5.49 Effect of number of rivets on damping factor for alumunium specimen using finite element method.	100
Figure 5.50 Effect of number of rivets on damping factor for alumunium specimen using experimental method.	101
Figure 5.51 Effect of number of rivets on damping factor for alumunium specimen using all methods.	101
Figure 5.52 Effect of number of rivets on damping factor for mild steel specimen using classical method.	102
Figure 5.53 Effect of number of rivets on damping factor for mild steel specimen using finite element method.	102
Figure 5.54 Effect of number of rivets on damping factor for mild steel specimen using experimental method.	103
Figure 5.55 Effect of number of rivets on damping factor for mild steel specimen using all methods.	103
Figure 5.56 Mode shapes for alumunium specimen for fixed fixed configuration.	104
(a) Mode 1 (b)Mode 2 (c)Mode 3	104
Figure 5.57 Mode shapes for mild steel specimen for fixed fixed configuration.	105
(a) Mode 1 (b)Mode 2 (c)Mode 3	105

Figure 5.58 Mode shapes for aluminium specimen for simply supported simply supported configuration.	106
(a) Mode 1 (b)Mode 2 (c)Mode 3	106
Figure 5.59 Mode shapes for mild steel specimen for simply supported simply supported configuration.	107
(a) Mode 1 (b)Mode 2 (c)Mode 3	107
Figure 5.60 Mode shapes for aluminium specimen for fixed simply supported configuration.	108
(a) Mode 1 (b)Mode 2 (c)Mode 3	108
Figure 5.61 Mode shapes for mild steel specimen for fixed simply supported configuration.	109
(a)Mode 1 (b)Mode 2 (c)Mode 3	109

List of tables

Table 3.1 Polynomial Constants for varying thickness ratios.....	53
Table 5.1 Structural data of specimens used for analysis	68
Table 5.2 Elastic modulus of materials used.	79

1. Introduction to dynamics and damping of jointed structures

1.1 Genesis

Structures consisting of two or more layers of thin bars and plates connected by an array of bolts, rivets, weldments or adhesives have widespread mechanical, civil and aerospace applications. The advantages of such structures are their low vibration, high damping, low weight, low cost, decreased fatigue and flutter. A typical feature of these jointed structures is that the mechanism to improve damping properties can be introduced during the process of their design and operation. When subjected to varying and fluctuating load, vibration levels are significantly enhanced when frequency of excitation force tallies with natural frequency of the body. In these conditions high repeated stresses occur that may result in the premature failure of the body. It is imperative, therefore, to have a forehand knowledge of natural frequencies and normal modes of such bodies. In actual practice these structures are either fixed, free, simply supported or elastically supported at their extreme ends. Dynamic analysis of these structures is of great significance, considering their wide spread industrial application.

Introduction of these structural elements in mechanical and structural systems improves damping level leading to reduction in vibration and noise. Free vibration analysis of these structures is of great importance to evaluate their dynamic and damping characteristics. If the frequency of impressed or disturbing force matches with natural frequency of the system, resonant condition prevails which leads to unwanted large vibrations. Most structural failures take place due to this condition. Under free vibration, the amplitude is maximum and at the outset and goes on decreasing with time and eventually it becomes zero. It is known that the rate of decrease in amplitude is dependent on the amount of damping. Soon after the free vibration is started higher modes are damped out leaving the system to vibrate mainly at its fundamental mode and damping characteristics can be estimated from the decay rate of the amplitudes.

In order to improve the damping properties of these structures additional measures are necessary to dissipate energy. The solid structures are heavy and possess poor damping. Fabrication of these structures in layers connected by means of joints enhances the flexibility of the built up structure and has significant contribution to improved damping performance. The low material damping of monolithic structures are compensated by use of layered structures. The use of mechanical joints also has a great role in improvement of damping. The deteriorating effects such as fretting corrosion and loss of static stiffness can be overcome by suitable design [1, 2, 3]. The influence of friction joints on the reduction of vibration level have been reported in [4-11].

Damping due to friction occurs when two surfaces have relative motion between them in presence of friction. Relative motion is a function of normal load arising from the tightening of the joints holding the connected parts. If the joint is loose, contact surfaces experience pure slip. Since no work is required to be done to overcome friction, no dissipation of energy takes place. On the contrary, when the joint is very tight, high normal loads cause the whole contact interface to stick. This results in no energy dissipation because of no relative motion. When normal load lies between these two extreme cases i.e. pure slip and no relative motion, energy is dissipated. But between these two extreme conditions energy gets dissipated and maximum value of energy dissipation takes place within the range.

It has been reported [4] that the modeling of the joints of layered structures vastly improves their damping. However not much work is reported on damping of layered structures compared to that on real and solid structures. The reason behind is the complex energy dissipation mechanism affected by interface pressure, coefficient of friction and relative slip at the interface. Proper evaluation of these influencing parameters is of considerable importance in determining damping capacity correctly. Clamping action of the joints produces contact pressure between the surfaces which influences the joint properties. The profile of interface pressure distribution assumes great significance in this context. The pressure is non uniform across the interface. It is maximum at the joint and decreases radially outwards. Because of this uneven pressure distribution, a local relative motion known as microslip occurs at the interfaces of the connecting members. The presence of friction in the connecting points largely influences the damping capacity of

the structure. It is known that the joint friction arises only when the contacting layers tend to move relatively under the action of transverse vibration and serves as a booster for energy dissipation. Coulomb's law of friction is widely used to represent dry friction at the connected surfaces. Work in this respect are presented in [12-17]. It is wanted for all structures to possess adequate damping such that their response to the external excitation is minimized (32).

The mechanism by which mechanical joints dissipate energy is microslip. This is shown in Figure 1.1 when excitation level is low. When excitation level is increased, both micro and macro-slips occur at the jointed interface. Usually the macroslip is ignored as it may lead to structural damage. The contribution of microslip is important in spite of its low magnitude and is generally considered in design of structural joints.

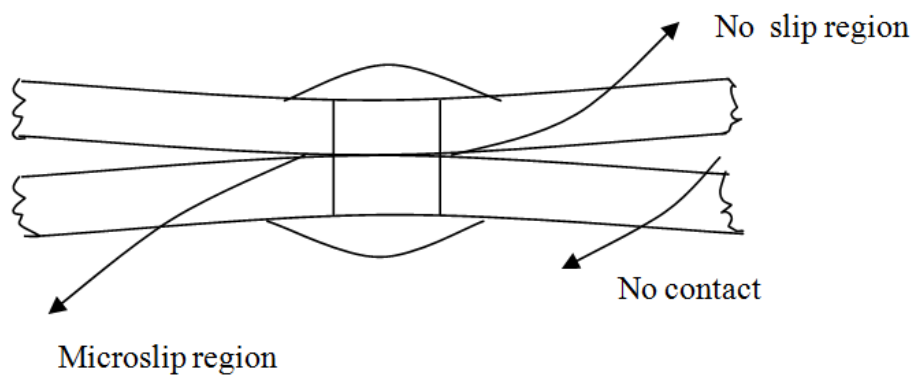


Figure 1.1 Mechanism of microslip at the jointed interface

The damping due to energy dissipation is quite small in real solid structures. In the present investigation an effort has been made to study dynamics and damping analysis of rivet-jointed layered structures with various boundary conditions.

1.2 Motivational aspects

Bolts, rivets, weldments are generally the elements used to fabricate built up structures. It has been established that the welded joints do not contribute appreciably to overall damping of the system. Hence they are discarded where damping is necessary. Damping

mechanism in case of bolts or rivets are the same, but interface pressure distribution is different in each case. Zone of influence and preload in case of bolted joints is different from those in case of riveted joints. Relative dynamic slip at the interface is therefore different leading to variation of damping action. In addition, axial load on a bolt can be changed by applying the torque as per the clamping necessity while the preload on the rivet is constant.

A number of research work has been reported in respect of bolted structures. Analytical, experimental and computational work in respect of bolted joint for fixed free boundary conditions has been reported. Study of damping of rivet jointed structures with respect to fixed fixed, fixed simply supported and simply supported simply supported boundary conditions has been the motivation for the present investigation.

1.3 Problem formulation

Structural problems are analyzed considering them either linear or non linear. In case of linear systems the excitation force and response are linearly related. Over certain operating ranges this relation is valid in most cases. Working with the linear models is relatively simple from analytical and experimental point of view. Principle of superposition holds good in these cases. For beams undergoing small amplitudes of vibration, linear beam theory is used to calculate natural frequencies, normal modes and response for a given excitation. Referring to Figure 1.2 linear and non linear systems agree well at small values of excitation while deviations are observed at higher level of excitation.

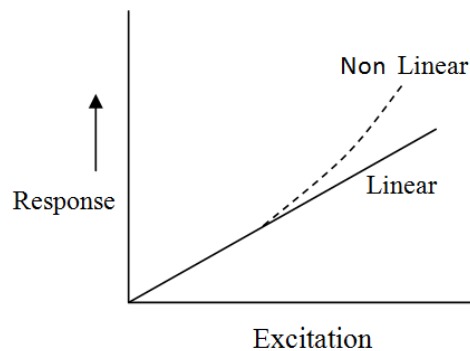


Figure 1.2 Comparison of Linear and Nonlinear system

The linear vibration theory is used when the beam is vibrated at small amplitudes and low frequencies. The present study primarily focuses on the analysis of damping of jointed beams at lower levels of excitation which is assumed to be linear.

1.4 Structure Modeling

The structure is modeled as a beam which is widely used as components of airplane wings, gun barrels, robot manipulators, multi-storey buildings, helicopter rotor blades, space craft antennae, satellites, long span bridges, naval frame works, and machine tool foundations and so on. Study of static and dynamic response of such beams both theoretically and experimentally are of great significance. Dynamic analysis of beams is carried out using either Euler-Bernoulli beam theory or Timoshenko beam theory. If the lateral dimensions of beam are less than one tenth of its length, the effect of shear deformation and rotary inertia are neglected for beams vibrating at low frequencies. The no transverse shear assumption implies that the rotation of cross section is due to bending only and corresponding beam is known as Euler-Bernoulli beam. If the lateral dimensions are more than one tenth of length of beam, the effects of shear deformation and rotary inertia are considered. Such beams are called Timoshenko beams. The present investigation is based on the assumption of Euler Bernoulli beam theory as the beam is excited at low frequencies and the dimensions of the test specimens have small lateral dimensions compared to length which satisfied thin beam theory.

Analytical modeling of the present problem is based on continuous model approach and finite element model approach. A continuous model is formulated using partial differential equations involving spatial and time co-ordinates. This is applicable for uniform beams and plates with simple geometry, end conditions and material properties. Actual engineering structures are not so simple. These are complex in shape, boundary conditions and material properties. For such problems approximate methods are used for the analysis. Finite element model in such cases is quite suitable. It consists of discretization of structure to a number of linear elements. Each element consists of two nodes at its ends. Each node has two degrees of freedom, i.e. transverse displacement and

rotation. Equations of motion are expressed by a set of coupled ordinary differential equations.

Theoretical modeling has to be justified by using experimental techniques. Several experimental methods are available to determine natural frequencies and level of damping in a structure. Frequency and time domain approach is a widely used method. It is based on frequency response and forced vibration. Time domain methods are based on the observation of time history of energy dissipation leading to the attenuation of amplitude of vibration. This method is applicable to both free and forced vibration problems. The logarithmic decrement method is commonly used for determining damping in time domain and is mostly applicable for free vibration response of a lightly damped linear system having low and medium frequency range. This method is useful for both single and multi degree freedom systems. Damping is separately obtained if the decay of initial excitation occurs in one mode of vibration for multiple degree of freedom systems. The half power bandwidth method is used to determine damping factor of beams assigned to harmonic expectations. Most research work has been reported to evaluate damping using these methods.

1.5 Outline of the present work

Dynamics and damping are important aspects of vibrating structures. Evaluation of these characteristics by analytical and experimental methods is of considerable significance. Usually the structures possess low damping and to improve their damping these are fabricated in layers incorporating joints. The introduction of joints causes energy dissipation through frictional contacts and shear displacements at the interfaces of the structural members which varies with boundary condition of the structure.

The present work is concerned with evaluation of dynamic characteristics of multilayered fixed fixed, fixed simply supported and simply supported simply supported beams with riveted joints. The primary reason for choosing rivets in place of welding or bolting is that these riveted connections are vastly used in trusses, pressure vessels, aircrafts in their various forms. The analysis are carried out on the basis of Euler-Bernoulli beam theory

since the dimensions of test specimens have been taken corresponding to thin beam theory and the beam is vibrated at low and medium frequencies.

The damping characteristics in rivet jointed structures with fixed fixed boundaries are significantly influenced by intensity of pressure distribution, relative dynamic slip and dynamic coefficient of friction at the interfaces which have to be precisely determined. Thickness ratio of the layers of beams also greatly influences these parameters.

The present work comprises of theoretical analysis and experimental analysis. The theoretical analysis consists of two different methods to calculate natural frequencies and damping parameters. These are classical method and finite element method. The classical method is applied to simple systems and produces an almost exact solution. The finite element method is applicable for practical problems with diversity and versatility, although results are reasonably accurate. In this method the beam is discretized into several elements and matrix equations are developed and solved to determine dynamic characteristics. The experimental analysis is carried out by use of frequency response curves and bandwidth method. Damping factor and log decrement are determined and compared with theoretical results for validity of theoretical analysis. Finally, conclusions have been drawn for dynamics and damping of rivet jointed layered beams with different boundary configurations.

1.6 Theoretical Assumptions

Several assumptions have been made in the present study to evaluate dynamic and damping characteristics.

- (a) Each layer of the beam undergoes uniform transverse deformation.
- (b) The beam is subjected to small amplitudes of vibration.
- (c) There is no overall microslip at the joint.
- (d) Effect of local mass of the joint area on behavior of beam is ignored.
- (e) Rivet holes in test specimens are completely filled by the rivets
- (f) There are no displacements and rotations at the clamped ends.
- (g) The material of the beam possesses linear characteristics
- (h) Coulomb's law of friction is used for the analysis.

- (i) The deflections are considered to be small compared to the thickness of beam.
- (j) The effects of shear deformation and rotary inertia are neglected.

1.7 Layout of the thesis

The whole thesis has been divided broadly into seven chapters which have been further subdivided into several sub chapters. The salient features of subject matter contained in each chapter are described as follows:

Chapter 1: The present chapter is introduction to study of dynamics and damping of jointed beams with various boundary conditions. It describes the significance and applications of these structures, motivation for the present work, aim and objective and brief outline of the research work.

Chapter 2: This chapter embodies a thorough review of literature related to vibration analysis of jointed structures. A good number of earlier research studies by various investigators have been reported. This chapter also describes different aspects of vibration, types and mechanism of damping and methods for improvement of damping.

Chapter 3: A detailed description of theoretical formulation for determining vibration characteristics and damping parameters in jointed beams of different boundary conditions are presented in this chapter. Determination of non uniform pressure distribution within the influencing zone of each rivet, estimation of normal and frictional forces at the interfaces, evaluation of log decrement and damping factor have been reported.

Chapter 4: Finite element method has been formulated to solve the present problem and forms the subject matter of this chapter. Discretizations of the jointed beam, derivation of element, global and reduced stiffness and mass matrices of the beam have been discussed. The steps to determine natural frequencies, mode shapes and damping factors using one dimensional linear element have been presented.

Chapter 5: This chapter is concerned with experimental analysis carried out to verify the theoretical results obtained by classical and finite element method. Development and fabrication of the experimental setup, preparations of the test specimens, instrumentation

and circuit diagrams, testing procedures are described. Comparison of analytical and experimental results is presented in graphical and tabular forms.

Chapter 6: A comprehensive discussion on the results in respect of dynamics and damping of rivet jointed layered beams by analytical and experimental methods have been reported in this chapter.

Chapter 7: Conclusion drawn on the basis of discussions over the results is presented in this chapter. The scope for further work in respect of the present work has been reported.

2. Literature Survey

2.1 Introduction

Over the years the study of vibration and damping of jointed structures have acquired great significance. Extensive research work involving classical and numerical methods have been carried out to predict vibration and damping behavior of these structures. Experimental techniques have been reported to measure their free and forced vibration response and damping performance. In the present chapter, the cause and effects of vibration and damping, classification of damping, methods of measurement of damping and improved performance related to damping and brief review of work conducted with regards to dynamics and damping in these areas have been presented.

2.2 Vibration and damping

Vibration is concerned with oscillatory motion of dynamic systems consisting of mass and parts capable of relative motion. All bodies having mass and elasticity are amenable to vibration. The vibratory motion of the system may be objectionable, trivial or necessary for performing a task. Unwanted vibrations in a machine may cause loosening of parts, its malfunctioning or its eventual failure. On the contrary, vibrating conveyors, shakers and vibrators in testing machines require vibration. Many engineering structures in general are subjected to undesirable vibrations and failure and damping is provided to attenuate vibrations and prevent failure. The ability of the structure to dissipate energy, mainly influence the damping properties and is released as heat.

It is essential to have a forehand knowledge of damping for design and working of a system. Damping may be desirable or undesirable and depends on the application. It is wanted for all structures to possess adequate damping such that their response to the external excitation is minimized (32). Damping not only reduces vibration, noise and dynamic stresses but also increases fatigue life of structures. Any unbalance in machines with rotating parts such as fans, ventilators, centrifugal separators, washing machines, lathes, centrifugal pumps, rotary presses, turbines, can cause undesirable vibrations. Buildings and structures experience vibrations due to operating machinery, passing

vehicular, air and rail traffic or natural calamities such as earthquakes and cyclones. Proper design of these systems is necessary for control of their vibrations.

In particular, structural systems possess low damping capacities and require additional damping such as passive or active damping treatments [33, 34]. Passive damping is provided by adding extra materials such as high damping visco-elastic materials during manufacturing of structure to control the vibration [36]. The layered and jointed constructions are most commonly considered for passive damping. Active damping however, refers to energy dissipation from the system by external elements such as actuators and sensors for detection and control of vibration. The energy of vibration is dissipated by several mechanisms, such as internal or material damping and structural damping.

2.2.1 Material Damping

The material damping is related to energy dissipation within the volume of material and is attributed to micro and macro structures, thermo elasticity, grain boundary, viscosity of the constituent material [24, 36]. Material damping is of two types, namely hysteretic damping and viscoelastic damping.

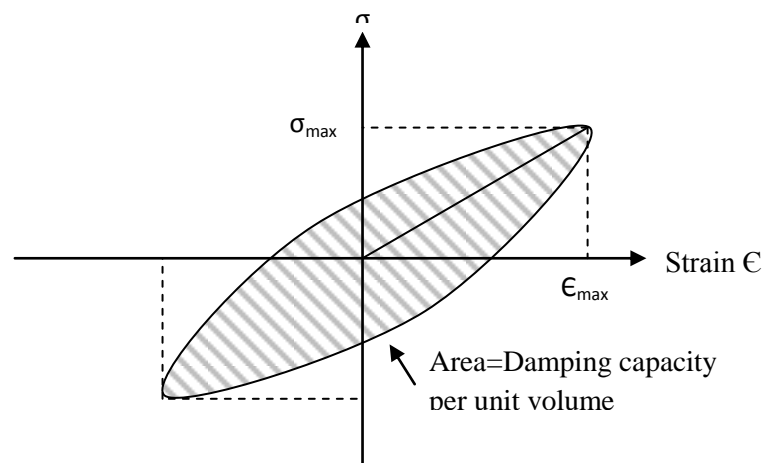


Figure 2.1 A typical hysteresis loop for material damping

When materials are critically stressed, energy is dissipated within the material itself and is proportional to the stiffness of the system and square of amplitude of vibration. This type of damping is known as hysteretic damping and energy loss per cycle is given as $E = \pi K \lambda A^2$, where k , λ and A are stiffness of the system, non dimensional damping factor and amplitude of vibration respectively. The stress-strain diagram for a body into hysteretic damping and subjected to vibration is shown in Figure 2.1. The area of the hysteresis loop represents the energy loss per unit volume of the material per stress cycle [26, 37]. This is termed as specific damping capacity and expressed as $\psi = \int \sigma d\epsilon$

The use of viscoelastic materials in structures provide passive damping and have widespread commercial and aerospace applications. The long chain molecules of viscoelastic or elastomeric materials when deformed convert mechanical energy into thermal energy. The relation between the stress and strain of a viscoelastic material is expressed as a linear differential equation with respect to time. The commonly used

Kelvin-Voigt model [26] uses the stress strain relation as $\sigma = E\epsilon + E^* \frac{d\epsilon}{dt}$ where E and

E^* are real and complex components of modulus of material respectively. The term $E\epsilon$ represents elastic behavior of body and does not contribute to damping. The other term

$E^* \frac{d\epsilon}{dt}$ contributes to damping. The specific damping capacity is given by $d_v = E^*$

$$\int \frac{d\epsilon}{dt} d\epsilon.$$

2.2.2 Structural Damping

Because of poor damping of structural materials, other methods are used to provide improved damping through joints and interfaces of structures. The damping in such cases is obtained by the energy dissipated due to rubbing friction resulting from relative motion between the parts and intermittent contact at the joints in a jointed structural system. The energy dissipated is affected by the interface pressure and extent of slip between the parts at the interfaces. Fretting corrosion also contributes to interfacial slip [32]. However, it is harmful for a safe joint design. Joint surfaces manufactured using cyanide hardening and

electro discharge machining greatly minimizes the fretting effect and improves high joint damping. The inclusion of joints reduces the stiffness of structure marginally. But through suitable design, loss of stiffness can be compensated. To enhance inherent damping in a structure it is easy and cheap to use joints to provide adequate damping and stiffness. The damping mechanism is most effective at low frequencies and at first few modes of vibration, since, the amplitudes are large enough to provide significant slip [32].

2.3 Measurement of structural damping

The damping properties of structures are generally expressed in terms of time response or frequency response methods depending on mathematically modeling of the problem. Logarithmic decrement, δ is assessed using time domain and quality factor R, by frequency domain methods. Other parameters such as damping ratio ζ , specific damping capacity ψ and loss factor η are evaluated from any one of the above two techniques for measurement of damping.

2.3.1 Logarithmic decrement

The log-decrement method is most popular technique to determine damping from the free decay of amplitudes of the time history curve [26, 32, 39, 40]. When the structure is set into free vibration, the lowest mode is predominant and higher modes are damped out in a short time. The logarithmic decrement represents the rate at which the amplitude of free damped vibration attenuates. It is defined as the natural logarithm of the ratio of any two consecutive amplitudes. Mathematically the logarithmic decrement “ δ ” is obtained as

$$\delta = \ln \frac{x_1}{x_2} = \frac{2\pi\zeta}{\sqrt{1-\zeta^2}} \text{ where } x_1 \text{ and } x_2 \text{ are the two successive amplitudes and } \zeta \text{ is the}$$

damping ratio. For small damping i.e. $\zeta \ll 1$, $\delta = 2\pi \zeta$. Log decrement can also be expressed as

$$\delta = \frac{1}{n} \ln \left(\frac{x_1}{x_{n+1}} \right) \text{ where } x_1, x_{n+1} \text{ are the amplitudes of 1}^{\text{st}} \text{ and last cycles}$$

respectively and n is number of cycles.

2.3.2 Quality factor (R)

The half power point bandwidth method is a frequency domain method to determine damping in terms of quality factor R. When a structure is subjected to forced vibration by a harmonic excitation force, the ratio of maximum dynamic displacement (X_{\max}) at steady state condition to the static displacement (X_s) under static force of same magnitude is called the R factor. Hence,

$$R = \frac{X_{\max}}{X_s} = \frac{1}{2\zeta} \Rightarrow \zeta = \frac{1}{2R}$$

Hence, damping ratio can be known if frequency response curve is determined. It is observed from the above expression that the systems with high R factor have low damping and systems with high damping have low R factor.

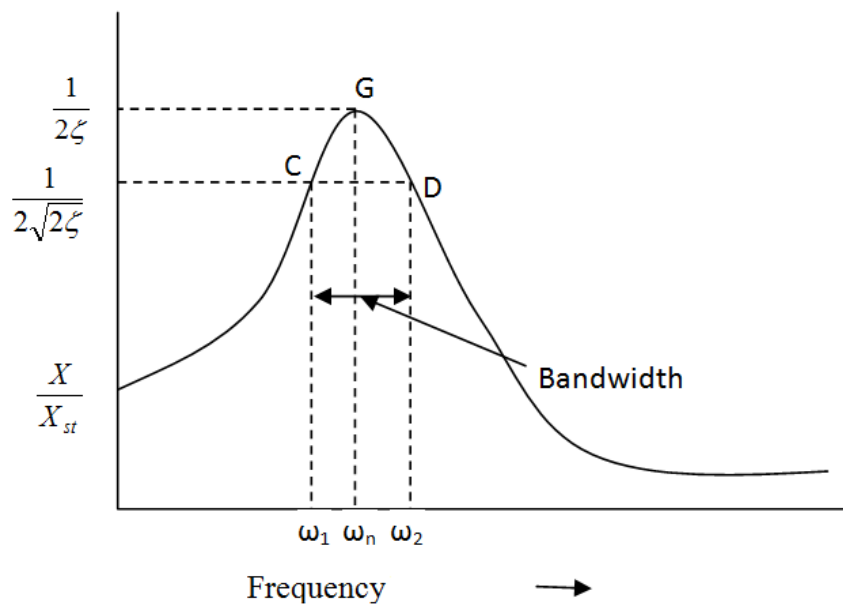


Figure 2.2 R-factor method of measuring ' ζ '

The points where amplitude ratio is $\frac{R}{\sqrt{2}}$ are known as half power points. With reference to Figure 2.2, C and D are half power points. The energy absorbed at point G is $\frac{1}{2}m\omega^2 R^2$ and at points C and D are $\frac{1}{2}m\omega^2 \left(\frac{R}{\sqrt{2}}\right)^2 = \frac{1}{4}m\omega^2 R^2$. Making use of half power points in response equation and solving we have

$$\left(\frac{\omega}{\omega_n}\right)^2 = (1 - 2\zeta^2) \pm 2\zeta \sqrt{1 - \zeta^2}$$

If ζ is very small, $\left(\frac{\omega}{\omega_n}\right)^2 = 1 \pm 2\zeta$

and $\frac{\omega_2 - \omega_1}{\omega_n} = 2\zeta = \text{Band width}$.

Thus, evaluation of band width leads to measuring damping ratio ζ .

2.3.3 Specific damping Capacity (Ψ)

The energy dissipated per cycle of vibration is defined as damping capacity and is expressed in the integral form as:

$$\Delta U = \oint f dx$$

Where fd = damping force

The damping capacity is given by the area bounded by the hysteresis loop in the displacement force plane. The ratio of energy dissipated per cycle to the total energy of vibration of the system is known as specific damping capacity (Ψ). If the initial (total) energy of the system is expressed as U_{\max} , then the specific damping capacity is given by

$$\Psi = \frac{\Delta U}{U_{\max}}$$

2.3.4 Loss factor (η)

The specific damping capacity per radian of damping cycle is known as loss factor η [41-43]. In viscoelastic damping, this factor is used frequently.

$$\text{Mathematically, } \eta = \frac{\Delta U}{2\pi U_{\max}}$$

It may be noted that U_{\max} is experimentally equal to the maximum kinetic or potential energy of the system without damping. The overall relationship among various terms of damping measurement for systems with small values of damping is given by:

$$\frac{1}{R} = \frac{\Psi}{2\pi} = \eta = \frac{\delta}{\pi} = 2\zeta = \frac{\Delta U}{2\pi U_{\max}}$$

2.4 Methods to improve damping capacity

Structural systems should possess the source of dissipation of energy to reduce their vibration level. Internal or material damping in these systems being low, it is necessary to introduce external energy dissipating methods to augment their damping capacity. A number of techniques have been developed to provide higher energy dissipation elements. These are two layered and sandwich construction using unconstrained and constrained viscoelastic layers respectively, use of high damping inserts and layered and jointed structures.

2.4.1 Unconstrained and sandwich construction

One of the simplest arrangements for increased damping is that of a viscoelastic layer attached to an elastic layer. Bending vibrations of the structure, result in alternate extension and contraction of the viscoelastic layer which leads to dissipation of energy. A viscoelastic body possesses both viscous and elastic properties. Some of the energy stored in the viscoelastic system is dissipated in the form of heat and rest of the energy is recovered after withdrawal of load. Damping effectiveness of unconstrained layer damping treatment applied to rectangular plates has been studied both experimentally and analytically [48, 49]. It is reported that this type of damping treatment increases modal loss factor and decreases modal frequencies.

Sandwich beams and plates consisting of a pair of shaft elastic face layers separated by and bonded to a stiff central core layer have found widespread application as structural elements of aircrafts, spacecrafts, missiles and many other branches of structural engineering. The material of top and bottom layers are generally metals and the core is of high damping viscoelastic material. During vibration, when the system deforms, shear strains develop in the damping layer and the energy is lost due to shear deformation. The

effect of face layer is to increase the deformation of the viscoelastic core and results in higher dissipation of energy. Kerwin [50] and Di Taranto [51] have developed mathematical modeling and wave theory of simply supported sandwich beams. Modeling for compressional damping in such beams has been presented by Douglas and Yang [52] and Duglas [53]. Sylwan [54] has studied a model combining shear and compressional effects and showed that energy loss is increased over a wider frequency range. Lee and Kim [55] have reported improved analytical results using thin viscoelastic layers. The theoretical work by Mead and Markus [56, 57] and Mead [58] reveals that the shearing of viscoelastic core is the only mechanism for energy dissipation with no effect of on energy loss due to compressional damping. The investigative work of Mead and Markus is widely recognized for analysis and damping of three layer sandwich beams and plates.

2.4.2 Use of high damping inserts

The inserts are either welded or attached by press fitting to structural members and are known to be improving damping capacity, as reported in articles [60-62]. It has been reported that the press fitting inserts are more damping effective than the welded ones. Welded inserts have limited size while the best results are obtained with shrink fit solid inserts. Rahmathullah and Mallik [63] have experimentally determined the damping capacity of aluminum cantilever strips by using high damping inserts of cast iron, Bakelite and Perspex. It has been found that with suitable selection of insert material, considerable improvement of damping capacity can be achieved by introducing little amount of high damping material.

2.4.3 Use of layered and jointed structures

Control of vibration of structure by providing sufficient damping mechanism is of great significance for their increased life expectancy. Rigid and robust solid structures designed in this context are heavy and expensive. The method of reducing vibration by fabricating the structures in layers and connecting them with mechanical joints has been widely recognized. It is known that the overall damping of a structural system is greater than the sum of the material damping of individual structural components of the system. The damping in structures such as beams is increased by fabricating them in layers and

connecting them by fasteners like bolts or rivets. The interfacial slip between layers takes place during their vibration and produces frictional damping. A good number of research work [64-66] shows that the joints mainly account for damping and are major sources of passive vibration control. The energy dissipation is undesirable because of fretting corrosion but desirable to reduce vibration amplitude [67]. A good number of researchers [59, 68-71] have reported experimental and analytical results related to joint damping.

The mechanism of dissipation of energy in a joint is a complex phenomenon which is greatly affected by interfacial pressure, slip and friction between contacting surfaces [16]. It is cumbersome to evaluate damping because of variation of coefficient of friction under dynamic conditions. However, it is generally accepted that the friction force at the interface is dependent on contacting materials and varies with normal force across the interface. At the location of the joint, sliding takes place in a micro scale and Coulomb's law of friction is assumed to be applicable.

2.5 Review of literature on joint damping

Engineering structures are generally of built-up constructions with mechanical joints connecting the structural elements. Two sources of damping namely internal or material damping [72] and structural damping [72-74] are present in these systems. While material damping is low, structural damping is 90% of the total damping of the structure. The jointed connections are major sources of energy dissipation and greatly influence dynamics and damping of the structures [12, 16, 67]. Apart from shear at the interfaces of joints, relative slip at the interfaces of joints, coefficient of friction and pressure distribution contribute largely to damping performance of the joints. In built-up structures energy dissipation occurs either due to micro slip or macro slip [75]. On application of excitation forces, the small portions of interface break which results in slipping. These localized motions are called micro slip and no relative motion at contact surfaces occur when excitation frequencies are low. As the force is increased, entire contact area slips giving rise to macro slip. In majority of structures micro slip occurs, but no macro slip. Macro slip leads to failure of joint and is generally avoided. While the micro slip is an

excellent source of energy dissipation, without causing damage of the joint and usually introduced in the design of the system.

In recent years most of work is involved with the concept of micro slip and macro slip [76, 77]. These concepts have been utilized to analyze dynamic behavior of jointed structures having frictional contact [6-11, 78-83]. Several researchers [84-88] have studied micro slip phenomenon by assuming the friction surface as a rigid body with low normal load. However, a number of researchers [9, 10, 89, 90] have used micro slip concept, considering friction surface as elastic body. In this case, the interface undergoes partial slip under high normal load. Mesuko et al [27] and Nishiwaki et al [28] have reported energy loss in jointed cantilever beam considering micro slip and normal force at the interface. Olofsson et al [92] stated that micro slip occurs at an optimal frictional force and presented a model for micro slip between smooth and rough flat surfaces covered with ellipsoidal elastic bodies. Ying [94] has proposed a new micro slip model to study effect of joint friction for controlling dynamic response.

The friction at the interfaces of jointed layers occurs when the layers undergo relative motion due to transverse vibration. The friction in a joint arises from shearing between the parts and is controlled by the tension in the bolt or rivet, surface properties and materials in contact [95]. The steady state response of a friction damped system with Coulomb and viscous friction has been analyzed by Den Hartog [96]. A good number of researchers [15, 16, 37, 96-99] have presented reviews on the effect of joint friction on structural damping in built-up structures and have shown that the friction in joints is an important source of energy dissipation.

Damping capacity of jointed structures is significantly affected by the nature of pressure distribution across a beam layer. Most of the previous investigators have idealized the joints by assuming a uniform pressure profile which ignores the effects of surface irregularities and asperities [27-29, 74, 100, 101]. However, a good number of researchers [102-107] have shown through experimental work that the interface pressure is not uniform in actual condition. Gould et al [107] and Zaida [109] have observed that

the pressure variation at the interface of a bolted joint is parabolic in nature, in an area circumscribing the bolt which is roughly 3.5 times the bolt diameter and is independent of tightening load. Hisakads et al [110] have shown through experimental findings that the pressure distribution is not dependent on surface roughness. They measured pressure distribution of contacting two metals by noting the impression of the softer surface formed by the denting of harder asperities. Of late Nanda and Behera [30] have developed an analytical expression for the pressure profile at the interfaces of a bolted joint by curve fitting the earlier results reported by Zaida et al [109]. In this context, an eight order polynomial even function have been obtained in terms of radial distance from the centre of bolt such that the function is maximum at the centre of bolt and decreases radially away from the bolt. Nanda and Behera have succeeded in simulating uniform interface pressure over the beam length and investigating the effect of pressure on the damping behavior of interfacial slip.

Analytical work involving the study of effect of non uniform pressure on interfacial slip damping for layered beams for both static and dynamic loading has been reported [111, 112]. In these studies, it has been shown that non-uniform pressure profile and frequency variation greatly affect energy dissipation and logarithmic decrement. The amount of energy dissipation with slip damping under dynamic load is less than the same under static load. Olunloyo [113] have used other forms of polynomial or hyperbolic expression for pressure distribution.

Among the various methods used to measure the contact pressure between layers the ultrasonic wave method is most effective. Since, it measures contact pressure without affecting the properties of the contact surface. A normal probe [114, 115] has been used to obtain reasonably good result. On the other hand Minakuchi et al [31] have used angle probe for convenience and have reported that the contact pressure between two layered beams of different thicknesses by obtaining a relation between the mean pressure and sound pressure of reflected waves. This method has wider acceptability as the results fairly match with theoretical values. The present work uses the Minakuchi experimental results to obtain non uniform pressure distribution at the interfaces of a jointed beam.

A good deal of research study [27-29, 116-119] is related to energy dissipation due to slip and non uniform pressure distribution. The effect of clamping pressure on mechanisms of dissipation of energy has been reported by many authors [12, 18, 19]. Under high clamping pressure the slip is small and under low pressure the shear due to friction is small. Beards [122] has considered these two limits and demonstrated the existence of an optimum clamping force for maximum energy distribution. An algorithm for evaluating energy loss due to slip has been proposed by Jezequel [119]. When the normal force is varied with relative slip joint damping resembles viscous damping [70, 122-126].

Beards et al [7] did experimental work on a framed structure and stated that reasonable increase in damping can be attained by fitting joints tightly to stop linear slip, but not so tightly as to prevent rotational slip. Beards and Imam [6] have shown that the frictional damping of plates is increased by using jointed laminated plates having interfacial slip during vibration. Effect of controlled frictional damping in joints on the frequency response of a frame work under harmonic excitation has been experimentally studied by Bears and Woodwat [82]. However, Beards [14, 65, 121, 127, 128], has observed that due to reduction in stiffness and increased corrosion at the joint interfaces, relative motion between contact surfaces should be avoided. A power law relation between energy loss and lateral load due to micro slip at the joints has been obtained [130, 131] by researchers at Sandia National Laboratories. Heller, Foltete and Piranda [132] have determined non linear damping capacity of bolt jointed built up structures, using experimental procedure and studied the effect of interface pressure and area of contact on its dynamic characteristics. Walker et al [132] focused his discussion on the joint factors influencing damping of aerospace structure and observed that energy dissipation is less on riveted joints compared to bolted ones due to higher stiffness. They also concluded that damping increases with reduction in bolt torque and vice versa.

Proper modeling of structure using the known joint parameters is of significance for slip related energy dissipation. Many researchers [16, 134-136] have worked to this effect. Song et al [136] have suggested Adjusted Iwan Beam Element (AIBE) model using

nonlinearity effects of a bolt joined structure. Hartwigsen et al [76] have experimentally studied the effect of non linearity on shear lap joints of two structures consisting of a centrally bolt joined beam and frame with a bolt joined member. Their experimental results reveal several important parameters influencing stiffness and damping of lap joints. Miller and Quinn [138] have developed a two sided interface model for dissipation which is based on a series-series system in which the parameters are physically activated. The model is introduced into a large model to find damping. Khattak[139] et al have developed a parameter less model considering shear lap joints that can be applied for variation in loading, joint geometry, coefficient of friction and clamping pressure. Many investigators [12, 16, 30, 67] have evaluated damping by using time or frequency domain method of experimental analysis, which are applicable for lightly damped linear systems vibrating at low frequency and amplitude. Nishiwaki et al [28] have reported an improved band width method to experimentally measure logarithmic decrement of a bolted cantilever beam for its first three modes. Masuko et al [27] and Nishiwaki et al [21] have studied damping of a jointed fixed free beam using normal force and micro-slip at the interfaces. Damsa et al [111] have analyzed dynamic loads, frequency variation and non uniformities in pressure distribution and their effect on energy dissipation and logarithmic decrement in clamped layered beams. Analytical results in respect of log-decrement have been reported [139] for layered viscoelastic structures.

Wang et al [141] and Tsai et al [143] have demonstrated frequency domain technique to find the stiffness and damping of a single bolt jointed structure using Frequency Response Function (FRF) in different frequency ranges. Yin et al [144] have reported a method based on the wavelet transform of FRF for linear system to evaluate natural frequency and damping. Hwang [145] has presented a frequency domain response model to estimate stiffness constant and damping parameters of connected structures experimentally. Ahmadian and Jalali [144] have reported a parametric model for a beam with bolted lap joint at its mid-span. The analysis provides the FRF at any location of the beam due to excitation at some other location which is compared with experimentally obtained results.

Gavl and Lenz [136] have used Finite Element Model (FEM) to evaluate dynamic response of built up structures considering interfacial slip theory. Sainsbury and Zhang [147] have performed dynamic analysis of damped sandwich beams using Finite Element Analysis. Lee et al [142] have evaluated natural frequencies and mode shapes of jointed beams using FEM. Hartwigsen et al [76] have determined contact area of a bolt jointed interface with help of FEM and verified the same experimentally. Micro slip concept using FEM had been the subject of study of Chan and Deng [149] for structures under pane stress conditions. Using press-fit and lap shear joint modeling they have reported the influence of dry friction and slip on damping response of joints for determining energy dissipation during cyclic loading. Effect of dynamic friction on energy loss and preload on response of a bolted joint has been reported [150].

Most of the work reviewed so far is concerned with dynamics and damping study of bolt jointed structures. Comparatively, little work has been reported for riveted structures. Riveting constitutes a major source of fastening and has extensive applications in trusses, frames, bridges, trestles etc. Riveted joints are relatively cheap, reliable, strong and capable of providing high damping. Pian and Hewell [151] have presented the theory of structural damping in assembled beams connected with riveted straps. Pian [101] has reported the theoretical analysis of energy loss of continuously riveted spar and spar cap and got the results tallying with experimental values. Walker et al [133] have made experimental investigations to study the effect of joint properties affecting the damping of metal plates for aerospace use.

In both cases of bolted and riveted structures, the mechanism of damping is same while their functional parameters are different. These parameters are interface pressure profile, influencing zone and preload. The zone of interface pressure distribution spreads over circular area about the rivet centre of diameter equal to 4.125, 5.0 and 5.6 times the rivet diameter for layer thickness ratios of 1.0, 1.5 and 2.0 respectively. The same in case of bolted joint is 3.5 times the bolt diameter [152]. As a result the relative spacing among the joints will be different which changes the dynamic slip at the interfaces. In addition, the axial load on a bolt can be altered as per the clamping need by applying the tightening

torque, whereas, the preload on a rivet is constant. Therefore, controlling factors of preload for both the joints are different which affect damping significantly. The objective of present study is to develop the theory of damping mechanism and dynamics of rivet jointed structures using classical and finite element method with verification by experimental analysis.

2.6 Concluding Remarks

Engineering structures require high damping for their useful functioning since they possess low material damping. It is necessary to furnish extra damping for their safe and reliable function and jointed construction serves the purpose well. Dynamic response of such structures can be predicted with reasonable accuracy by knowledge of damping parameters obtained by using joint details. The prediction of damping in built up structures being complex, it is necessary to analyze the damping phenomenon and associated factors theoretically and verify the results experimentally.

From the literature survey it is clear that damping is produced by the energy dissipation during vibration of a structure when some relative motion occurs at the interfaces of joints with friction. This dissipation is required to reduce vibration and increase useful life of structure. Over the decades, a great deal of research work has been reported on the damping of bolted structures with less work reported in respect of riveted structures. The present work aims at evaluation of dynamic and damping characteristics of layered riveted structures with various boundary conditions.

3. Theoretical Formulation Using Classical Energy Method

3.1 Introduction

In earlier chapters it has been described that inclusion of joints in built-up structures is the major source of energy dissipation. The damping is because of frictional effects arising out of shear displacements at the interfaces of the layers. The damping parameters are influenced by the intensity of pressure distribution, micro slip and kinematic coefficient of friction at the interfaces which are to be considered for determination of loss of energy. These characteristics are also greatly dependent on boundary configuration of the structure. The present chapter gives a detailed discussion of the theoretical formulation by classical method for determining damping properties of jointed layered fixed fixed, fixed simply supported and simply supported simply supported beam with riveted joints.

3.2 Classification of beam model

Vibrating systems are generally classified into two groups, i.e. discrete and continuous systems. In discrete system, mass is assumed to be rigid and concentrated at discrete points. The motion of discrete systems is governed by ordinary differential equations and the number of masses generally defines the number of degrees of freedom. The solution of discrete systems has been accomplished by using Finite Element Method presented in the next chapter.

In non discrete or continuous systems, the mass and elasticity are considered to be distributed parameters. Vibration of the system is described by partial differential equations. These systems are considered to be infinite degrees of freedom systems and they possess infinite number of natural frequencies and modes. However, the first few modes of vibration influence the dynamics of the system considerably.

3.3 Governing equations for free transverse vibration

A fixed fixed beam undergoing free transverse vibration is shown in Figure 3.1. In deriving the governing equations of motion, Euler-Bernouli beam is used. It is based on

the assumptions that the rotation of differential element is negligible compared to translation and the angular distortion due to shear is small in relation to flexural deformation. This assumption is justified where ratio of length of beam to its depth is large as in the present case.

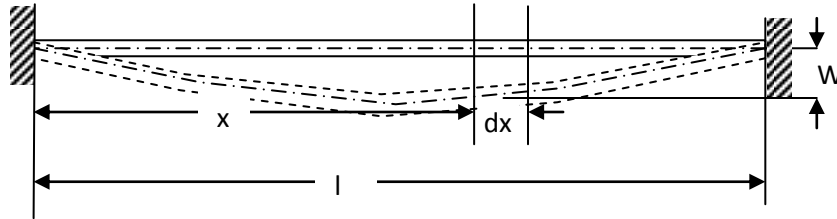


Figure 3.1 Differential Analysis of Fixed Fixed beam

The beam motion is depicted by partial differential equation in terms of spatial variable 'x' and time variable 't'. The governing equation for free transverse vibration is given by

$$c^2 \frac{\partial^4 w(x,t)}{\partial x^4} = - \frac{\partial^2 w(x,t)}{\partial t^2} \quad 3.1$$

where $c = \sqrt{\frac{EI}{\rho A}}$ and E, I, ρ , A are Young's modulus of elasticity, moment of inertia, mass density and cross sectional area of beam, respectively.

The solution of Eq 3.1 which is of fourth order has four unknown constants and hence requires four boundary conditions for their determination. The second order time derivative also requires two initial conditions, one for the displacement and another for velocity. The above equation is solved using the technique of separation of variables. In the method the displacement $w(x,t)$ is written as the product of two functions, one depending on space coordinate x and other depending on time coordinate 't'. Hence, the solution is given by:

$$w(x,t) = W(x) V(t) \quad 3.2$$

Where $W(x)$ and $V(t)$ are space and time functions respectively.

Using equation (3.2) in Equation (3.1) we have

$$c^2 W''''(x) V(t) = - W(x) \ddot{V}(t) \quad 3.3$$

The time and space variables are separated by

$$c^2 \frac{W''''(x)}{W(x)} = -\frac{\ddot{V}(t)}{V(t)} = \omega_n^2 \quad 3.4$$

where ω_n^2 is the separation constant representing the square of natural angular frequency. Since, the first term in equation (3.4) is a function of 'x' only and second term is a function of 't' only, the entire equation can be satisfied for arbitrary values of 'x' and 't' only, if each of them is a constant. This equation yields two ordinary differential equations given by

$$W''''(x) - \left(\frac{\omega_n}{c}\right)^2 W(x) = 0 \quad 3.5$$

and

$$\ddot{V}(t) + \omega_n^2 V(t) = 0 \quad 3.6$$

Introducing, $\alpha^2 = \frac{\omega_n}{c}$, equation (3.5) is written as

$$W''''(x) - \alpha^4 W(x) = 0 \quad 3.7$$

The equation (3.7) is solved in the usual way with $W(x)$ as a sum of four terms and the solution is given by

$$W(x) = C_1 \cosh \alpha x + C_2 \sinh \alpha x + C_3 \cos \alpha x + C_4 \sin \alpha x \quad 3.8$$

where C_1, C_2, C_3 and C_4 are evaluated from the known boundary conditions of the fixed fixed beam. Equation 3.6 is the known free vibration equation of an undamped single degree freedom system and its solution is given by

$$V(t) = C_5 \cos \omega_n t + C_6 \sin \omega_n t \quad 3.9$$

where C_5 and C_6 are the constants to be determined from initial conditions.

Substituting the expressions of space and time functions i.e. equations (3.8) and (3.9) into equation (3.2), the complete solution for deflection at any section is written as

$$W(x,t) = (C_1 \cosh \alpha x + C_2 \sinh \alpha x + C_3 \cos \alpha x + C_4 \sin \alpha x) \times (C_5 \cos \omega_n t + C_6 \sin \omega_n t) \quad 3.10$$

3.3.1 Determination of constants C_1, C_2, C_3, C_4, C_5 and C_6 for a beam fixed at both ends

Using the expression for space function as per equation (3.8) following relations of its first and second derivatives are written

$$W(x) = C_1 \cosh \alpha x + C_2 \sinh \alpha x + C_3 \cos \alpha x + C_4 \sin \alpha x \quad 3.11(a)$$

$$W'(x) = C_1 \alpha \sinh \alpha x + C_2 \alpha \cosh \alpha x - C_3 \alpha \sin \alpha x + C_4 \alpha \cos \alpha x \quad 3.11(b)$$

$$W''(x) = C_1 \alpha^2 \cosh \alpha x + C_2 \alpha^2 \sinh \alpha x - C_3 \alpha^2 \cos \alpha x - C_4 \alpha^2 \sin \alpha x \quad 3.11(c)$$

The four boundary conditions for a fixed fixed beam are given by:

$$\text{At } x = 0, W(0) = 0 \quad 3.12(a)$$

$$\text{and at } x=0, W'(0) = 0 \quad 3.12(b)$$

$$\text{Again at } x = l, W(l) = 0 \quad 3.12(c)$$

$$\text{and at } x=l, W'(l) = 0 \quad 3.12(d)$$

$$\text{Using equation 3.12 (a), } W(0) = C_1 + C_3 = 0 \quad 3.12(e)$$

$$\text{and equation 3.12(b) } W'(0) = C_2 + C_4 = 0 \quad 3.12(f)$$

Using equations 3.12 (c) and 3.12 (e)

$$W(l) = C_1 \cosh \alpha l + C_2 \sinh \alpha l + C_3 \cosh \alpha l + C_4 \sinh \alpha l = 0$$

$$\text{or } W(l) = C_1 (\cosh \alpha l - C_2 \cos \alpha l) + C_2 (\sinh \alpha l - \sin \alpha l) = 0 \quad 3.12(g)$$

Using equation 3.12(d)

$$W'(l) = C_1 \alpha \sinh \alpha l + C_2 \alpha \cosh \alpha l - C_3 \alpha \sin \alpha l + C_4 \alpha \cos \alpha l = 0$$

$$\text{or } W'(l) = C_1 (\sinh \alpha l + \sin \alpha l) + C_2 (\cosh \alpha l - \cos \alpha l) = 0 \quad 3.12(h)$$

The equations 3.12(g), 3.12 (h) can be written in the matrix form as follows:

$$\begin{bmatrix} \cosh \alpha l - \cos \alpha l & \sinh \alpha l - \sin \alpha l \\ \sinh \alpha l + \sin \alpha l & \cosh \alpha l - \cos \alpha l \end{bmatrix} \begin{Bmatrix} C_1 \\ C_2 \end{Bmatrix} = \begin{Bmatrix} 0 \\ 0 \end{Bmatrix} \quad 3.13$$

For non zero solution of the constant, determinant of the matrix = 0, i.e.

$$\begin{vmatrix} \cosh \alpha l - \cos \alpha l & \sinh \alpha l - \sin \alpha l \\ \sinh \alpha l + \sin \alpha l & \cosh \alpha l - \cos \alpha l \end{vmatrix} = 0 \quad 3.14$$

Equation (3.14) can be simplified as

$$\cosh \alpha l \cdot \cos \alpha l = 1 \quad 3.15$$

This transcendental equation is the required condition for the coefficient matrix to yield a non trivial solution and can be solved to evaluate natural frequencies of vibration

using equation 3.12 (f), $C_2 = -1$, if $C_4 = 1$

And from equation 3.13 we have

$$\left. \begin{aligned} C_1 &= \frac{\sinh \alpha l - \sin \alpha l}{\cosh \alpha l - \cos \alpha l}, \quad C_2 = -1 \\ C_3 &= -\frac{\sinh \alpha l - \sin \alpha l}{\cosh \alpha l - \cos \alpha l}, \text{ and } C_4 = 1 \end{aligned} \right\} \quad 3.16$$

The space function $W(x)$ is expressed as

$$W(x) = \frac{(\sinh \alpha l - \sin \alpha l)(\cosh \alpha x - \cos \alpha x) - (\cosh \alpha l - \cos \alpha l)(\sinh \alpha x - \sin \alpha x)}{\cosh \alpha l - \cos \alpha l} \quad 3.17$$

Different mode shapes of vibration can be determined using equation 3.17 for fixed fixed beam. The expression for deflection and its time derivative at any section of beam are given by,

$$w(x,t) = W(x) (C_5 \cos \omega_n t + C_6 \sin \omega_n t) \quad 3.18$$

$$\text{and } \frac{\partial w(x,t)}{\partial t} = W(x) (-C_5 \omega_n \sin \omega_n t + C_6 \omega_n \cos \omega_n t) \quad 3.19$$

Using initial condition of fixed fixed beam

$$\frac{\partial w\left(\frac{l}{2}, 0\right)}{\partial t} = 0 \text{ at } t = 0, \text{ we have } C_6 = 0$$

and $w(x,t) = W(x) C_5 \cos \omega_n t$

considering initial deflection at mid point of beam as $W\left(\frac{l}{2}\right)$,

$$C_5 = \frac{w\left(\frac{l}{2}, 0\right)}{W\left(\frac{l}{2}\right)} \quad 3.20$$

Hence the general expression for modal displacement can be written as

$$w(x,t) = W(x) \frac{w\left(\frac{l}{2}, 0\right)}{W\left(\frac{l}{2}\right)} \cos \omega_n t \quad 3.21$$

3.3.2 Determination of constants C_1, \dots, C_6 for a beam simply supported at both ends

The four boundary conditions for the beam with simply supported ends are:

$$\text{At } x = 0, \quad W(0) = 0 \quad 3.22(a)$$

$$M(0) = 0 \rightarrow d \frac{\partial^2 W(0)}{\partial x^2} = 0 \quad 3.22(b)$$

$$\text{And at } x = l, \quad W(l) = 0 \quad 3.22(c)$$

$$M(l) = 0, \quad \frac{\partial^2 W(l)}{\partial x^2} = 0 \quad 3.22(d)$$

Substituting condition 3.22(a) in 3.11 (a) and 3.22 (b) in 3.11(c) we obtain

$$C_1 + C_3 = 0 \quad 3.22(e)$$

$$\text{And } C_1 - C_3 = 0 \quad 3.22(f)$$

which implies that

$$C_1 = 0 \quad 3.22(g)$$

$$\text{And } C_3 = 0 \quad 3.22(h)$$

Using equation 3.22(g), 3.22(h) and condition 3.22(c) in equation 3.11(a) we have

$$C_2 \sinh \alpha l + C_4 \sin \alpha l = 0 \quad 3.22(i)$$

Using condition 3.22(d), equation 3.22(g) and 3.22(h) in equation 3.11(c), we have

$$C_2 \sinh \alpha l - C_4 \sin \alpha l = 0 \quad 3.22(j)$$

From equation 3.22(i) and (j) we have

$$C_2 \sinh \alpha l = 0 \quad 3.22(k)$$

$$\text{and } C_4 \sin \alpha l = 0 \quad 3.22(l)$$

Since, $\sinh \alpha l$, in general, cannot be zero, $C_2 = 0$ and

$$W(x) = C_4 \sin \alpha x \quad 3.22(m)$$

$$\text{And since } C_4 \neq 0, \sin \alpha l = 0 \quad 3.22(n)$$

Which yields $\alpha l = n\pi$ ($n = 0, 1, \dots, \infty$)

Considering $C_4 = 1$

$$W(x) = \sin \frac{n\pi}{l} \cdot x \quad 3.22(o)$$

Equation 3.22(o) represents mode shape for a simply supported beam.

Using the same procedure as used for fixed fixed beam

$$w(x,t) = W(x) \frac{w\left(\frac{l}{2},0\right)}{W\left(\frac{l}{2}\right)} \cos \omega_n t \quad 3.23$$

3.3.3 Determination of constants C_1, \dots, C_6 and mode shape of a beam fixed at one end and simply supported at the other end

The boundary conditions for such a beam are:

(i) At the fixed end, i.e. at $x = 0$, $W(0) = 0$ which gives $C_1 + C_3 = 0$

(ii) At $x = 0$, $\frac{\partial W(0)}{\partial x} = 0$, gives $C_2 + C_4 = 0$

At the simply supported end, $w(l)=0$, and $\frac{\partial^2 W(l)}{\partial x^2} = 0$

Hence we have from equation 3.11(a) and 3.11(c)

$$(\cosh \alpha l - \cos \alpha l)C_1 + (\sinh \alpha l - \sin \alpha l)C_2 = 0 \quad 3.24(a)$$

$$\text{and } (\cosh \alpha l + \cos \alpha l)C_1 + (\sinh \alpha l + \sin \alpha l)C_2 = 0 \quad 3.24(b)$$

The non trivial solution for C_1 and C_2 requires that the determinant for their coefficients be zero, i.e.

$$\begin{vmatrix} (\cosh \alpha l - \cos \alpha l) & (\sinh \alpha l - \sin \alpha l) \\ (\cosh \alpha l + \cos \alpha l) & (\sinh \alpha l + \sin \alpha l) \end{vmatrix} = 0 \quad 3.24(c)$$

Expanding the determinant yields the frequency equation

$$\cos \alpha l \cdot \sinh \alpha l - \sin \alpha l \cdot \cosh \alpha l = 0$$

$$\tan \alpha l = \tanh \alpha l \quad 3.24(d)$$

The above equation yields $\alpha l = 3.92, 7.07, 10.1$ for first three modes of vibration.

Solving for α , we obtain the expression for $W(x)$ as given in equation 3.17 and displacement of beam as

$$w(x,t) = W(x) \frac{w(l',0)}{W(l')} \cos \omega_n t \quad 3.25$$

where l' defines the point on the beam having maximum displacement (i.e. $l' = 0.58l$).

3.4 Evaluation of micro slip at the interfaces of jointed beams

The interfaces of contacting beam layers contain microscopic asperities of different shapes and sizes which deform elastically or plastically and may collapse during motion. Partial slippage between layers may occur due to deformation and subsequent tangential motion. Semi-rigidness of the connected members is another source of micro slip. Due to clamping force, no slippage occurs at the riveted joint. But the normal force away from the joint is relatively small and permits micro slip over a fraction of region of contact. The contact pressure at the jointed interface is non-uniform in nature which is maximum at the site of rivet hole and is gradually reduced with the distance away from the rivet hole. First occurrence of micro slip takes place in the region where contact pressure is inadequate to overcome the shear stress. In a nutshell, micro slip is due to several factors, notably deformation and breakage of asperities, semi rigid nature of joints and non uniform pressure distribution at the interfaces. The micro slip is solely responsible for energy dissipation. At higher levels of excitation, both micro slip and macro slip occur. Because of structural failure macro slip is undesirable. On the contrary, micro slip occurs at lower levels of vibration and provides a reasonable level of energy dissipation and damping without causing any structural malfunctioning. Considering the above factors, the relative dynamic slip at the interfaces is analyzed. The slope at any section of beam is obtained by differentiating Eq 3.25 with respect to x , as follows:

$$\frac{\partial w(x,t)}{\partial x} = \frac{\partial W(x)}{\partial x} * \frac{w\left(\frac{l}{2}, 0\right)}{W\left(\frac{l}{2}\right)} \cos \omega_n t \quad 3.26$$

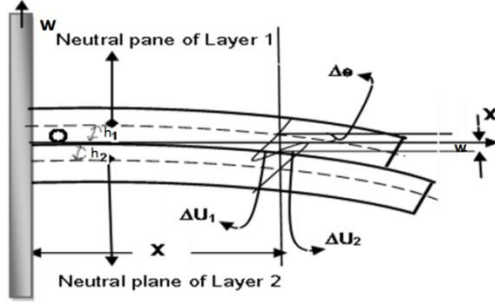


Figure 3.2 Mechanism of microslip at the interface

As shown in Figure 3.2, the relative displacement at a distance x from the fixed end of the beam is given by

$$u_0(x,t) = \Delta u_1 + \Delta u_2 = (h_1 + h_2) \frac{\partial w(x,t)}{\partial x} \quad 3.27$$

However, the actual micro slip $u_r(x,t)$ between the interfaces is always less than $u_0(x,t)$ and is given by

$$u_r(x,t) = \alpha' u_0(x,t) \quad 3.28$$

where α' is a constant known as dynamic slip ratio and is defined as the ratio of actual micro slip $u_r(x,t)$ in the presence of friction to the ideal micro slip $u_0(x,t)$, in the absence of friction. α' is a function of pressure distribution and surface irregularities at the interfaces of layers. The maximum relative micro slip under a connecting rivet is obtained by

$$U_{,M} = \left[\alpha' \frac{(h_1 + h_2)}{2} \right] \left[(\sinh \alpha x + \sin \alpha x)(\sinh \alpha l - \sin \alpha l) - (\cosh \alpha x - \cos \alpha x)(\cosh \alpha l - \cos \alpha l) \right] \\ \times \left\{ \frac{\alpha w \left(\frac{1}{2}, 0 \right)}{W \left(\frac{1}{2} \right)} \right\} (\cosh \alpha l - \cos \alpha l)^{-1} \quad 3.29$$

Considering 'n' number of rivets, equispaced along the beam.

$$U_{rM} = \alpha' \frac{(h_1 + h_2)}{2} X \alpha W \left(\frac{l}{2}, 0 \right) \quad 3.30$$

where

$$X = \left[(\sinh \alpha l - \sin \alpha l) \sum_{i=1}^n (\sinh \alpha x_i + \sin \alpha x_i) - (\cosh \alpha l - \cos \alpha l) \sum_{i=1}^n (\cosh \alpha x_i - \cos \alpha x_i) \right] / [W(l/2) \times (\cosh \alpha l - \cos \alpha l)] \quad 3.31$$

For the simply supported simply supported beam configuration, the equation 3.30 is valid

$$\text{for } U_{rM} \text{ with } X = \sum_{i=1}^n \cos \alpha x_i / W \left(\frac{l}{2} \right) \quad 3.31(a)$$

For fixed simply supported beam configuration, the expressions for U_{rM} and X remain the same as given in equations 3.30 and 3.31 respectively with $(l/2)$ replaced by l' .

3.5 Normal force under each rivet

The rivet jointed structure holds the members together at the interfaces. Because of clamping of rivets, the pressure is developed at the contacting surface. To evaluate energy dissipated due to friction it is necessary to determine interface pressure and the resultant normal force. A circular area of contact is formed around the rivet with a separation occurring at a certain distance away from the rivet hole as shown in Fig 3.3(a,b)

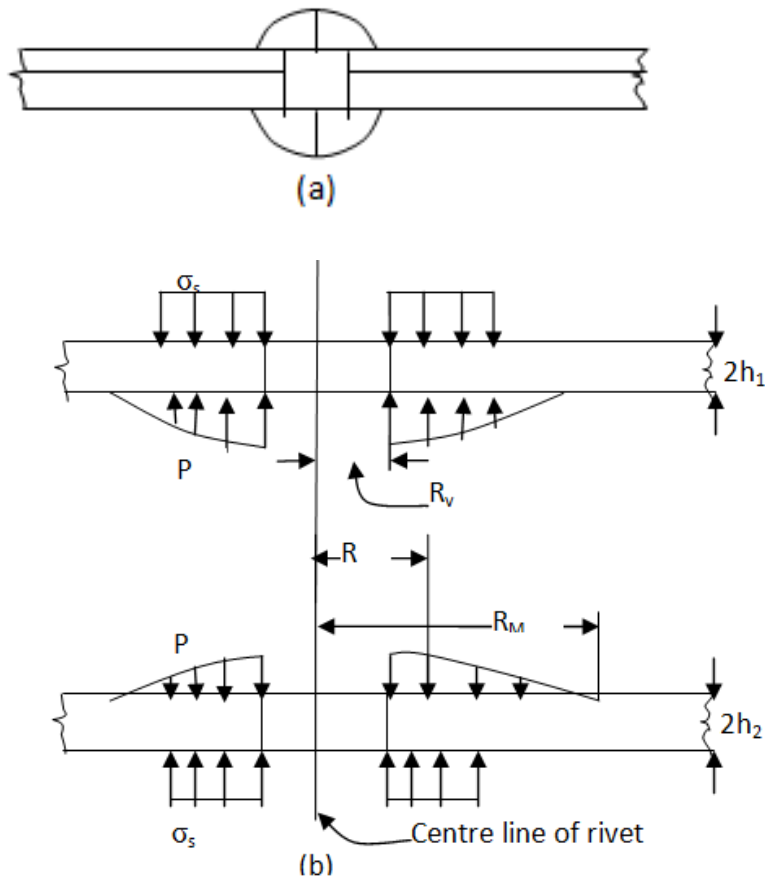


Figure 3.3 (a) Plates clamped by a rivet

Figure 3.3 (b) Surface stress and interfacial pressure distribution around rivet

The interfacial pressure is non uniform being maximum at the rivet hole and decreasing with distance away from the rivet. As a result, localized slipping occurs at the interfaces while the overall joint remains fixed. The pressure is also affected by the component beams with different thickness ratios. It has been found by Minakuchi, et al [32] that the interface pressure distribution is parabolic with a circular influence zone surrounding the rivet with diameter equal to 4.125, 5.0 and 5.6 times the diameter of rivet for thickness ratios 1.0, 1.5 and 2.0 respectively.

The pressure distribution around the rivet is a non dimensional polynomial for jointed structure is assumed as

$$\frac{p}{\sigma_s} = A_1 \left(\frac{R}{R_v} \right)^{10} + A_2 \left(\frac{R}{R_v} \right)^8 + A_3 \left(\frac{R}{R_v} \right)^6 + A_4 \left(\frac{R}{R_v} \right)^4 + A_5 \left(\frac{R}{R_v} \right)^2 + A_6 \quad 3.32$$

where p , σ_s , R and R_v are the interface pressure, surface stress on the structure due to riveting, and radius within the influence zone and radius of the connecting rivet respectively. A_1 to A_6 are the constants determined from the numerical data of Minakuchi et al [32] as given in Table 3.1. The surface stress, σ_s is obtained by the ratio P/A' where P is initial tension on the rivet and A' is the area under rivet head.

The expression (Eq. 3.32) is a tenth order polynomial in respect of non-dimensional radial distance from the centre of rivet so that it assumes its maximum value at the centre and diminishes radially. It is observed from Table 3.1 that the contribution of first four coefficients to distribution of pressure is negligible which indicates a linear distribution of pressure across the interface. Damisa et al [111] have used linear pressure profile in their analysis. But, in the present study a higher order polynomial as stated has been used for non uniform pressure profile.

Table 3.1 – Polynomial Constants for varying thickness ratios

Thickness Ratio	A1	A2	A3	A4	A5	A6
1	1.45E-06	-5.80E-05	6.04E-04	3.09E-03	-9.58E-02	5.38E-01
1.5	-1.74E-07	1.40E-05	-4.59E-04	8.17E-03	-8.77E-02	4.88E-01
2	-7.42E-08	7.45E-04	-2.98E-04	6.22E-03	-7.46E-02	4.60E-01

From Table 3.1 it is seen that the polynomial constants are different for different thickness ratios. Therefore, pressure distribution varies and depends on the thickness ratio of the layered beam.

According to Shigley, et al [153] the area A' under the rivet head is given by

$A' = \pi[(1.75R_v)^2 - R_v^2] = 2.0625\pi R_v^2$, Hence, interface pressure

$$p = \left[A_1 \left(\frac{R}{R_v} \right)^{10} + A_2 \left(\frac{R}{R_v} \right)^8 + A_3 \left(\frac{R}{R_v} \right)^6 + A_4 \left(\frac{R}{R_v} \right)^4 + A_5 \left(\frac{R}{R_v} \right)^2 + A_6 \right] \frac{P}{2.0625\pi R_v^2} \quad 3.33$$

Taking a differential element in the form of an annular ring of radius R and width dR (Figure 3.4) the normal force on the element is given as

$$dN = pdA = 2\pi R dR$$

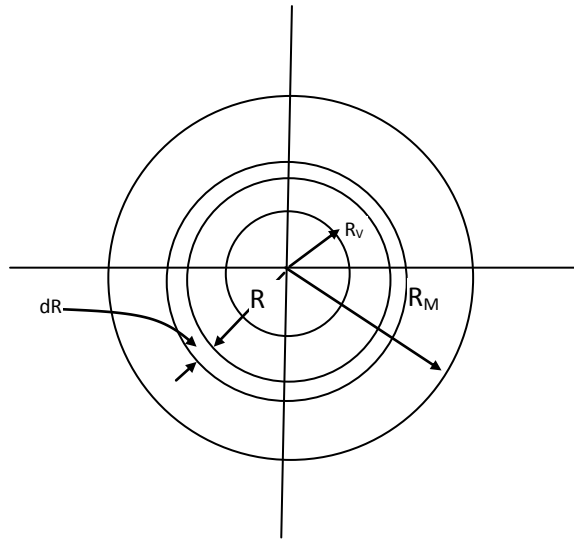


Figure 3.4 – Circular zone of influence of interfacial pressure

Therefore, net normal force under each rivet

$$N = 2\pi \int_{R_v}^{R_M} p R dR$$

$$\begin{aligned} \text{or } N = \frac{P}{2.0625} & \left[\frac{A_1}{6} \left\{ \left(\frac{R_M}{R_v} \right)^{12} - 1 \right\} + \frac{A_2}{5} \left\{ \left(\frac{R_M}{R_v} \right)^{10} - 1 \right\} + \frac{A_3}{4} \left\{ \left(\frac{R_M}{R_v} \right)^8 - 1 \right\} \right] + \\ & \left[\frac{A_4}{3} \left\{ \left(\frac{R_M}{R_v} \right)^6 - 1 \right\} + \frac{A_5}{2} \left\{ \left(\frac{R_M}{R_v} \right)^4 - 1 \right\} + A_6 \left\{ \left(\frac{R_M}{R_v} \right)^2 - 1 \right\} \right] \end{aligned} \quad 3.34$$

where R_M = Limiting radius of influencing zone and

P = Initial tension on the rivet = Force with which the members are tightened together

= $\sigma_0 \cdot A_0$, where σ_0 = Initial stress on the rivet = 100 N/mm^2 (For power driven rivets as per Maitra and Prasad [154] and A_0 = Cross sectional area of rivet = πR_v^2

Friction occurs due to relative motion between two surfaces in contact and accounts for dissipation of energy. Since, Coulomb's law of friction is valid the maximum frictional force is given as $F_M = \mu N$, where μ = kinematic coefficient of friction. Energy dissipation

per cycle of vibration is determined from the hysteresis loop shown in Fig 3.5 and is given in the integral form as

$$E_f = \oint F_r du_r = 2F_{rM} u_{rM} \quad 3.35$$

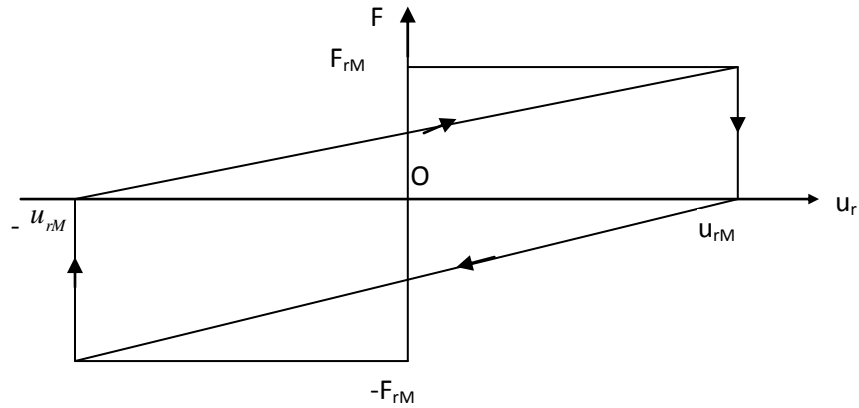


Figure 3.5 F_r vs u_r during one cycle

3.6 Determination of damping factor

Damping capacity of a jointed beam is normally obtained by using the logarithmic decrement method. Logarithmic decrement ‘ δ ’ is defined as the natural logarithm of the ratio of two consecutive amplitudes on the same side of mean line of vibration. From the data of experimentally obtained curve of decaying amplitudes log-decrement is determined. However, energy method is used to evaluate theoretically the log decrement. According to Nishiwaki et al [29] log decrement is given by

$$\delta = \frac{1}{2} (E_{\text{loss}}/E_n) \quad 3.36$$

The energy loss E_{loss} consists of the sum of energy loss (E_f) due to friction at the joints and the energy loss E_0 due to material of the beam and damping at the support.

$$\delta = \delta_f + \delta_0 = \frac{1}{2} \frac{E_f}{E_n} + \frac{1}{2} \frac{E_0}{E_n} \quad 3.37$$

However, in the present investigation the damping is considered because of joint friction only. Hence, equation (3.37) is simplified as

$$\delta = \frac{1}{2} \frac{E_f}{E_n} = \delta_f \quad 3.38$$

The energy is stored in the system in form of flexural strain energy when the fixed fixed beam is excited at its midspan. The amount of energy stored in the system per cycle of motion, E_n is given by

$$E_n = \frac{1}{2} k \left[w \left(\frac{l}{2}, 0 \right) \right]^2 \quad 3.39$$

where k is the static bending stiffness of the layered and jointed beam which is less than that of its equivalent solid beam. The static stiffness the beam is determined experimentally to evaluate the energy stored in the system. Using the expressions of E_f and E_n as per equation (3.35) and (3.39) we have

$$\delta = \frac{\mu N \alpha' (h_1 + h_2) X \alpha}{k w \left(\frac{l}{2}, 0 \right)} \quad 3.40$$

If thickness of each layer is same, i.e., $2h_1 = 2h_2 = 2h$, equation (3.40) is modified as

$$\delta = \frac{2\mu N \alpha' h X \alpha}{k w \left(\frac{l}{2}, 0 \right)} \quad 3.41$$

For a beam with 'm' layers, the number of interfacial layers is 'm-1'. Hence, 'δ' is given by

$$\delta = \frac{2\mu N \alpha' (m-1) h X \alpha}{k w \left(\frac{l}{2}, 0 \right)} \quad 3.42$$

And damping factor is given by, $\zeta = \delta/2\pi$ 3.43

Energy dissipation mainly depends on 'μ' the kinematic coefficient of friction and 'α'' the dynamic slip ratio. It is difficult to evaluate damping produced in joints due to variation of these two parameters. However, they are interdependent and inversely related to each other. In other words, if one of them is increasing, the other is decreasing and vice versa. However their product $\alpha' \cdot \mu$ is found to be constant for a particular specimen despite the surface condition. Hence, the product (α' , μ) is obtained by

$$\alpha' \cdot \mu = \frac{k w \left(\frac{l}{2}, 0 \right) \delta}{N(h_1 + h_2) X \alpha} \quad 3.44$$

This product has been found from experimental results for a particular rivet diameter and later used to find log decrement for other conditions of the beam using equation 3.40.

3.8 Chapter Summary

In the present chapter, an exact analysis for the distributed mass model of the beam has been presented. Neglecting shear deformation and rotary inertia, governing equation of the free flexural vibration of the jointed beam has been deduced. The total relative dynamic slip at the interfaces has been determined, considering slope and deflection. The interface pressure has been evaluated which is seen to be non uniform being maximum at the rivet location and decreasing radially away from the rivet. The normal force and frictional force have been evaluated and used subsequently to determine logarithmic decrement for two as well as multilayered beam joints with rivets. Analysis has been made for the multilayered beams with fixed fixed, fixed-simply supported and simply supported simply supported boundary conditions.

4. Finite Element Analysis of Jointed Structures

4.1 Introduction

Classical and conventional method of analysis of vibration and damping of rivet jointed beams has been formulated in Chapter 3. The physical structures are in general complex ones having variations in shape, size and properties of materials, loading and end constraints. Finite difference and finite element methods are extensively used to solve such problems. Developments of high speed computers and software packages have considerably facilitated the analysis of structural problems by using these methods. In the present chapter finite element approach has been demonstrated to evaluate dynamic and damping characteristics of rivet jointed beams of different end conditions.

In the finite difference method, the derivative terms in differential equations describing motion of the beam is substituted by finite difference equivalent at nodal points. As a result, a set of linear simultaneous algebraic equations involving nodal variables are derived and solved to determine nodal properties and subsequently the required characteristics of the beam. Finite element method is actually an outgrowth of the finite difference method and consists of discretization, choice of displacement function, evaluation of shape function, stiffness matrix, mass matrix and solution of the matrix equations, leading to determination of desirable parameters of the structure. Finite element method is widely used for its diversity and flexibility.

4.2 Finite Element Concept

The finite element method is based on the representation of structure by an assemblage of sub divisions called finite elements. The finite elements are obtained by means of fictitious cuts through the original structure. Adjoining elements may be considered as being connected at common points, termed as nodes. Then simple functions are chosen to approximate the variation of actual displacement over each finite element. Such assumed functions are called displacement functions or displacement models. The unknown magnitudes of displacement functions are called nodal displacements. The idealized model is analyzed by using the principle of minimum potential energy to obtain a set of equilibrium equations for each element. The equilibrium equations for the entire body are obtained by combining the equations for the individual elements in such a way that continuity of displacements is preserved at the interconnecting nodes. These equations presented in matrix forms are modified for the given boundary conditions and are solved to evaluate unknown displacements. In extending the problem for vibration analysis, kinetic and strain energies of the element are derived in the form of nodal displacement. Using Lagrange's equation, element mass and stiffness matrix are derived for each element and assembled to obtain overall mass and stiffness matrix for the whole domain. Thus, each individual element and its contribution are considered in determining global model of the structure. Introduction of boundary conditions in the equations involving global matrices gives the reduced matrix equations which are finally expressed as Eigen

value problems. These matrices are solved to determine Eigen values and natural frequencies and Eigen vectors or mode shapes of the beam.

4.3 Governing equations of motion

To apply the finite element theory for the vibrations of jointed beam, the differential equation describing motion of the beam in terms of physical and geometrical parameter is considered. For this purpose, Euler Bernoulli equation for the beam modified for free transverse vibration is given by:

$$EI \frac{\partial^4 w(x,t)}{\partial x^4} = 0 \quad 4.1$$

Solution for $w(x,t)$ can be written in terms of the shape functions which are functions relating nodal displacements with intermediate displacement of the isolated beam element as shown in figure 4.2 which has been discretized into 'n' linear elements (Fig 4.1).

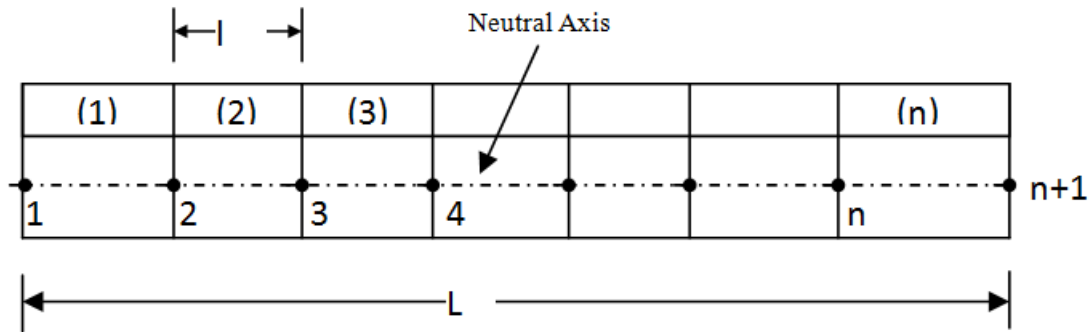


Figure 4.1 Discretization of beam

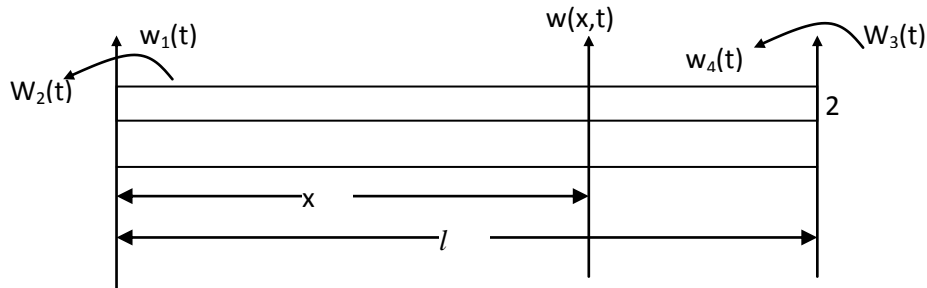


Figure 4.2 A typical beam element showing nodal and intermediate displacement

$$\text{Hence, } w(x,t) = \sum_{i=1}^4 N_{ix} w_i(t) = [S]\{w(t)\} \quad 4.2$$

The displacement and slope at the nodal points of the element are zero. Using equation 4.2 in equation 4.1, and the boundary conditions, the shape functions are evaluated as

$$\left. \begin{aligned} N_{1x} &= 1 - \frac{3x^2}{l^2} + \frac{2x^3}{l^3} \\ N_{2x} &= x - \frac{2x^2}{l} + \frac{x^3}{l^2} \\ N_{3x} &= \frac{3x^2}{l^2} - \frac{2x^3}{l^3} \\ N_{4x} &= -\frac{x^2}{l} + \frac{x^3}{l^2} \end{aligned} \right\} \quad 4.3$$

Now, kinetic energy($T(t)$) and potential energy($v(t)$) of the beam element are given by

$$T(t) = \frac{1}{2} \int_0^l m \left(\frac{\partial w(x,t)}{\partial t} \right)^2 dx \quad 4.4$$

$$\text{and } v(t) = \frac{1}{2} \int_0^l EI \left(\frac{\partial^2 w(x,t)}{\partial x^2} \right)^2 dx \quad 4.5$$

Evaluating the integrals and simplifying

$$\begin{aligned} T(t) &= \frac{ml}{840} [156\dot{w}_1^2(t) + 4l^2\dot{w}_2^2(t) + 156\dot{w}_3^2(t) + 4l^2\dot{w}_4^2(t) + 44l\dot{w}_1(t)\dot{w}_2(t) + 108l\dot{w}_1(t)\dot{w}_3(t) \\ &\quad - 26l\dot{w}_1(t)\dot{w}_4(t) + 26l\dot{w}_2(t)\dot{w}_3(t) - 6l^2\dot{w}_2(t)\dot{w}_4(t) - 44l\dot{w}_3(t)\dot{w}_4(t)] \quad 4.6 \end{aligned}$$

$$\begin{aligned} v(t) &= \frac{EI}{2l^3} [12w_1^2(t) + 4l^2w_2^2(t) + 12w_3^2(t) + 4l^2w_4^2(t) + 12lw_1(t)w_2(t) - 24w_1(t)w_3(t) + 12lw_1(t)w_4(t) \\ &\quad - 12lw_2(t)w_3(t) + 4l^2w_2(t)w_4(t) - 12lw_3(t)w_4(t)] \quad 4.7 \end{aligned}$$

The Lagrange's equation for free vibration of beam is given by

$$\frac{\partial}{\partial t} \left(\frac{\partial T(t)}{\partial \dot{w}_i(t)} \right) + \frac{\partial v(t)}{\partial w_i(t)} = 0 \quad 4.8$$

Using equations 4.6 and 4.7 in equation 4.8 and simplifying, the four equations in terms of, $w_1(t)$, $w_2(t)$, $w_3(t)$ and $w_4(t)$ are obtained. Collecting these equations in matrix form we get

$$[m^e] \{\ddot{w}(t)\} + [k^e] \{w(t)\} = 0 \quad 4.9$$

where $[m^e]$ = Element mass matrix $[k^e]$ =Element stiffness matrix and these are given as

$$[m^e] = \frac{ml}{420} \begin{bmatrix} 156 & 22l & 54 & -13l \\ 22l & 4l^2 & 13l & -3l^2 \\ 54 & 13l & 156 & -22l \\ -13l & -3l^2 & -22l & 4l^2 \end{bmatrix} \quad 4.10$$

$$\text{and } [k^e] = \frac{EI}{l^3} \begin{bmatrix} 12 & 6l & -12 & 6l \\ 6l & 4l^2 & -6l & 2l^2 \\ -12 & -6l & 12 & -6l \\ 6l & 2l^2 & -6l & 4l^2 \end{bmatrix} \quad 4.11$$

4.4 Global and reduced mass and stiffness matrices

A beam discretized into 'n' elements has n+1 nodes. Each node has two degrees of freedom given by displacement and slope. Therefore, the beam has 2(n+1) degrees of freedom and nodal displacement vector consists of same number of elements. The assembled overall or global mass matrix $[M_0]$ and global stiffness matrix are each of the order $2(n+1) \times 2(n+1)$. The (4x4) stiffness matrix of i^{th} element is converted to $2(n+1) \times 2(n+1)$ matrix by using auxiliary rectangular matrix $[A_i]$ of the order $2(n+1) \times 4$.

For a 3 element beam, the transpose of auxiliary matrix $[A_2]$ of element 2 is given by :

$$[A_2]^T = \begin{bmatrix} 0 & 0 & 1 & 0 & 0 & 0 & 0 & 0 \\ 0 & 0 & 0 & 1 & 0 & 0 & 0 & 0 \\ 0 & 0 & 0 & 0 & 1 & 0 & 0 & 0 \\ 0 & 0 & 0 & 0 & 0 & 1 & 0 & 0 \end{bmatrix} \quad 4.12$$

$$\text{Hence, } [K_0] = \sum_{i=1}^n [A_i][k_i][A_i]^T \quad 4.13$$

$$\text{and } [M_0] = \sum_{i=1}^n [A_i][m_i][A_i]^T \quad 4.14$$

By introducing displacement boundary conditions, the global mass and stiffness matrices are converted to reduce mass and stiffness matrices. The corresponding equation of motion using reduced matrices are obtained as

$$[M]\{\ddot{w}_0(t)\} + [K]\{w_0(t)\} = 0 \quad 4.15$$

The global stiffness and mass matrices assembled for a beam discretized into 3 elements of identical physical and geometrical parameters are given by

$$[K] = \frac{EI}{l^3} \begin{bmatrix} 12 & 6l & -12 & 6l & 0 & 0 & 0 & 0 \\ 6l & 4l^2 & -6l & 2l^2 & 0 & 0 & 0 & 0 \\ -12 & -6l & 24 & 0 & -12 & 6l & 0 & 0 \\ 6l & 2l^2 & 0 & 8l^2 & -6l & 2l^2 & 0 & 0 \\ 0 & 0 & -12 & -6l & 24 & 0 & -12 & 6l \\ 0 & 0 & 6l & 2l^2 & 0 & 8l^2 & -6l & 2l^2 \\ 0 & 0 & 0 & 0 & -12 & -6l & 12 & -6l \\ 0 & 0 & 0 & 0 & 6l & 2l^2 & -6l & 4l^2 \end{bmatrix} \quad 4.16$$

$$[M] = \frac{ml}{420} \begin{bmatrix} 156 & 22l & 54 & -13l & 0 & 0 & 0 & 0 \\ 22l & 4l^2 & 13l & -3l^2 & 0 & 0 & 0 & 0 \\ 54 & 13l & 312 & 0 & 54 & -13l & 0 & 0 \\ -13l & -3l^2 & 0 & 8l^2 & 13l & -3l^2 & 0 & 0 \\ 0 & 0 & 54 & 13l & 312 & 0 & 54 & 13l \\ 0 & 0 & -13l & -3l^2 & 0 & 8l^2 & 13l & 3l^2 \\ 0 & 0 & 0 & 0 & 54 & 13l & 156 & -22l \\ 0 & 0 & 0 & 0 & -13l & 3l^2 & -22l & 4l^2 \end{bmatrix} \quad 4.17$$

Reduced stiffness and mass matrices for fixed fixed 3 element beam are given by

$$[K] = \frac{EI}{l^3} \begin{bmatrix} 24 & 0 & -12 & 6l \\ 0 & 8l^2 & -6l & 2l^2 \\ -12 & -6l & 24 & 0 \\ 6l & 2l^2 & 0 & 8l^2 \end{bmatrix} \quad 4.18$$

$$[M] = \frac{ml}{420} \begin{bmatrix} 312 & 0 & 54 & -13l \\ 0 & 8l^2 & 13l & -3l^2 \\ 54 & 13l & 312 & 0 \\ -13l & -3l^2 & 0 & 8l^2 \end{bmatrix} \quad 4.19$$

Corresponding matrices for fixed-simply supported 3 element beam are given by

$$[K] = \frac{EI}{l^3} \begin{bmatrix} 24 & 0 & -12 & 6l & 0 \\ 0 & 8l^2 & -6l & 2l^2 & 0 \\ -12 & -6l & 24 & 0 & -12 \\ 6l & 2l^2 & 0 & 8l^2 & 2l^2 \\ 0 & 0 & 6l & 2l^2 & 4l^2 \end{bmatrix} \quad 4.20$$

$$[M] = \frac{ml}{420} \begin{bmatrix} 312 & 0 & 54 & -13l & 0 \\ 0 & 8l^2 & 13l & -3l^2 & 0 \\ 54 & 13l & 312 & 0 & 54 \\ -13l & -3l^2 & 0 & 8l^2 & 13l \\ 0 & 0 & 54 & 13l & 156 \end{bmatrix} \quad 4.21$$

Reduced matrices for simply supported simply supported 3 element beam are given by

$$[K] = \frac{EI}{l^3} \begin{bmatrix} 4l^2 & -6l & 2l^2 & 0 & 0 & 0 \\ -6l & 24 & 0 & -12 & 6l & 0 \\ 2l^2 & 0 & 8l^2 & -6l & 2l^2 & 0 \\ 0 & -12 & -6l & 24 & 0 & -12 \\ 0 & 6l & 2l^2 & 0 & 8l^2 & -6l \\ 0 & 0 & 0 & -12 & -6l & 12 \end{bmatrix} \quad 4.22$$

$$[M] = \frac{ml}{420} \begin{bmatrix} 4l^2 & 13l & -3l^2 & 0 & 0 & 0 \\ 13l & 312 & 0 & 54 & -13l & 0 \\ -3l^2 & 0 & 8l^2 & 13l & -3l^2 & 0 \\ 0 & 54 & 13l & 312 & 0 & -13l \\ 0 & -13l & -3l^2 & 0 & 8l^2 & -3l^2 \\ 0 & 0 & 0 & -13l & -3l^2 & 4l^2 \end{bmatrix} \quad 4.23$$

4.5 Determination of natural frequencies & mode shapes.

Assuming the solution for $\{w_0(t)\}$ as $\{W_0\}e^{i\omega t}$, the equation 4.15 is simplified as

$$-\omega^2 [M]\{W_0\} + [K]\{W_0\} = 0 \quad 4.24$$

$$\text{or } [-\omega^2 [M] + [K]]\{W_0\} = 0 \quad 4.24(a)$$

The above equation is an eigen value problem. The characteristic determinant is obtained as

$$|[D] - \lambda[I]| = 0 \quad 4.25$$

Where $[D] = \text{Dynamic matrix} = [M]^{-1} [K]$ and $[I] = \text{Identity matrix}$

Expansion of the above determinant leads to a polynomial of order 'n'. By solving polynomial equation, eigen values λ_i and eigen vectors are obtained. The i^{th} Natural frequency is given by

$$\omega_i = \sqrt{\lambda_i}$$

Eigen vectors of equation 4.25 corresponding to respective eigen values are plotted to determine mode shapes.

4.6 Determination of damping factor

As stated in the previous chapter the nature of interfacial pressure variation along the beam layer and its magnitude is dependent on thickness ratio. By summing up the pressure over influencing zone, the net normal force 'N' under each rivet is calculated (equation 3.31). The maximum frictional force is found as

$$F_{rM} = \mu N \quad 4.26$$

When the beam is excited at its mid span, relative motion takes place at the contacting faces to generate the desirable damping. The relative dynamic slip under a connecting rivet is written as

$$u_r(x, t) = \alpha'(h_1 + h_2) \frac{\partial w(x, t)}{\partial x} = \alpha'(h_1 + h_2) \left[\frac{ds}{dx} \right] \{w(t)\} \quad 4.27$$

The magnitude of slip under one rivet differs from another due to their varying slope which depends on location of rivet along the beam length. Considering the effect of all rivets maximum dynamic slip for all considered boundary conditions is given by

$$u_{rM} = \alpha' (h_1 + h_2) Y \quad 4.28$$

$$\text{where } Y = \sum_{i=1}^q \frac{ds}{dx} \{w^i(t)\} \quad 4.29$$

and q = Total number of rivets

Energy loss per cycle of vibration is given by

$$E_f = 2 \alpha' \mu N (h_1 + h_2) Y \quad 4.30$$

The energy stored per cycle of motion is given by

$$E_n = \frac{1}{2} [d^T] [K_0] [d] \quad 4.31$$

The damping capacity in terms of damping factor can be written as

$$\zeta = \frac{\delta}{2\pi} = \frac{E_f}{4\pi E_n} = \frac{\alpha' \mu N (h_1 + h_2) Y}{\pi [d]^T [K_0] [d]} \quad 4.32$$

For equally thick layer, $h_1 = h_2 = h$

$$\zeta = \frac{2\alpha'\mu NhY}{\pi[d]^T [K_0][d]} \quad 4.33$$

Many times for higher damping, multilayered beams are used in engineering applications. For a structure consisting of 'm' number of equally thick beam layers, the damping factor is evaluated as

$$\zeta = \frac{2(m-1)\alpha'\mu NhY}{\pi[d]^T [K_0][d]} \quad 4.34$$

4.7 Chapter summary

In the present chapter, finite element analysis has been carried out to determine natural frequencies, mode shapes and damping factor of rivet jointed layered structures. The whole beam structure is discretized into a number of finite elements and for each element, mass or inertia matrix and stiffness matrix are evaluated using strain energy, kinetic energy and Lagrange's equation of motion. Overall and reduced mass and stiffness matrices are derived by using appropriate boundary conditions. Number of discretizations has been decided by using convergence of results. The damping property of the jointed beam has been defined in terms of damping factor and log decrement which can be determined theoretically as well as experimentally.

5. Experimental Study

5.1 Introduction

As stated in earlier chapters, the dynamics and damping of built up structures depend on material and geometrical parameters, surface features, boundary conditions and a number of related factors. Classical and finite element methods are based on certain assumptions to simplify the analysis. Therefore, it is necessary to authenticate theoretical predictions by conducting tests. The objective of the present experimental work is to determine dynamic characteristics such as natural frequencies, normal modes and damping properties like damping factor by half power bandwidth method. Experimental details such as preparation of test specimens, development of experimental procedures, observations made and comparison of results with theoretical values are described in this chapter.

5.2 Preparation of test specimens

The riveted thin beam composite specimens are of mild steel and aluminum with different dimensions. These are prepared from the same stock of flats available in the market and presented in Table 5.1. Rivets of different diameters shown in the Table 5.1 are used to join the two layered specimens and are equispaced along the length of beam. Rivet pitch has been chosen such that clashing of influence zones under consecutive rivet heads is avoided. The width and length of the specimens are selected considering diameter of rivet and thickness ratio of beams with respect to the zone of influence. For thickness ratios of 1.0, 1.5 and 2.0, the centre distance between two adjacent rivets of specimens are taken as 4.125, 5.0 and 5.6 times the rivet diameter respectively as per zone of influence proposed in the theory. The length of the specimens is varied accordingly to connect with different number of rivets.

Table 5.1 Specification of specimens used for analysis

SL No.	Length	Width	No of	Thickness of	No of	Dia of	Material
	(mm)	(mm)	layers	layers (mm)	rivets	rivets(mm)	
1	370	41.25	2	3+3	6	8	MS
2	430	41.25	2	3+3	6	8	MS
3	500	41.25	2	3+3	6	8	MS
4	430	41.25	2	2.4+3.6	6	8	MS
5	430	41.25	2	2+4	6	8	MS
6	500	41.25	2	3+3	6	6	MS
7	500	41.25	2	3+3	6	10	MS
8	370	41.25	2	3+3	4	8	MS
9	370	41.25	2	3+3	8	8	MS
10	430	41.25	3	2+2+2	6	8	MS
11	430	41.25	4	1.5+1.5+1.5+1.5	6	8	MS
12	370	41.25	2	3+3	6	8	Al
13	430	41.25	2	3+3	6	8	Al
14	500	41.25	2	3+3	6	8	Al
15	430	41.25	2	2.4+3.6	6	8	Al
16	430	41.25	2	2+4	6	8	Al
17	500	41.25	2	3+3	6	6	Al
18	500	41.25	2	3+3	6	10	Al
19	370	41.25	2	3+3	4	8	Al
20	370	41.25	2	3+3	8	8	Al
21	430	41.25	3	2+2+2	6	8	Al
22	430	41.25	4	1.5+1.5+1.5+1.5	6	8	Al



Figure 5.1 Photograph of the thin riveted mild steel specimens

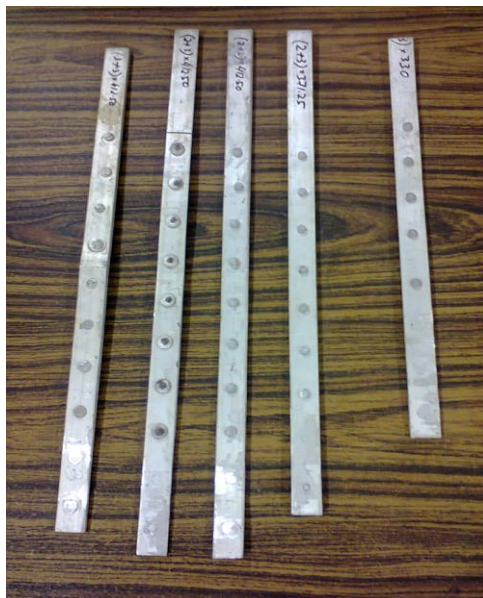


Figure 5.2 Photograph of the thin riveted aluminium specimens

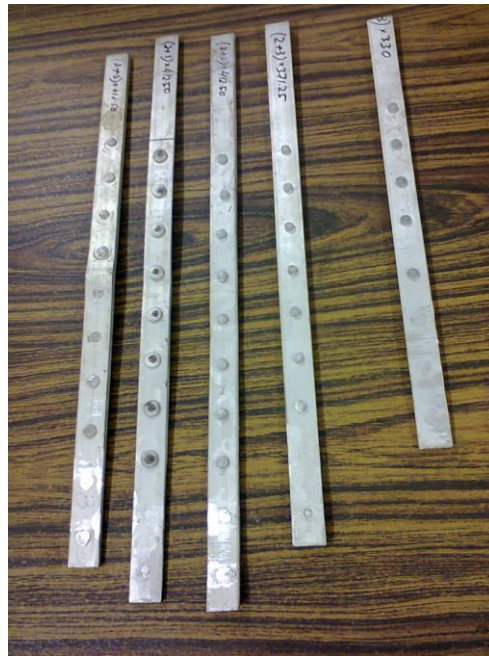


Figure 5.3 Photograph of the thin riveted aluminium specimens



Figure 5.4 Photograph of the riveted mild steel specimens

The interfaces of the specimens are cleaned, degreased and polished before connecting them with rivets. The rivet used has a cylindrical shank with a button type head and power riveting has been employed to make the joint. The heated rivet is entered into the hole and a head is formed on the blunt end with pneumatic pressure using a die. The shank is compressed till it fills the rivet hole fully. On cooling, the rivet produces a clamping force between the connecting members.

5.3 Description of the Experimental Set-up

The setup comprises of a welded frame work fabricated from steel channel sections grooved to a heavy and rigid concrete pedestal by means of anchoring bolts. The frame work has the provision to accommodate the beams of varying length using its slotted guide ways and to hold the fixed and simply supported ends of the beam specimens. The clamping is produced by using a vice which works on the screw jack mechanism consisting of a spindle and base plate with external and internal treading respectively. A lever is attached at the tip of spindle and its rotation moves the spindle axially downward imparting the necessary clamping force to the base plate. As a result, the specimen is held rigidly at its ends. The base plate prevents the specimen from rotating while applying the necessary clamping force. A spring mounted exciter is used to impart vibration at the midpoint of the specimens with controlled amplitudes. The use of spring in the exciter ensures zero initial velocity of the specimen at the time of excitation. It is attached with a dial gauge which is calibrated to read the initial amplitudes of vibration. The dial gauge is clamped to a vertical stand with a magnetic pedestal.

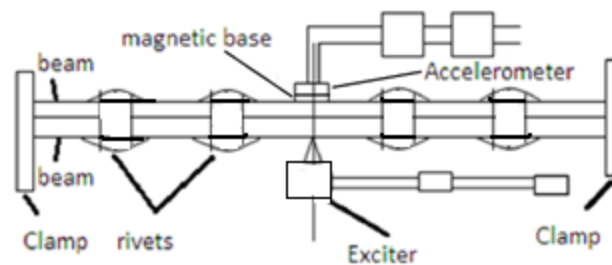


Figure 5.5 Schematic layout of the specimen in the set-up

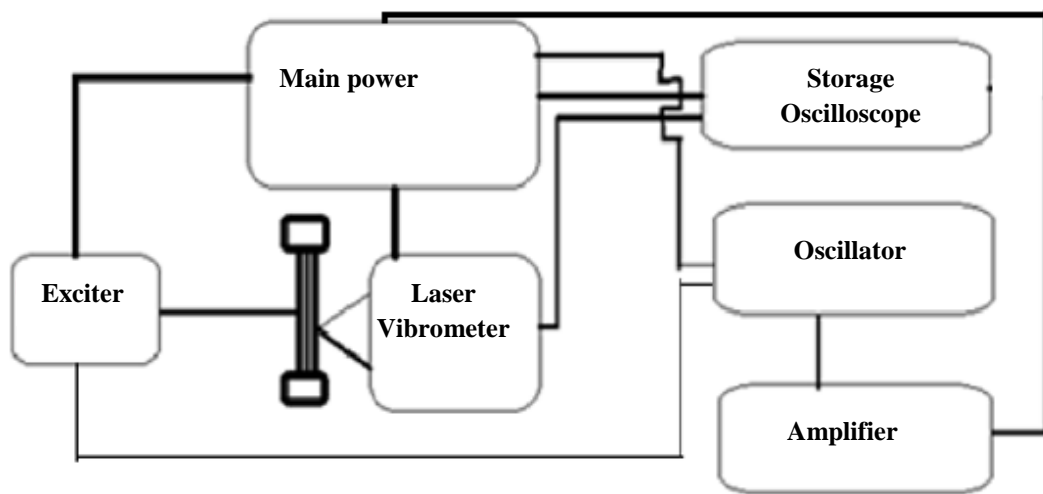


Figure 5.6 Schematic diagram of experimental setup

The instruments used in experimental set up are accelerometer, vibration pick up, dial gauge, digital storage oscilloscope, laser vibrometer, oscillator, exciter and amplifier. The operational features and the specification of the equipments are described below. Digital storage oscilloscope is used for processing and display of vibration signals. It consists of a display screen, input connectors, control knobs and bottoms on the front panel. The signal which is to be measured is fed to one of the connectors. In the display screen, a two dimensional graph of the time history curve is plotted.



Figure 5.7 Amplifier



Figure 5.8 Exciter



Figure 5.9 Oscillator



Figure 5.10 Ometron LASER vibrometer back view



Figure 5.11 Ometron LASER vibrometer with tripod



Figure 5.12 Dial gauge



Figure 5.13 Setup view for clamping beams at



Figure 5.14 DPO 4000 series oscilloscope.

Specifications:

Input voltage 100 V to 240 V $\pm 10\%$

- Input power frequency: 47 Hz to 66 Hz (100 v to 240 V)
- 400 HZ (100 V to 132 V)
- Power consumptions: 250 W maximum
- Weight: 5 kg.
- Clearance: 51 mm
- Operating temperature: 0 to 50⁰C.
- High operating humidity: 40 to 50⁰C 10 to 60% RTT
- Low operating humidty: 0 to 40⁰C 10 to 90% RTT

The accelerometer is a transducer changing mechanical quantities i.e. displacement, velocity or acceleration into varying electrical quantities i.e. voltage or current. One end

of the accelerometer is fixed magnetically to the vibrating surface and the other end is connected to one of the connectors of the oscilloscope. The accelerometer used is of contact type. The dial gauge is attached to a stand with a magnetic base and is of high precision range shock proof device to measure amplitude in the range of 0.01 to 10 mm. A distributor box is connected to 200-240 V power source and supplied AC power to storage oscilloscope with a voltage of 230 V at a frequency of 50 HZ.

The Surtronic 3+ surface measuring instrument is used for measuring roughness of mild steel and aluminum specimens.

Laser Vibrometer

The Scanning Laser Vibrometer or Scanning Laser Doppler Vibrometer is an instrument for rapid non-contact measurement and imaging of vibration.

Fields where they are applied include automotive, medical, aerospace, micro system and information technology as well as for quality and production control. The optimization of vibration and acoustic behavior are important goals of product development in all of these fields because they are often among the key characteristics that determine a product's success in the market. They are also in widespread use throughout many universities conducting basic and applied research in areas that include structural dynamics, modal analysis, acoustic optimization and non-destructive evaluation.

The operating principle is based on the Doppler effect, which occurs when light is back-scattered from a vibrating surface. Both velocity and displacement can be determined by analyzing the optical signals in different ways. A scanning laser vibrometer integrates computer-controlled X,Y scanning mirrors and a video camera inside an optical head. The laser is scanned point-by-point over the test object's surface to provide a large number of very high spatial resolution measurements. This sequentially measured vibration data can be used to calculate and visualize animated deflection shapes in the relevant frequency bands from frequency domain analysis. Alternatively, data can be acquired in the time domain to for example generate animations showing wave propagation across structures. In contrast to contact measuring methods, the test object is unaffected by the vibration measuring process.



Fig 5.15 Ometron Laser vibrometer lens view

5.4 Testing procedure

The schematic layout of the specimen in the experimental setup and the block diagram of equipments used for the test are shown in figure 5.5 and figure 5.6 respectively. The electro dynamic vibrator used for providing forced excitation to the specimen is driven by an oscillator cum amplifier. The inductance pick-up and accelerometer connected to storage oscilloscope are used to store time history curve of the response. Initially, elasticity modulus and static flexural stiffness of the specimen are measured by conducting static deflection tests. Thereafter, vibration level is changed by varying the frequency of excitation. Frequency response curve is plotted by noting the observations and damping factor is determined by using bandwidth method.

5.4.1 Measurement of elasticity modulus (E)

Few samples of solid beams were selected from the same block of mild steel and aluminum flats. These were mounted on the experimental setup and fixed at the ends by using screw clamps. Static loads (W) were applied at the midpoints and corresponding deflections at mid point along length of beam are recorded. Elasticity modulus was determined by using the relation $E = \frac{Wl^3}{192I\delta}$, where l , I , δ are length, moment of inertia and deflection of beam respectively. The average of five reading was found and measured values of E are given Table 5.5.

Table 5.5 Elastic modulus of materials used.

Material	E(GPa)
Mild steel	196
Aluminium	67.6

5.4.2 Measurement of Static bending stiffness (K)

The same static deflection tasks as used in case of elasticity modulus are conducted to measure the actual stiffness K of a jointed specimen using the relation, $K = W/\delta$. The bending stiffness of an identical solid fixed fixed beam is theoretically calculated from the expression $K' = 192EI/l^3$.

5.4.3 Measurement of modal frequencies

The specimens are mounted on the setup as per the required boundary conditions and are subjected to excitations by using the vibrator. Voltage signals obtained through the accelerometer are displayed in the screen of oscilloscope by varying the frequency of execution by the oscillator amplitude values against the recorded frequency. Modal frequencies corresponding to maximum amplitude are found. The accelerometer locations along the length of specimen varied for a particular modal frequency and the amplitude for various points of beam are noted and modal displacement curves are plotted.

5.4.4 Measurement of logarithmic decrement ‘ δ ’

The specimens used for testing were mounted successively on the setup. A spring operated exciter was used to excite the specimen at the mid points along the length of the specimen. The beam specimen was initially deflected and released to vibrate at its first mode. The response of the beam was sensed by a contacting type accelerometer attached at its mid point. One end of accelerometer was held magnetically to the vibrating surface and the other is connected to one of the connectors of the storage oscilloscope. The accelerometer output which is proportional to the square of frequency and amplitude of vibration was displayed on the oscilloscope for storage and processing. The data was then analyzed to determine logarithmic decrement. The attenuated response curve obtained from the oscilloscope was used to measure log decrement δ by using the expression

$$\delta = \ln (x_i/x_{i+z})/z$$

where x_i and x_{i+z} and z are the recorded values of amplitudes of the first cycle, last cycle and number of cycles respectively. Each test was repeated five times and the average value was determined.

5.4.5 Measurement of damping factor ‘ ζ ’

The set of specimens which were used for finding their elasticity modulus, flexural stiffness were mounted on the experimental set up to determine their damping factor. For

three separate boundary conditions, i.e. fixed -fixed, fixed-simply supported and simply supported -simply supported end conditions were tested. A spring loaded device called exciter is used to excite the specimens. The excitation is applied for a range of mid point amplitude of beam varying from 0.1 to 0.3 mm. In steps of 0.1 mm, the beam response is sensed by laser vibrometer by focusing the laser beam of light to the point under consideration. The signals are then passed on to the oscilloscope. The variation of response with frequency was plotted as frequency response curve. The range of frequencies is determined having response equal to 0.707 times resonant amplitude.

Using the expression, $\zeta = \frac{\omega_2 - \omega_1}{2\omega_n}$, damping factor is determined for various specimens.

Each test during experiment is repeated several times and the average value is obtained for accuracy in measurement. Thereafter, the boundary condition is changed and the experiments are conducted for another set of results.

While designing the experimental setup, energy loss due to support friction, air drag, connecting wires, accelerometer mountings, etc. are neglected. The specimens were prepared with proper care and the surface was maintained flat for perfect contact at the interfaces, to achieve identical pressure distribution under each rivet. While fixing the specimen for testing, adequate clamping was provided to ensure the desired boundary condition and reduce effect on damping. All the factors were considered during testing for minimizing the errors.

5.5 Experimental determination of α' μ

The dynamic slip ratio (α') and coefficient of friction (μ) are to be correctly assessed for determining energy dissipated. It is known that these factors are inversely proportional to each other and their product is constant. Thus, it is desirable to determine $\alpha' \mu$ as a single quantity. After evaluating ζ , $\alpha' \mu$ has been determined by using equation 3.43. α' and μ depends on frequency of excitation and amplitude of vibration. The product $\alpha' \mu$ increases with increase in frequency and decreases with increase in amplitude and have been obtained by extrapolating the results given in [155].

5.6 Comparative study of experimental and theoretical results

Theoretical analysis explained in chapters 3 and 4 are broadly based on assumptions as stated in introductory chapter. Dynamic and damping characteristics may, therefore differ from their true values. Experimental investigation has been performed to verify theoretical results. The structural specifications of the specimens such as length, width, thickness and number of layers, number and diameter of rivets and material has been presented in table 5.1. Experimental results for these specimens and corresponding theoretical values have been presented in graphical forms in figure 5.19 to figure 5.64. Comparison of the characteristics for various boundary conditions and for various methods of analysis has been shown graphically.

5.6.1 Experimental and theoretical comparison of damping factor for aluminium specimens

The variation of damping factor with length is shown in figure 5.19 to figure 5.22 and that with diameter of rivets in figure 5.27 to figure 5.30. Moreover variation of damping factor with thickness ratios, number of layers and number of rivets are shown in figures 5.35- 5.38, figure 5.43 and figures 5.51-5.54 respectively. It may be observed from the graphs that the theoretical values differ by 3% to 8% from the experimental values.

5.6.2 Experimental and theoretical comparison of damping factor for mild steel specimens

Figures 5.23-5.26 show the variation of damping factor with length and figures 5.31-5.34 show variation of damping factor with diameter of rivets. In addition effects of thickness ratio, number of layers and number of rivets on damping factor are shown in figure 5.39- 5.42 figure 5.44 and figures 5.55-5.58 respectively. The variation in damping factor in all these theoretical cases is within 6% of the experimental values.

5.6.3 Experimental and theoretical comparison of modal frequencies and mode shapes for aluminium specimens

The variation of 1st, 2nd and 3rd modal frequencies with length is shown in figures 5.42-5.44 respectively. Corresponding mode shapes for fixed- fixed, fixed- simply supported and simply supported- simply supported configurations are shown in figure 5.56, figure 5.58 and figure 5.60. There is a discrepancy of 4.5 % between theoretical and experimental values. Modal patterns as obtained by theoretical and experimental methods are found to be in good agreement.

5.6.4 Experimental and theoretical comparison of modal frequencies and mode shapes for mild steel specimens

The variation of 1st, 2nd and 3rd modal frequencies with length is shown in figures 5.45-5.47 respectively. Corresponding mode shapes for fixed fixed, fixed simply supported and simply supported simply supported configurations are shown in figure 5.57, figure 5.59 and figure 5.61. There is a discrepancy of 4 % between theoretical and experimental values. Modal patterns as obtained by theoretical and experimental methods are found to be in good agreement.

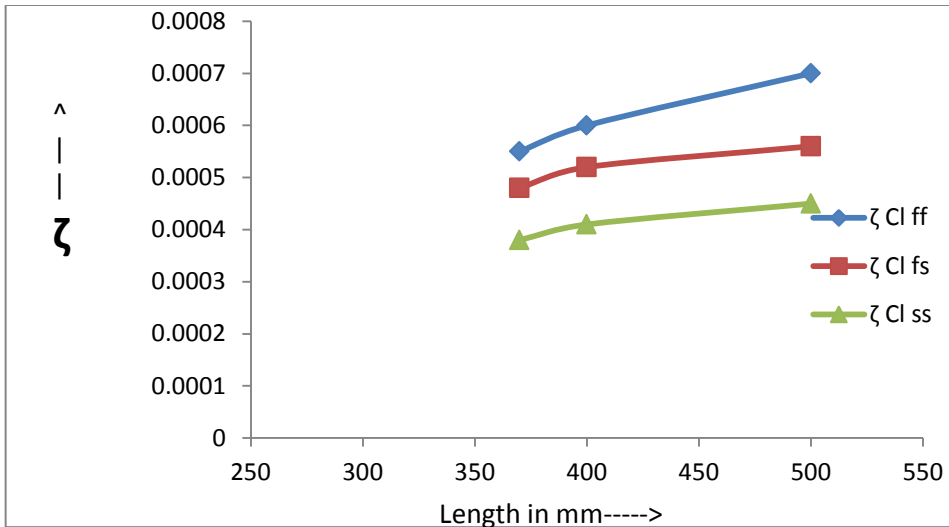


Figure 5.16 Effect of length on damping factor for aluminium specimen using classical method.

Cl: classical, **FEM:** Finite element method, **Exp:** Experimental, **ff:** fixed fixed, **fs:** fixed simply supported, **ss:** simply supported simply supported for all figures.

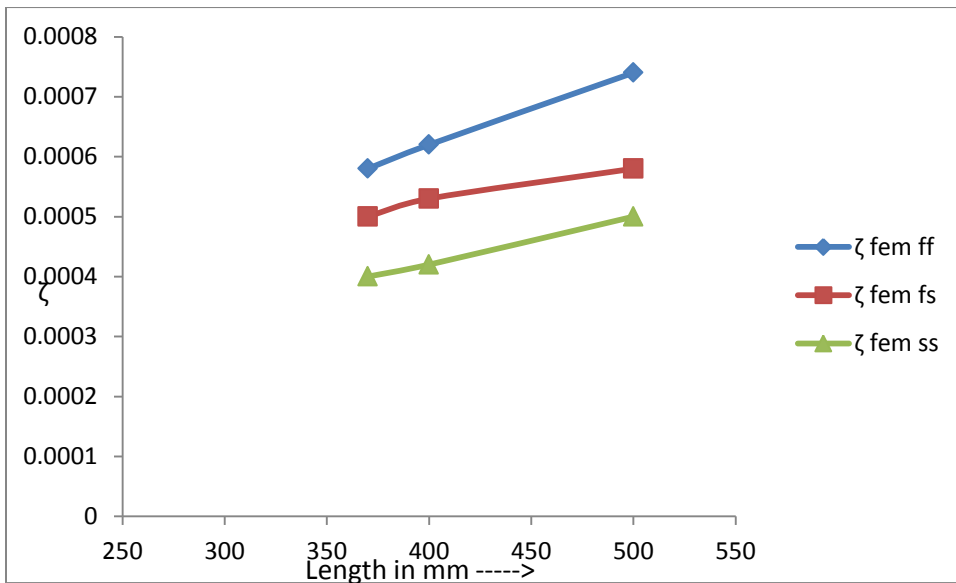


Figure 5.17 Effect of length on damping factor for Aluminium specimen using Finite Element method.

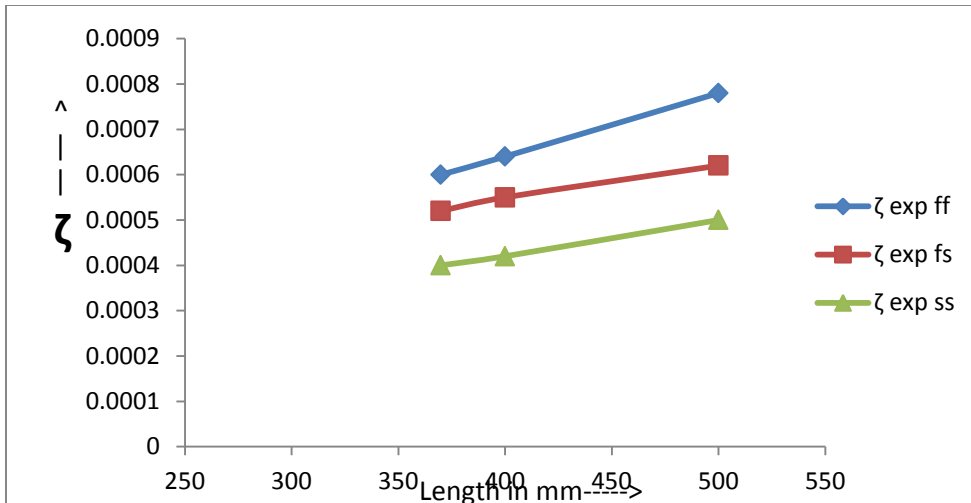


Figure 5.18 Effect of length on damping factor for aluminium specimen using experimental method.

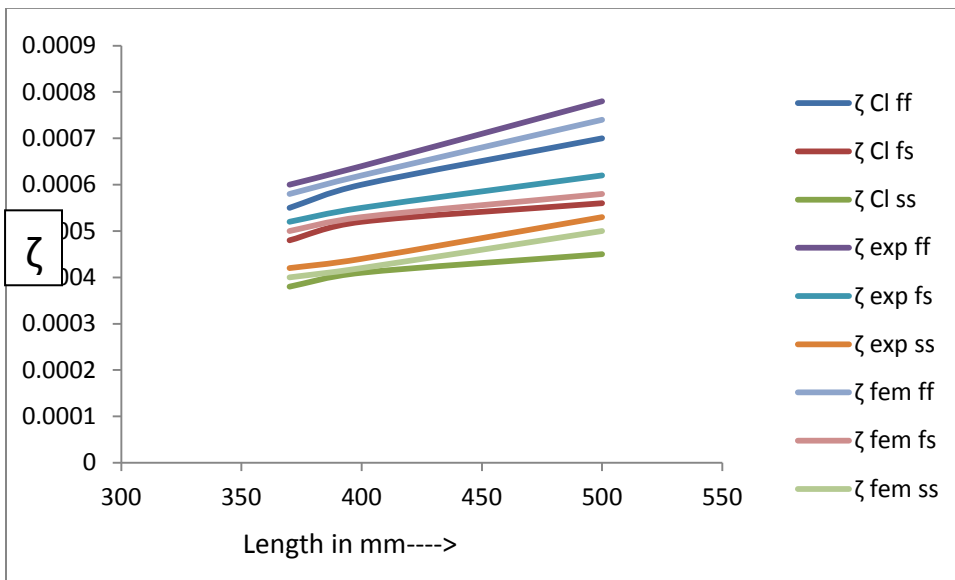


Figure 5.19 Comparison of effect of length parameter on damping factor for Aluminium specimen using all methods.

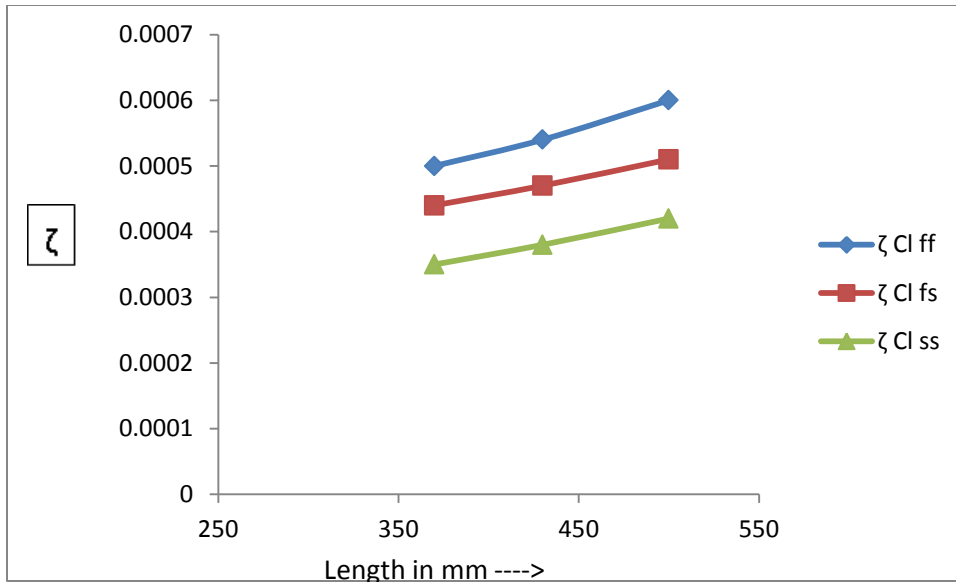


Figure 5.20 Effect of length on damping factor for Mild steel specimen using classical method.

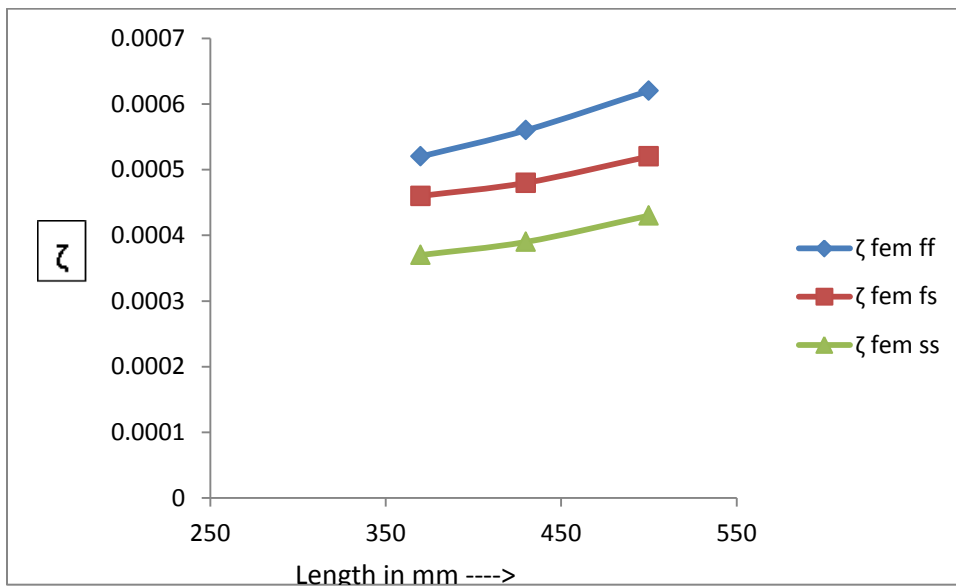


Figure 5.21 Effect of length on damping factor for Mild steel specimen using Finite Element method.

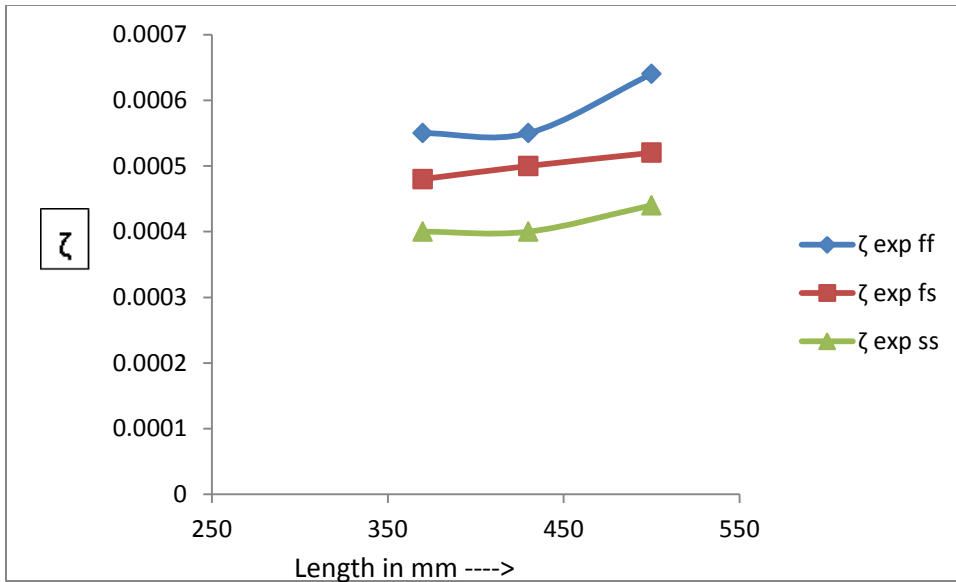


Figure 5.22 Effect of length on damping factor for Mild steel specimen using Experimental method.

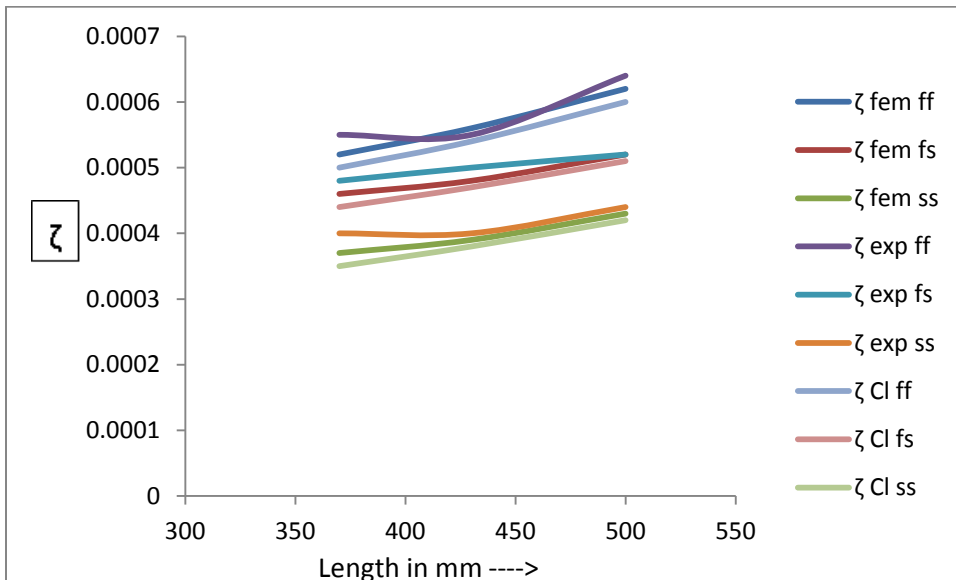


Figure 5.23 Comparison of effect of length parameter on damping factor for Mild steel specimen.

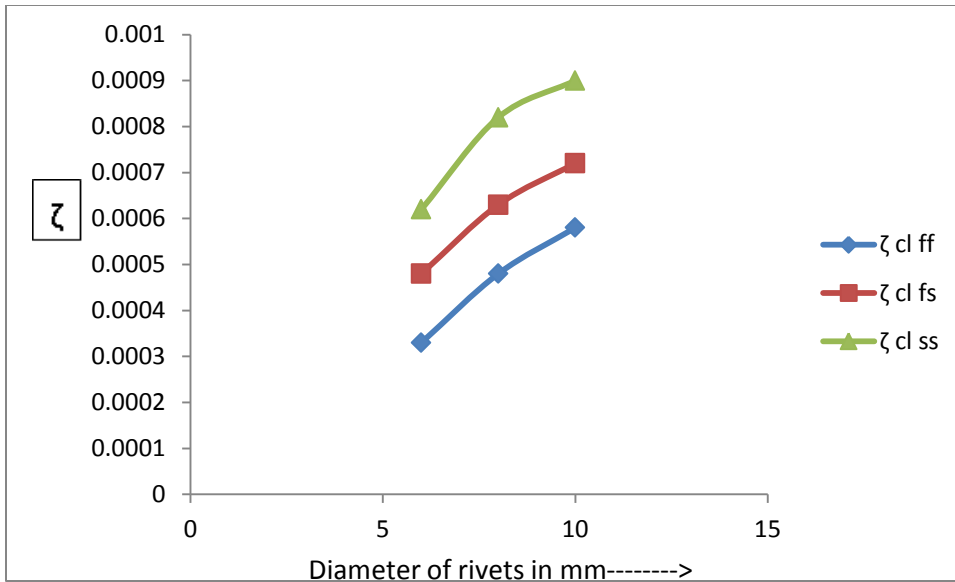


Figure 5.24 Effect of diameter of rivets on damping factor for Aluminium specimen using classical method.

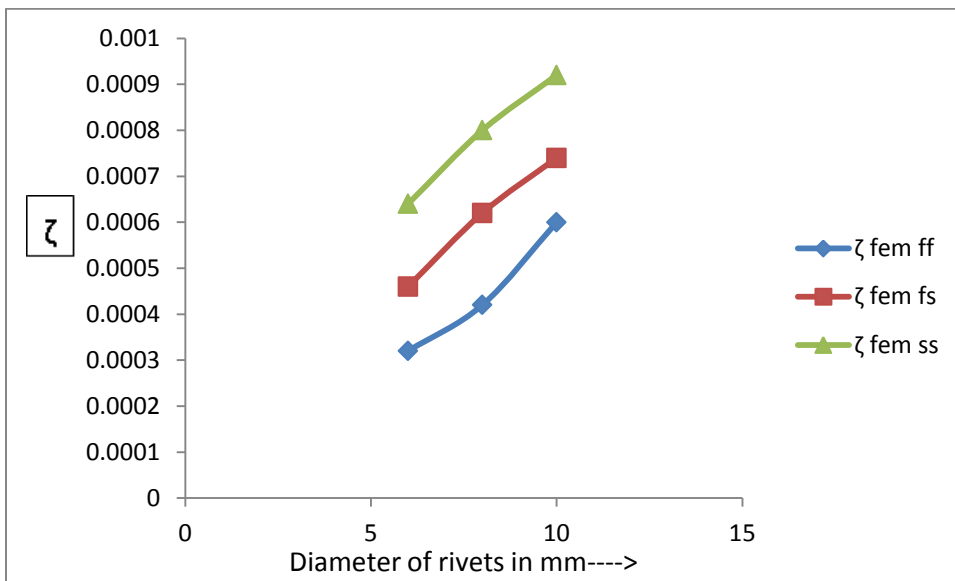


Figure 5.25 Effect of diameter of rivets on damping factor for Aluminium specimen using Finite Element method.

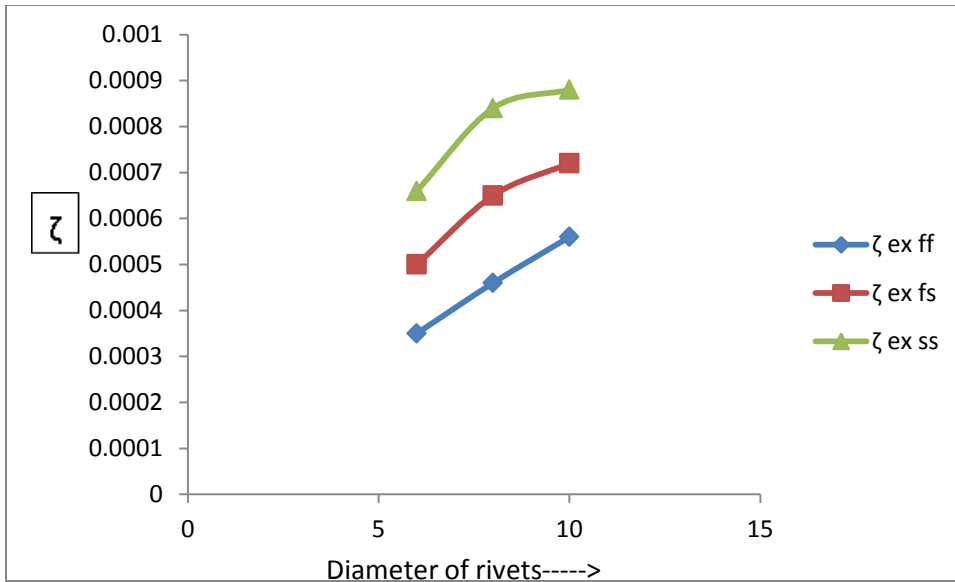


Figure 5.26 Effect of diameter of rivets on damping factor for Aluminium specimen using Experimental method.

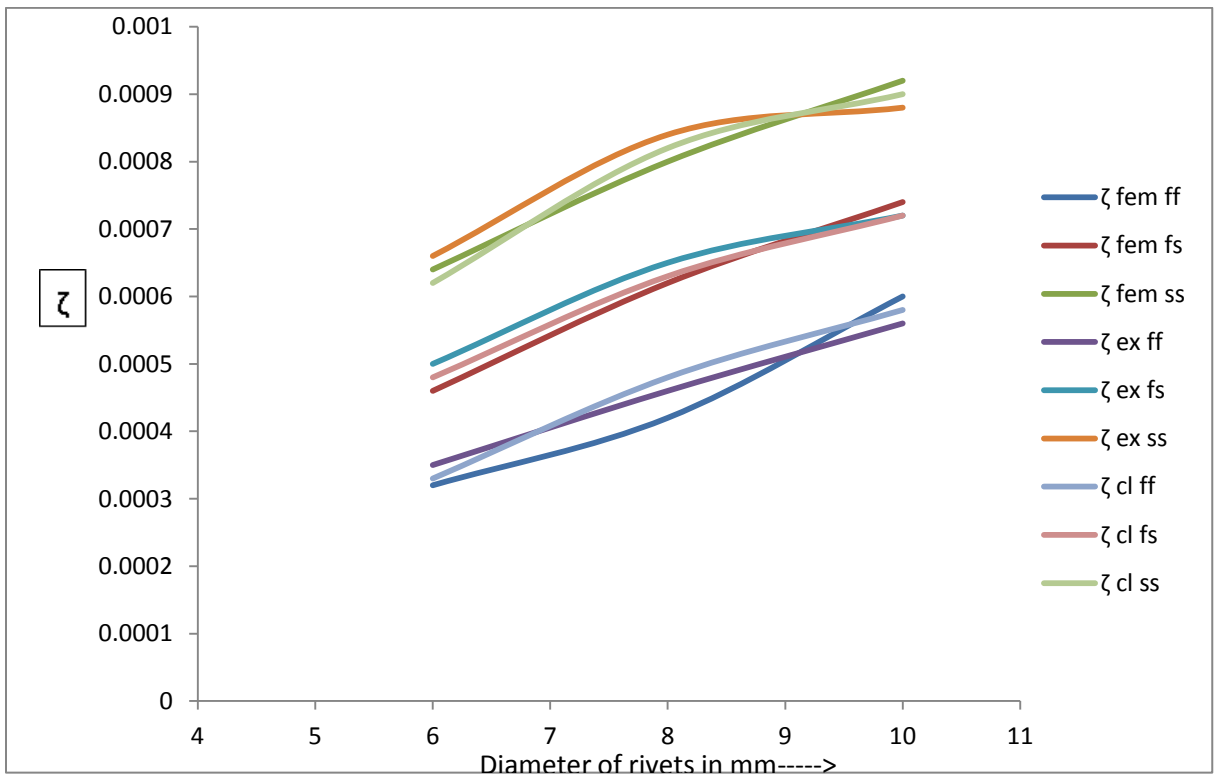


Figure 5.27 Comparison of effect of diameter of rivets on damping factor for Aluminium specimen using all methods.

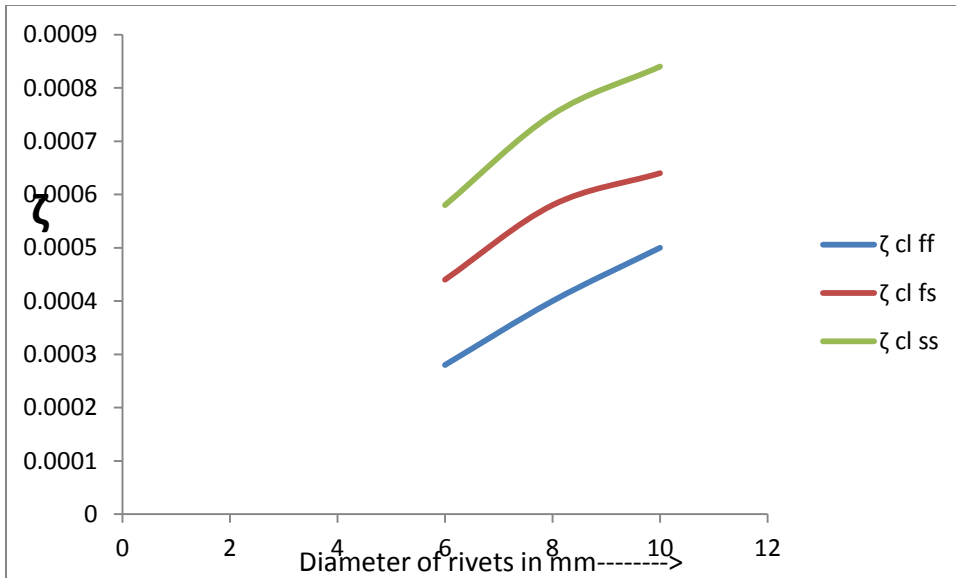


Figure 5.28 Effect of diameter of rivets on damping factor for Mild steel specimen using classical method.

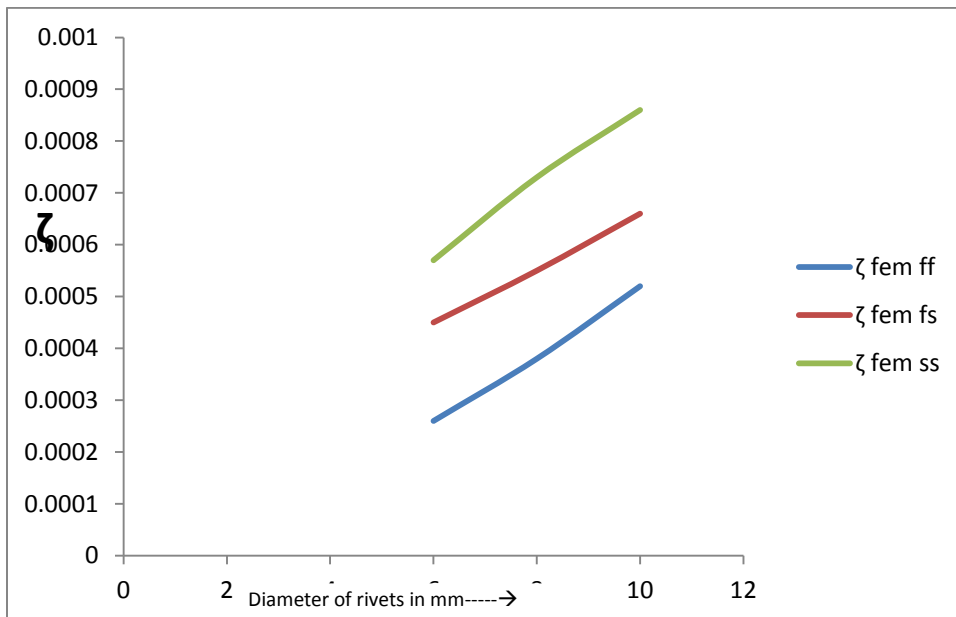


Figure 5.29 Effect of diameter of rivets on damping factor for Mild steel specimen using Finite element method.

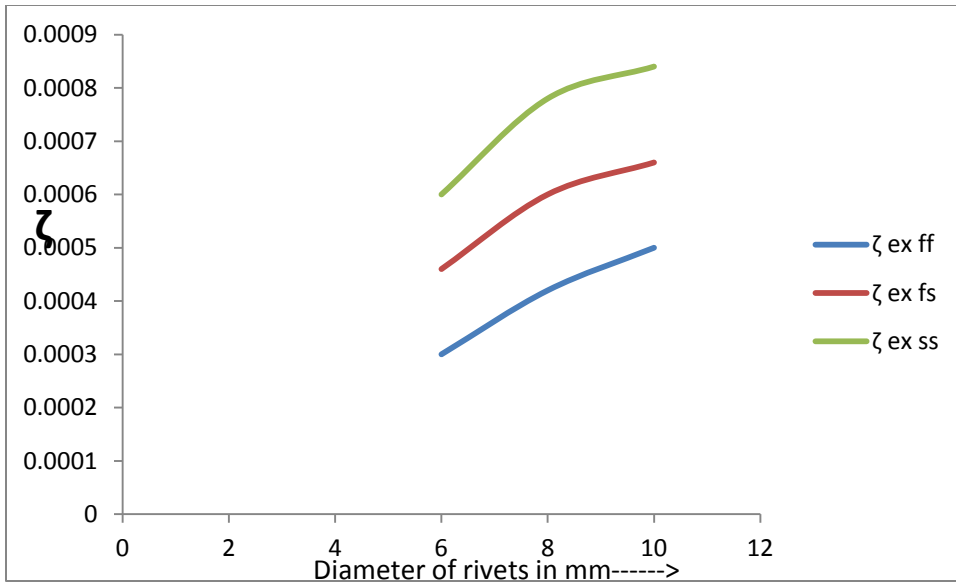


Figure 5.30 Effect of diameter of rivets on damping factor for Mild steel specimen using experimental method.

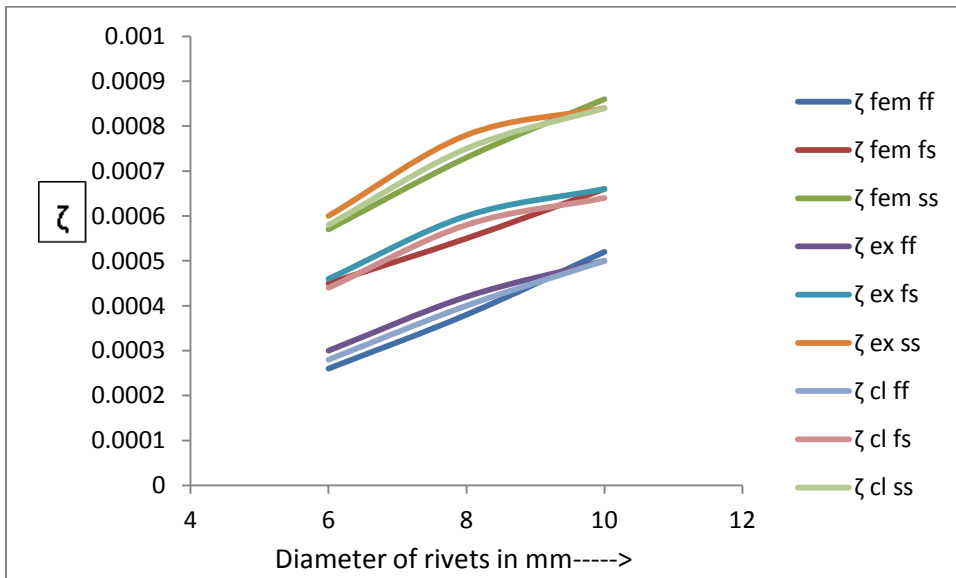


Figure 5.31 Comparison of effect of diameter of rivets on damping factor for Mild steel specimen using all methods.

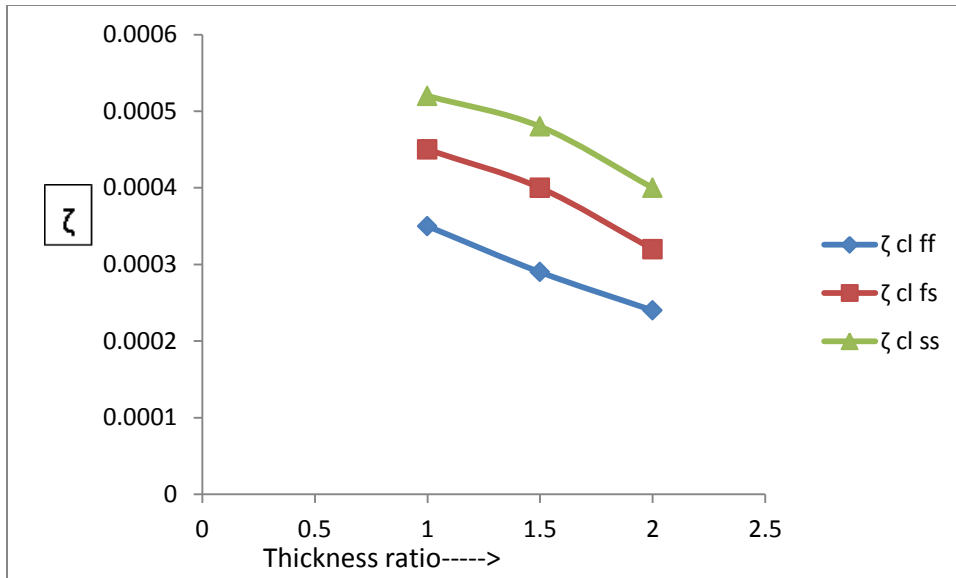


Figure 5.32 Effect of thickness ratio of beams on damping factor for Aluminium specimen using classical method.

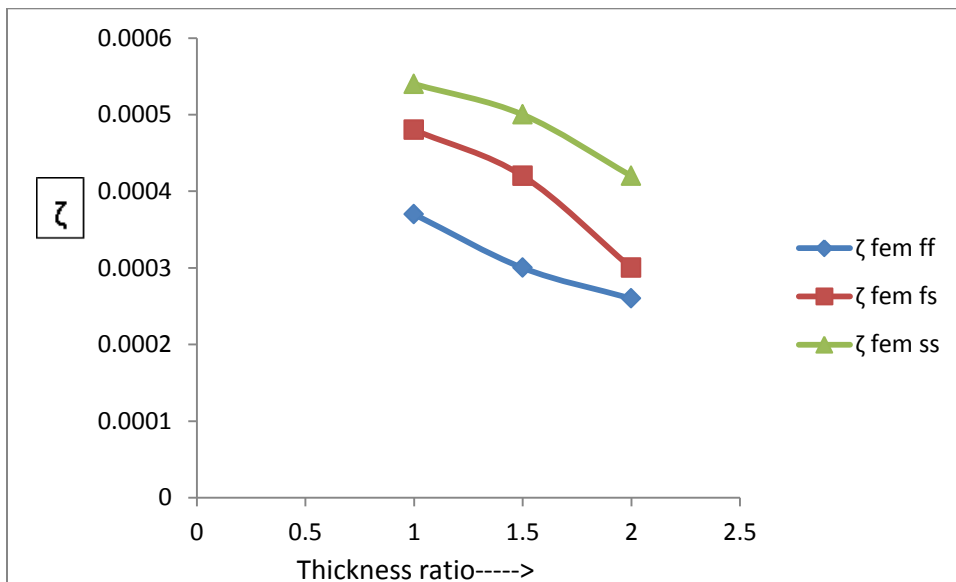


Figure 5.33 Effect of thickness ratio of beams on damping factor for aluminium specimen using Finite element method.

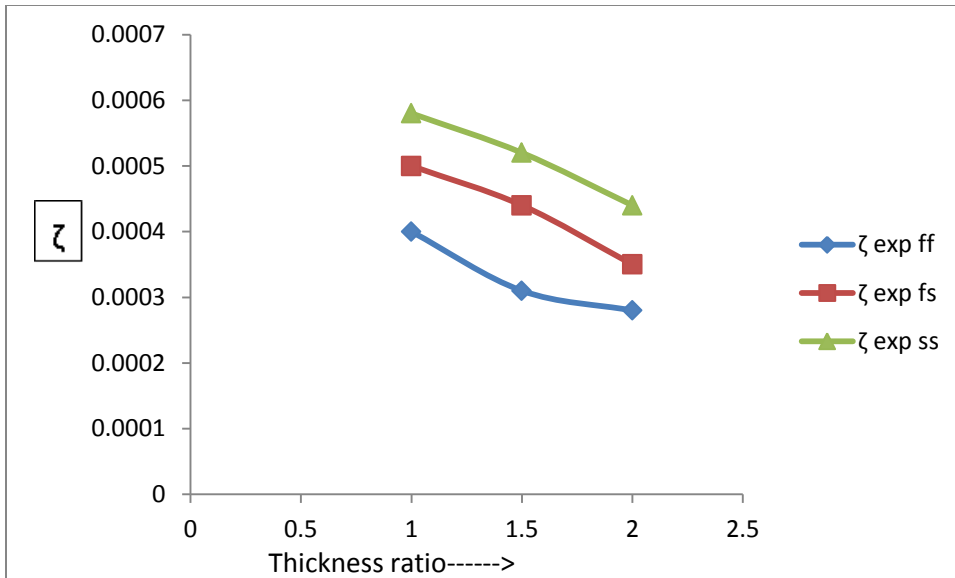


Figure 5.34 Effect of thickness ratio of beams on damping factor for aluminium specimen using experimental method.

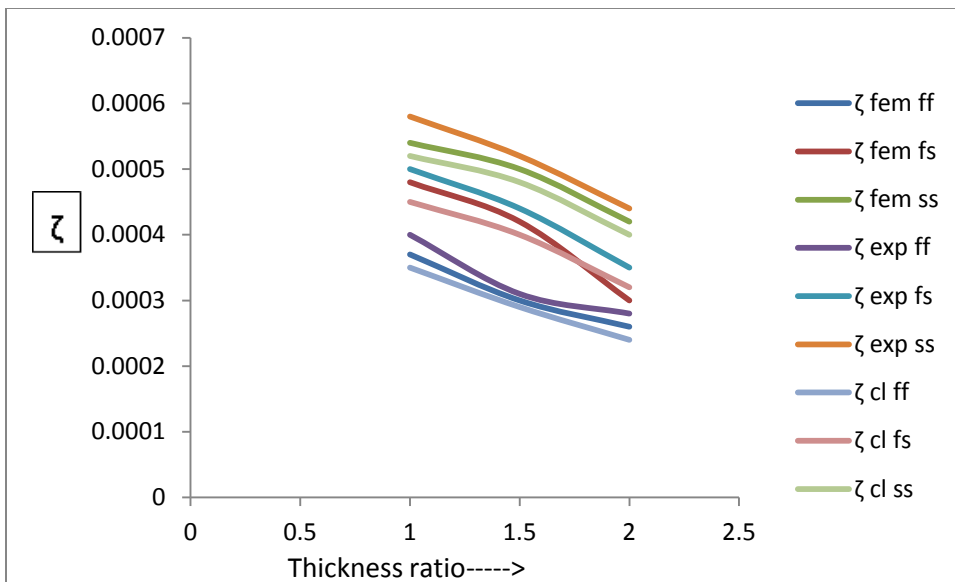


Figure 5.35 Comparison of effect of thickness ratio of beams on damping factor for aluminium specimen using all methods.

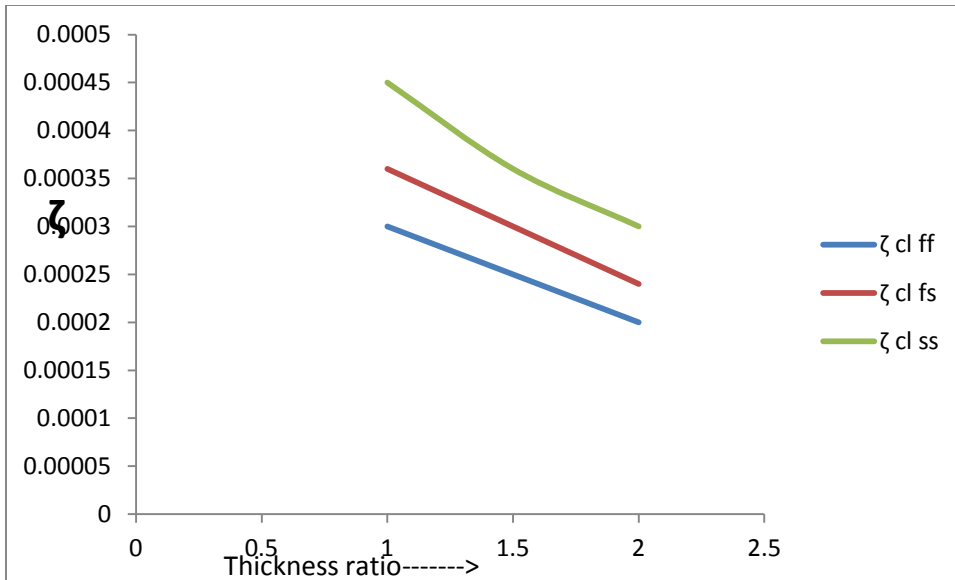


Figure 5.36 Effect of thickness ratio of beams on damping factor for mild steel specimen using classical method.

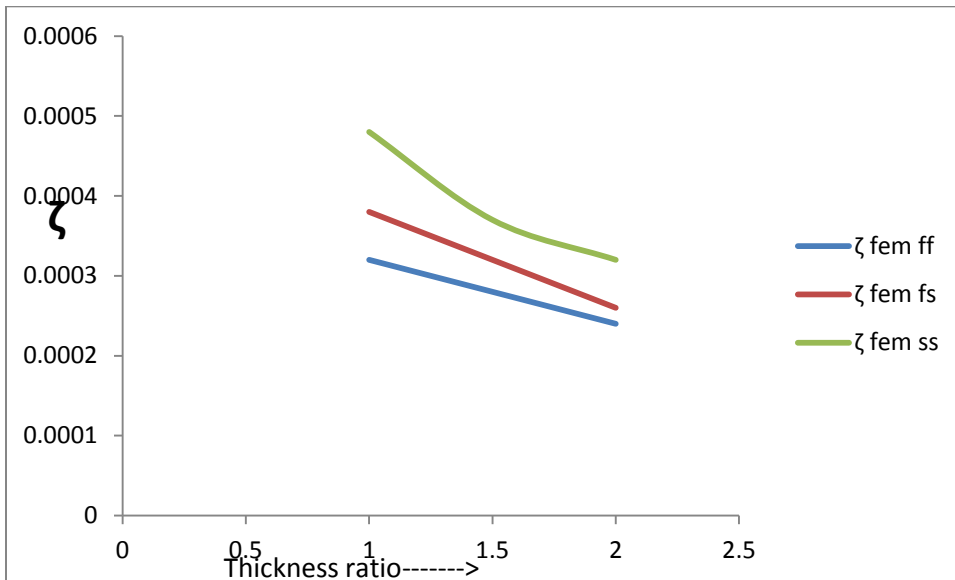


Figure 5.37 Effect of thickness ratio of beams on damping factor for mild steel specimen using finite element method.

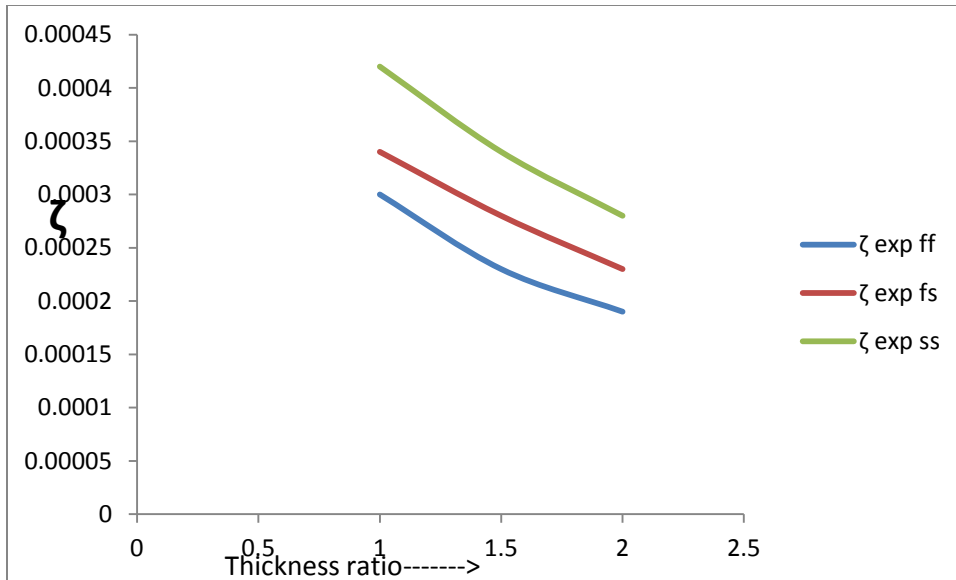


Figure 5.38 Effect of thickness ratio of beams on damping factor for mild steel specimen using classical method.

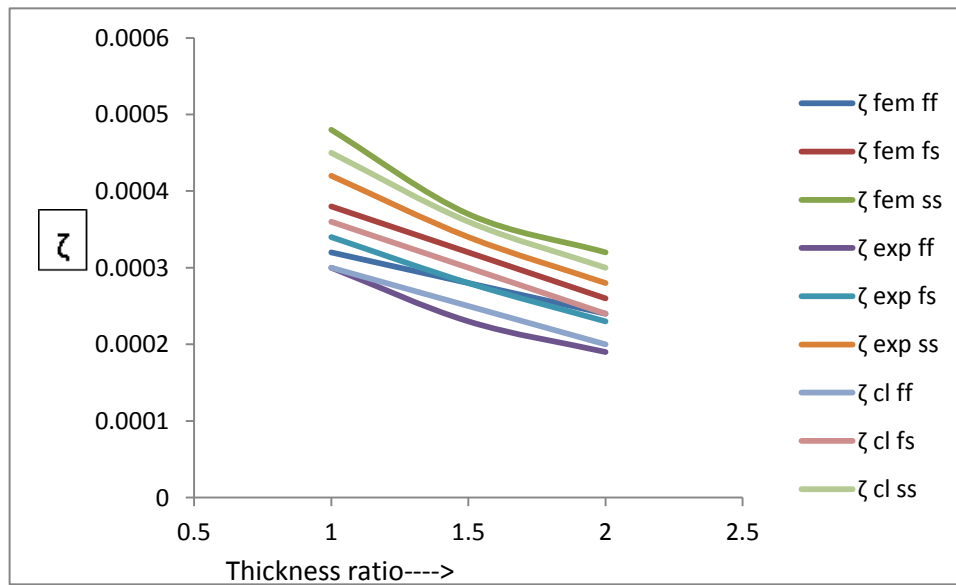


Figure 5.39 Comparison of effect of thickness ratio of beams on damping factor for mild steel specimen using all methods.

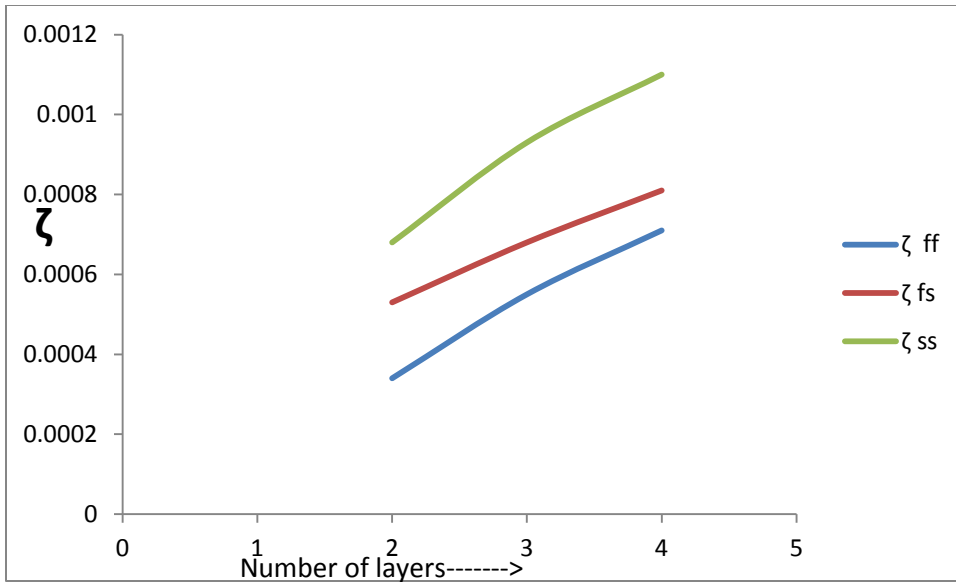


Figure 5.40 Effect of number of layers in composite beam on damping factor for aluminium specimen.

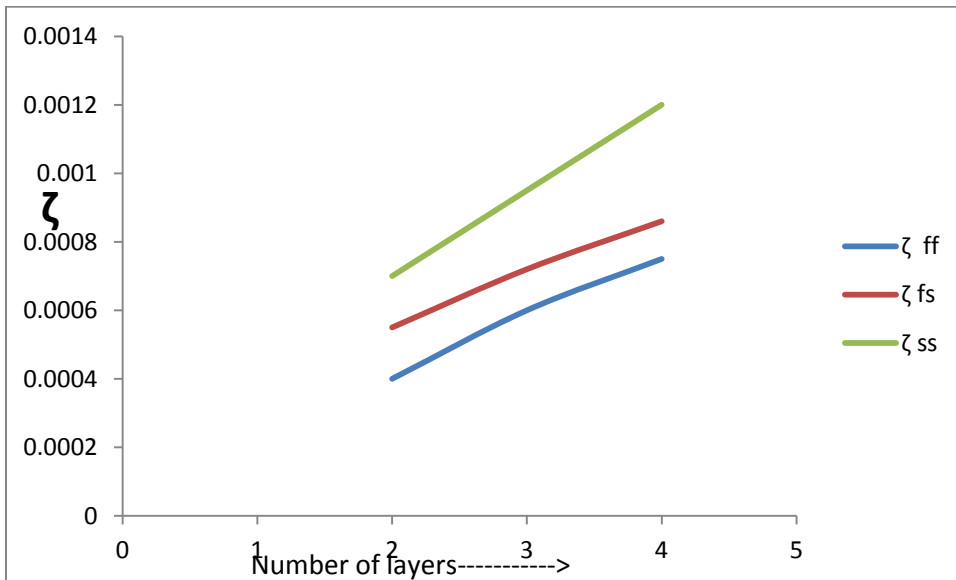


Figure 5.41 Effect of number of layers in composite beam on damping factor for mild steel specimen.

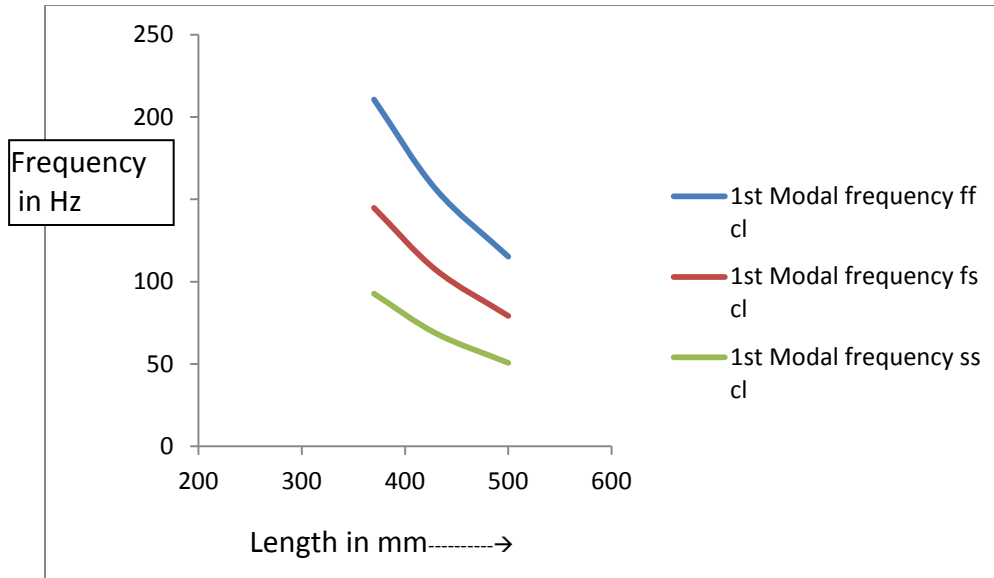


Figure 5.42 Variation of 1st modal frequency with length for aluminium specimen using classical method.

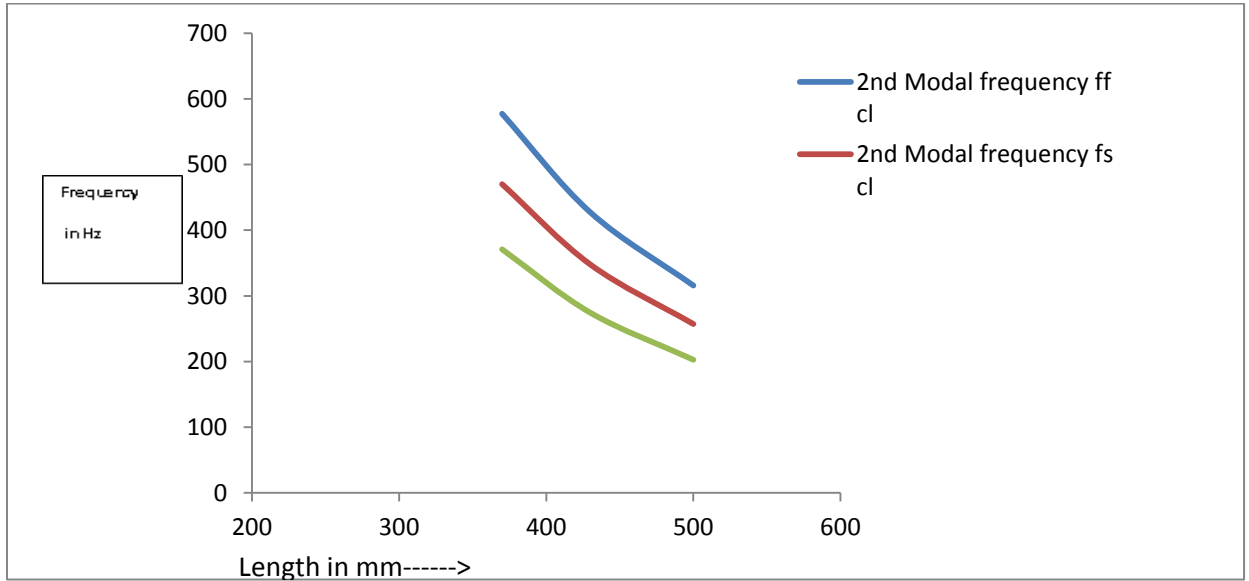


Figure 5.43 Variation of 2nd modal frequency with length for aluminium specimen using classical method.

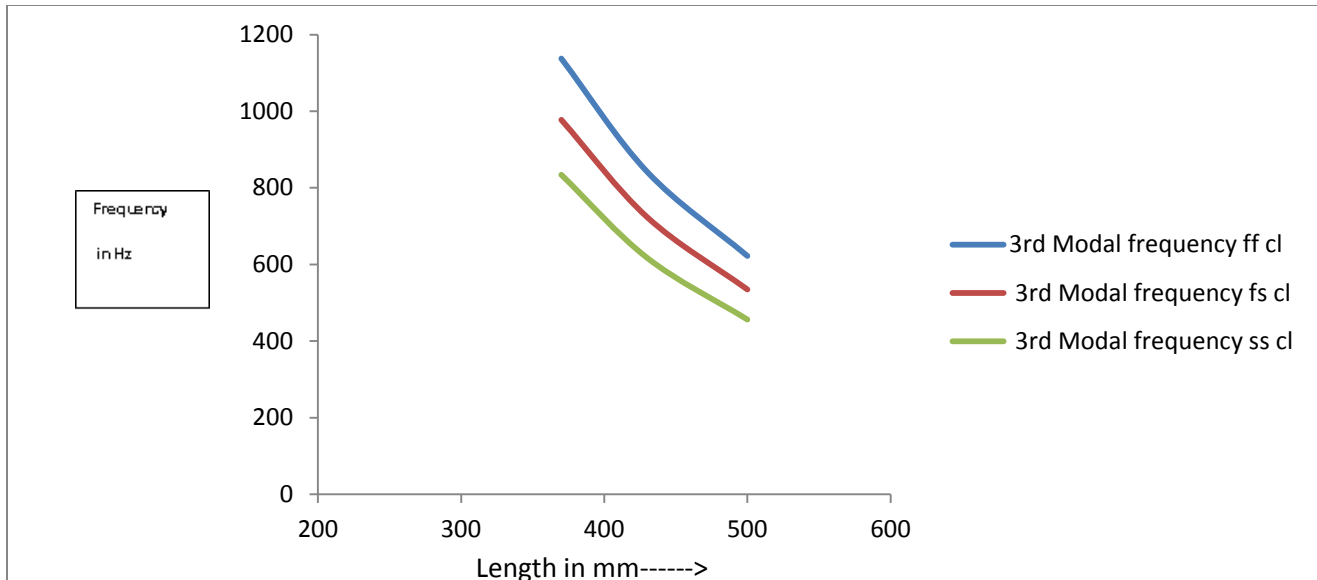


Figure 5.44 Variation of 3rd modal frequency with length for aluminium specimen using classical method.

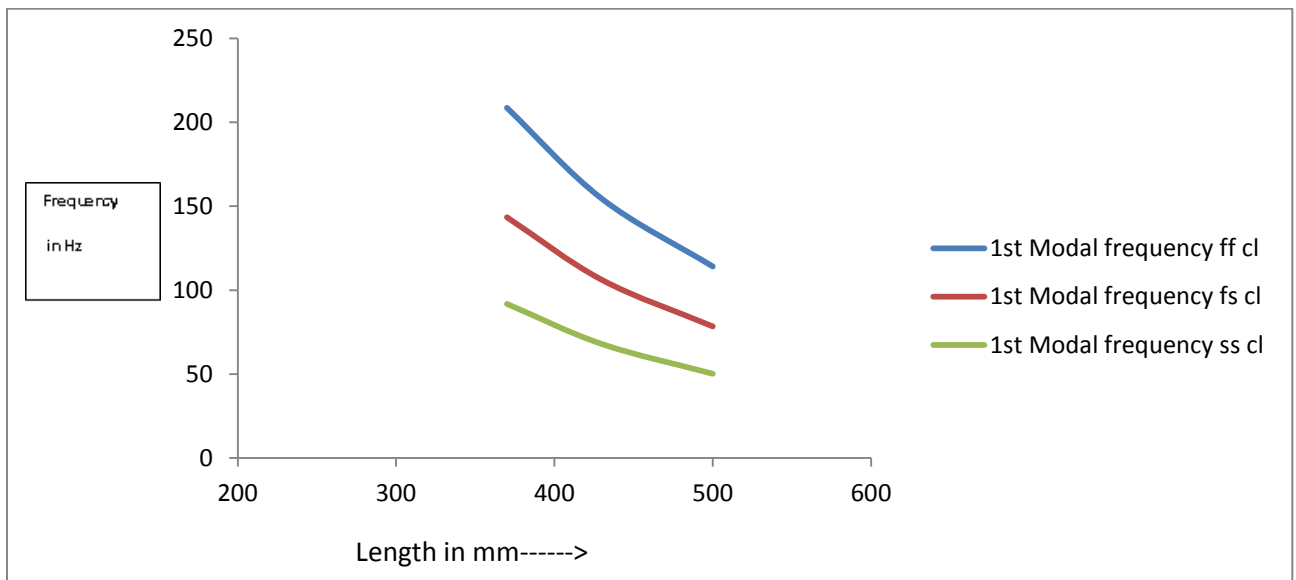


Figure 5.45 Variation of 1st modal frequency with length for mild steel specimen using classical method.

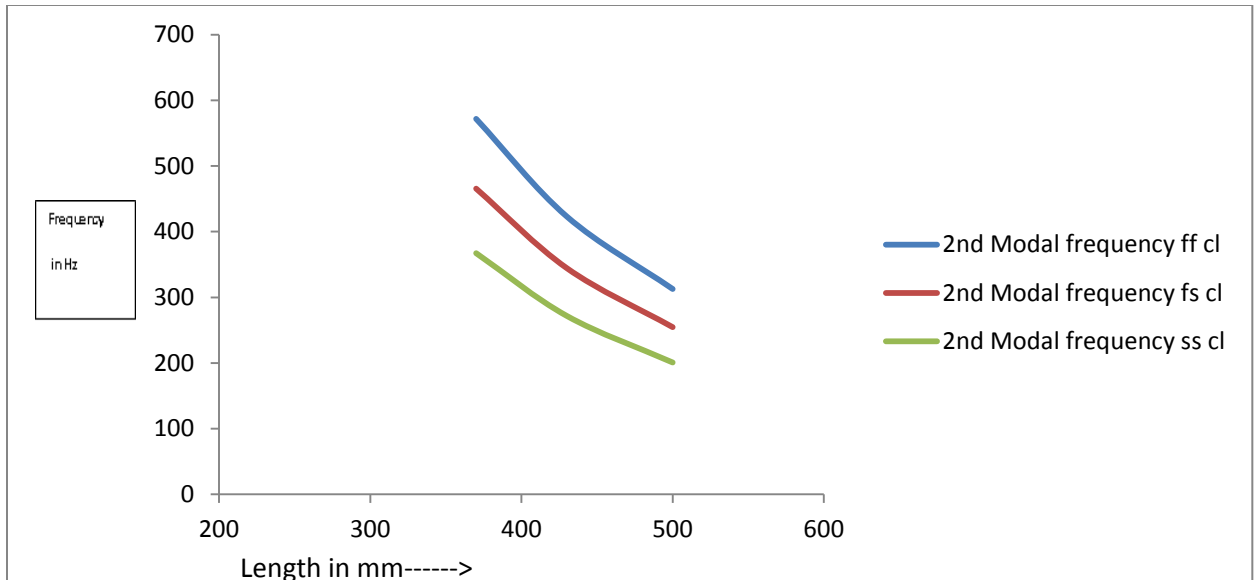


Figure 5.46 Variation of 2nd modal frequency with length for aluminium specimen using classical method.

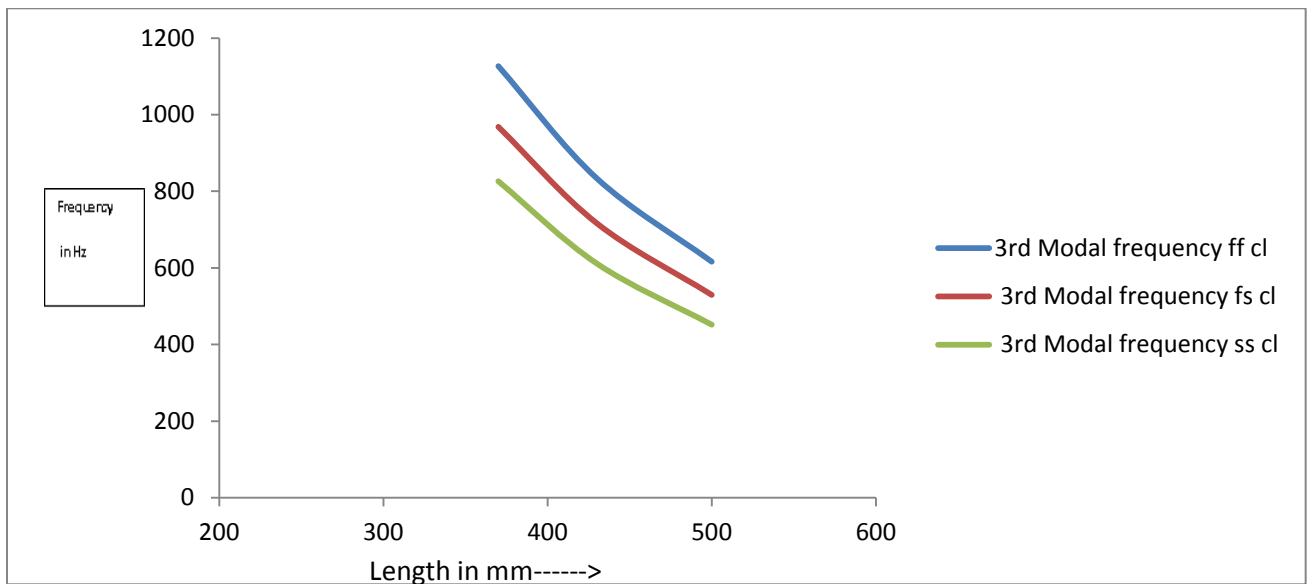


Figure 5.47 Variation of 3rd modal frequency with length for mild steel specimen using classical method.

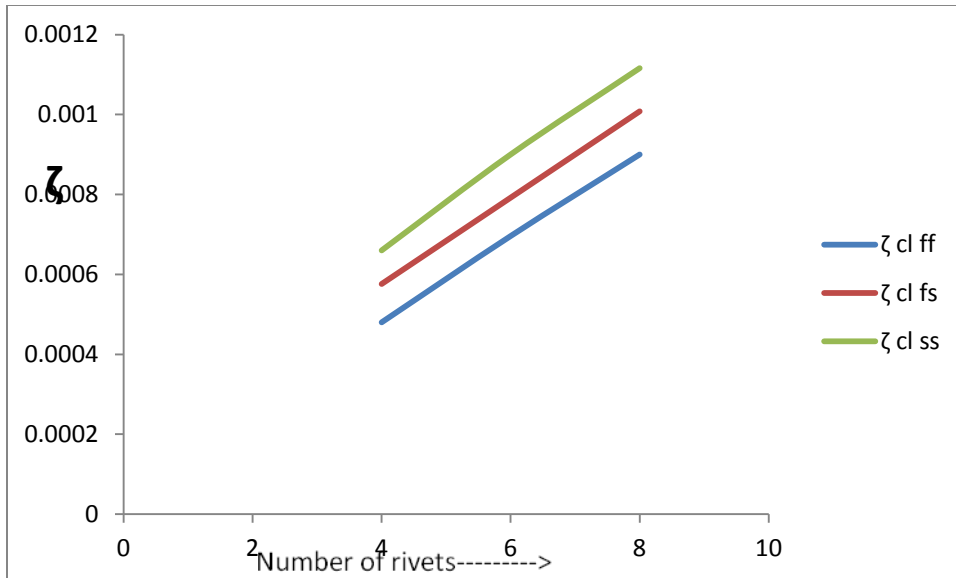


Figure 5.48 Effect of number of rivets on damping factor for aluminium specimen using classical method.

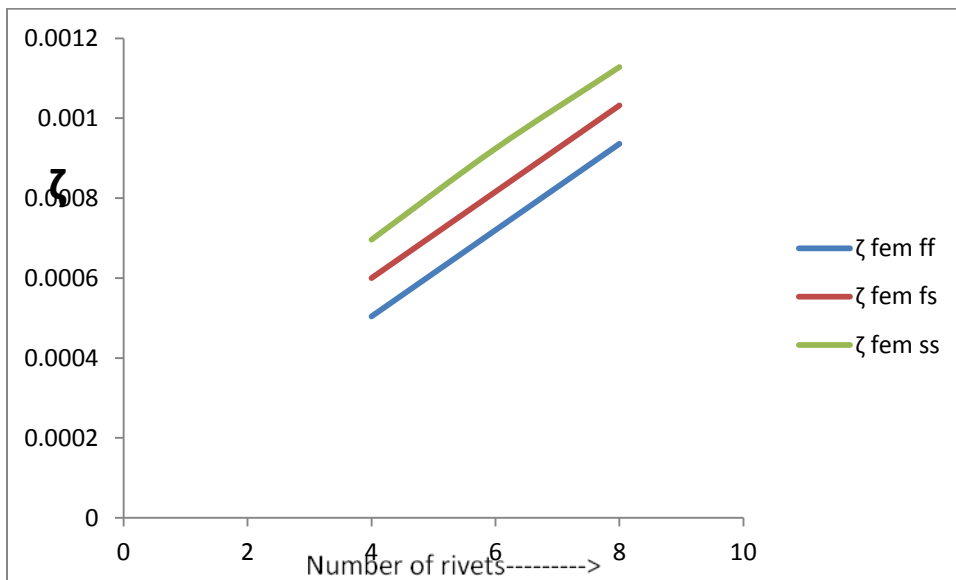


Figure 5.49 Effect of number of rivets on damping factor for aluminium specimen using finite element method.

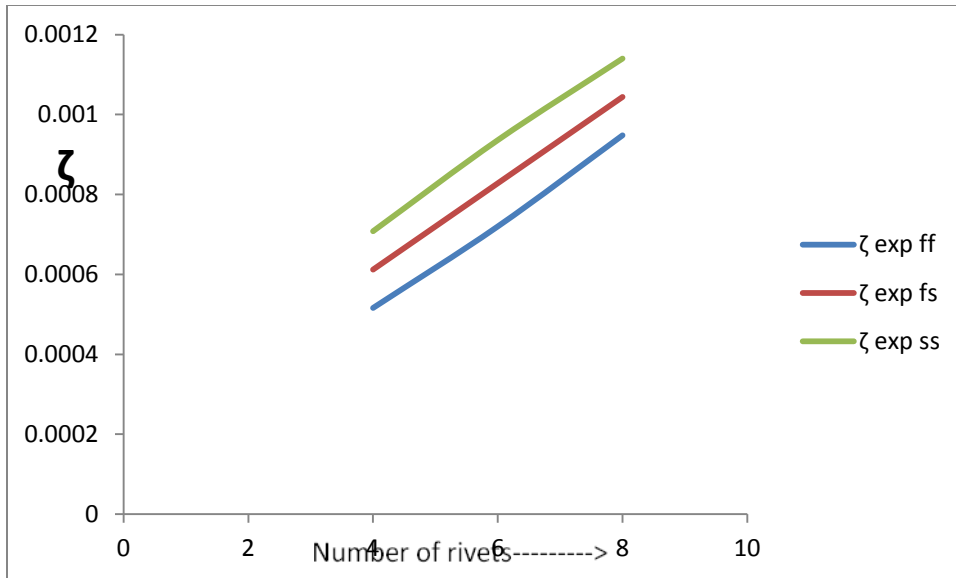


Figure 5.50 Effect of number of rivets on damping factor for aluminium specimen using experimental method.

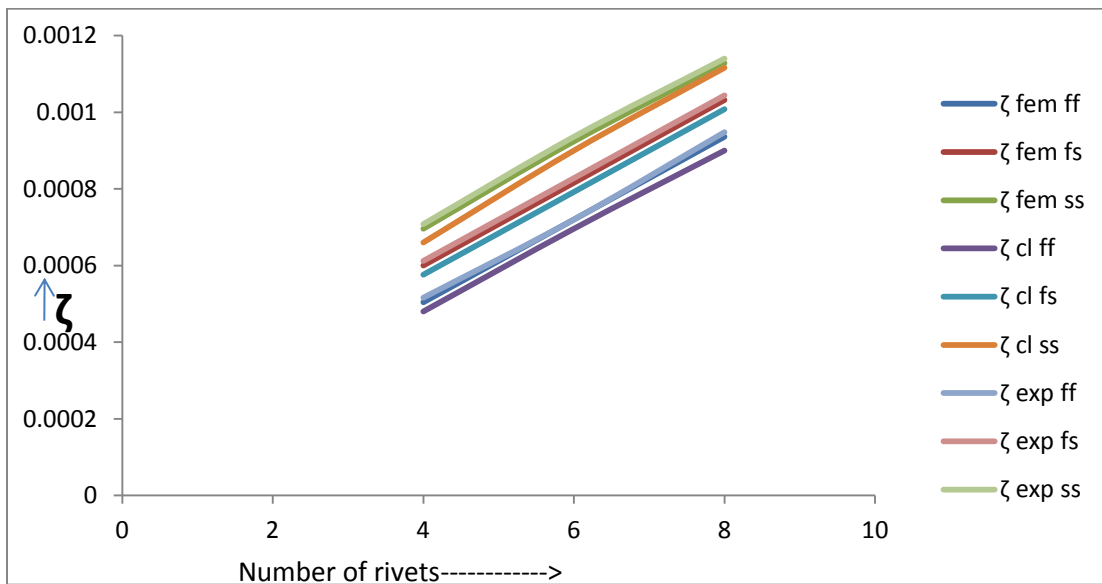


Figure 5.51 Effect of number of rivets on damping factor for aluminium specimen using all methods.

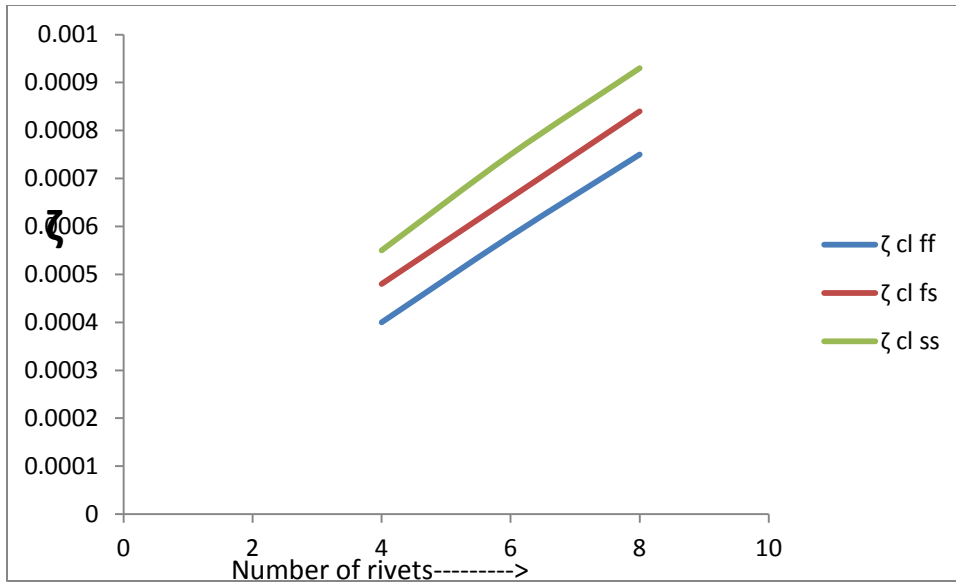


Figure 5.52 Effect of number of rivets on damping factor for mild steel specimen using classical method.

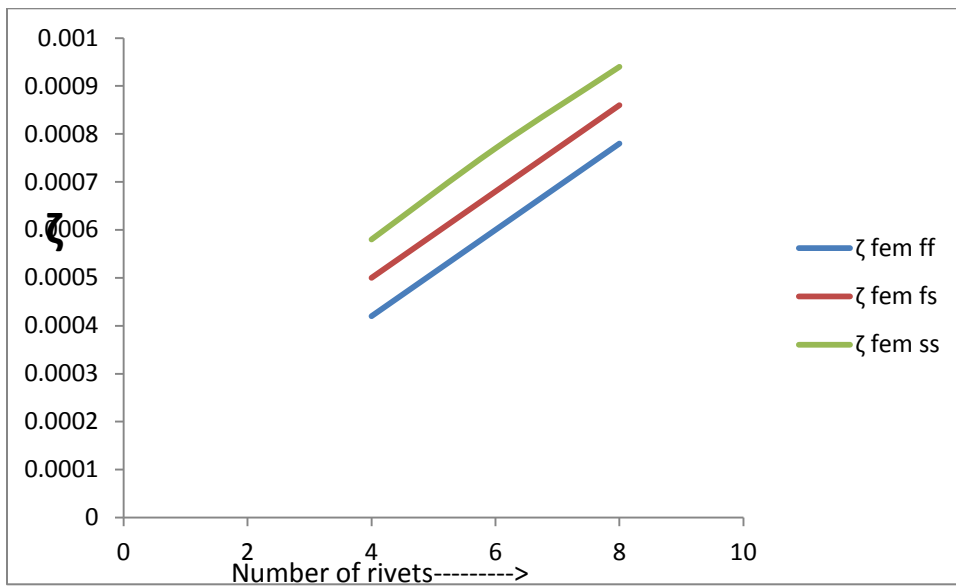


Figure 5.53 Effect of number of rivets on damping factor for mild steel specimen using finite element method.

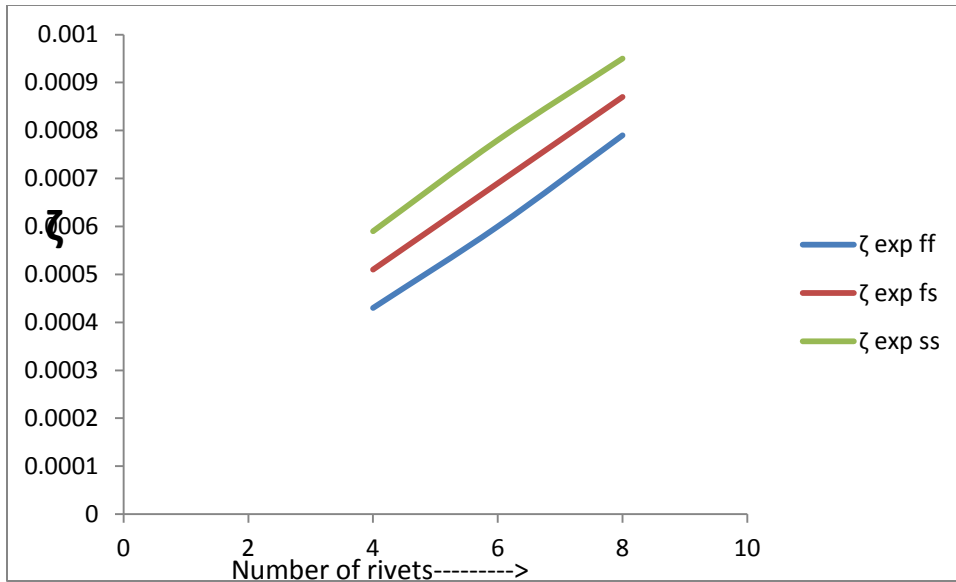


Figure 5.54 Effect of number of rivets on damping factor for mild steel specimen using experimental method.

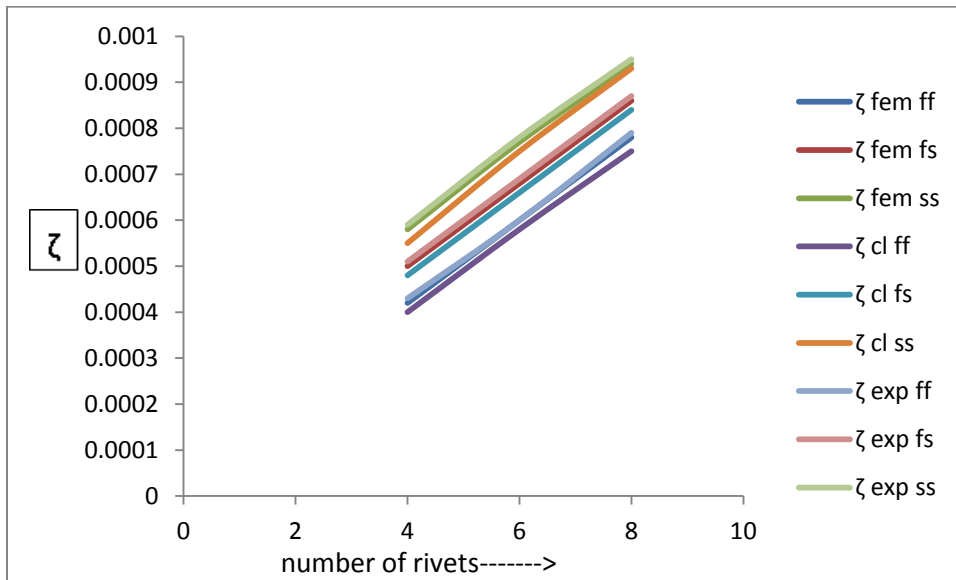


Figure 5.55 Effect of number of rivets on damping factor for mild steel specimen using all methods.

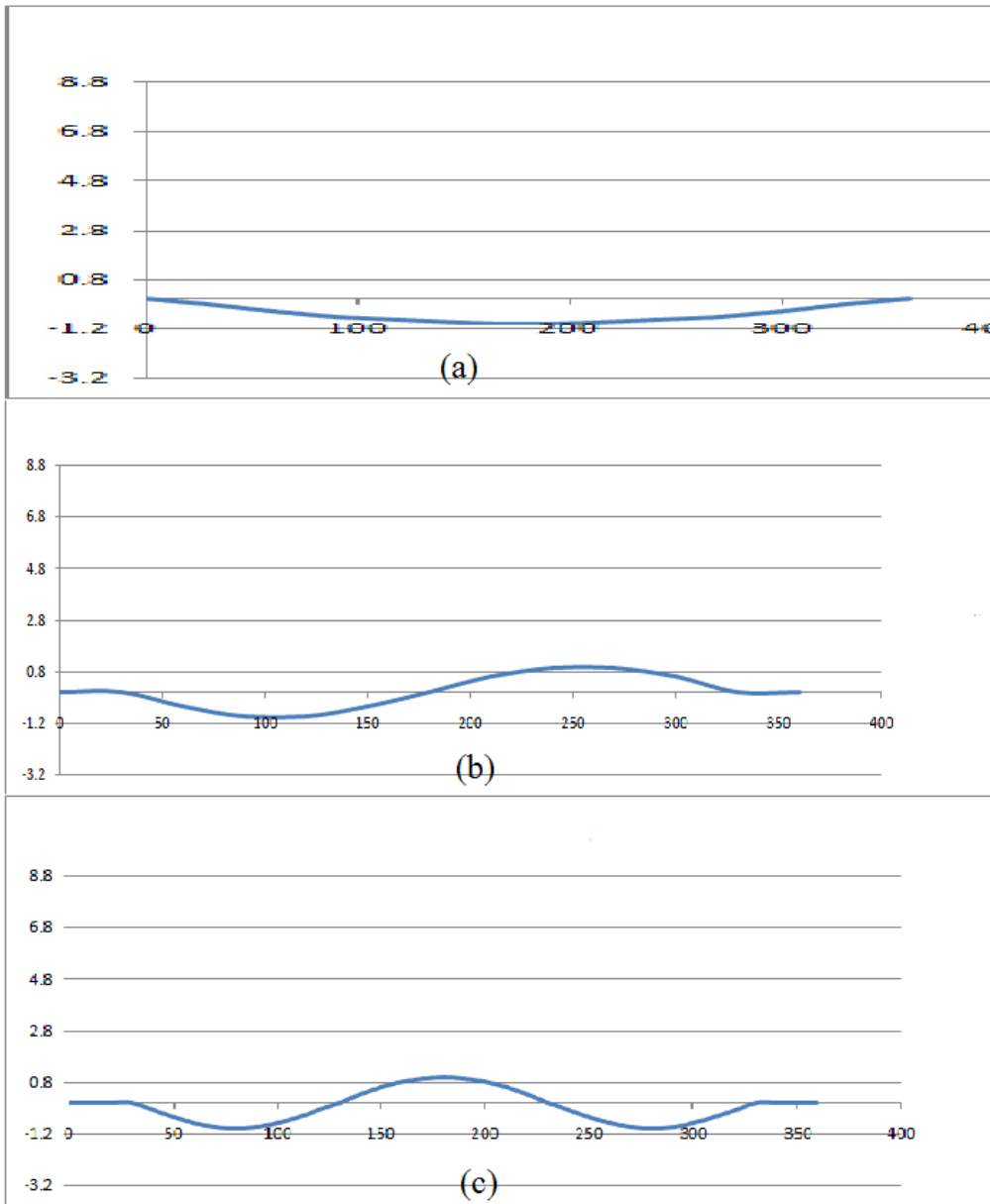


Figure 5.56 Mode shapes for aluminium specimen for fixed fixed configuration.

(a) Mode 1 (b) Mode 2 (c) Mode 3

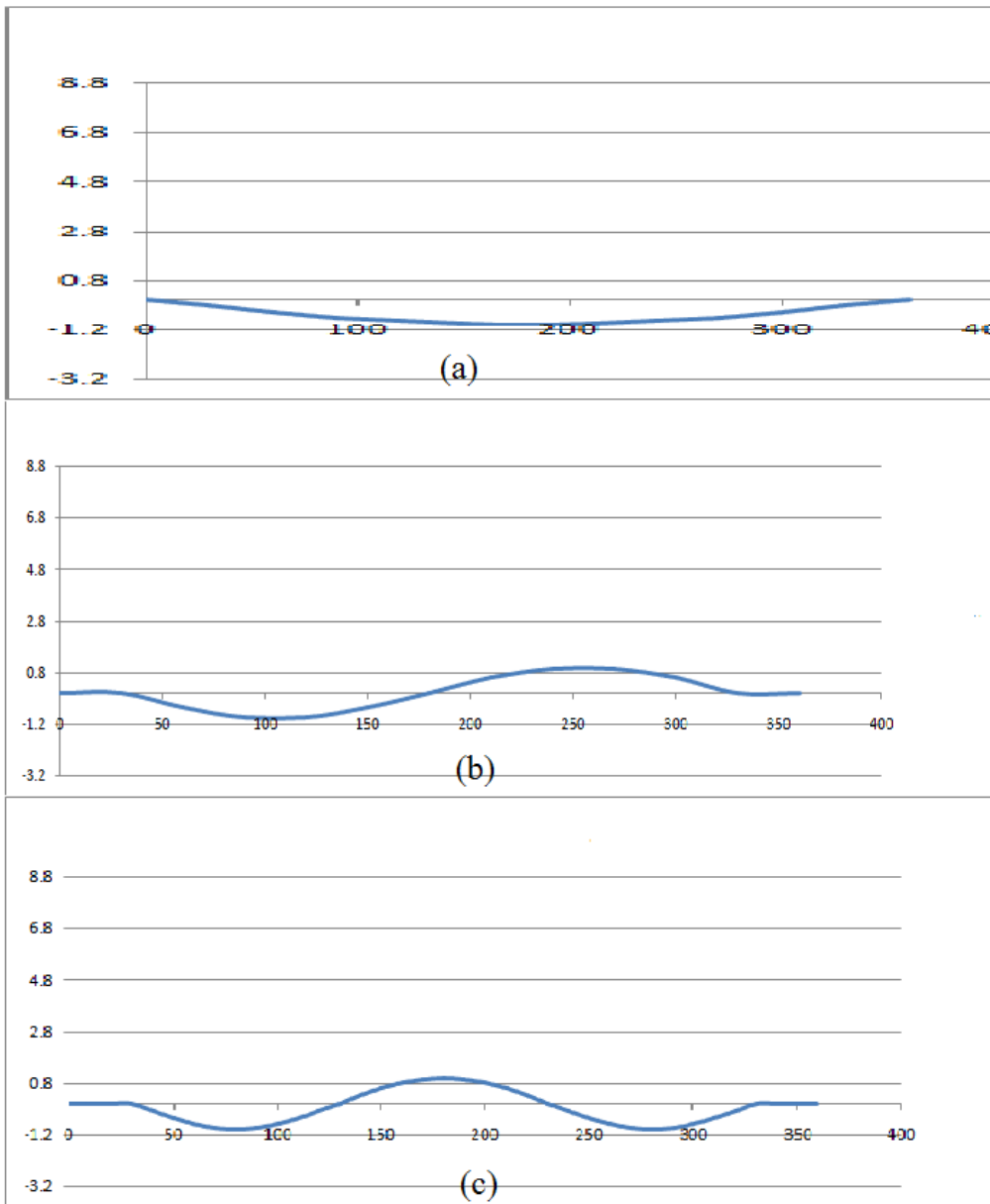


Figure 5.57 Mode shapes for mild steel specimen for fixed fixed configuration.

(a) Mode 1 (b) Mode 2 (c) Mode 3

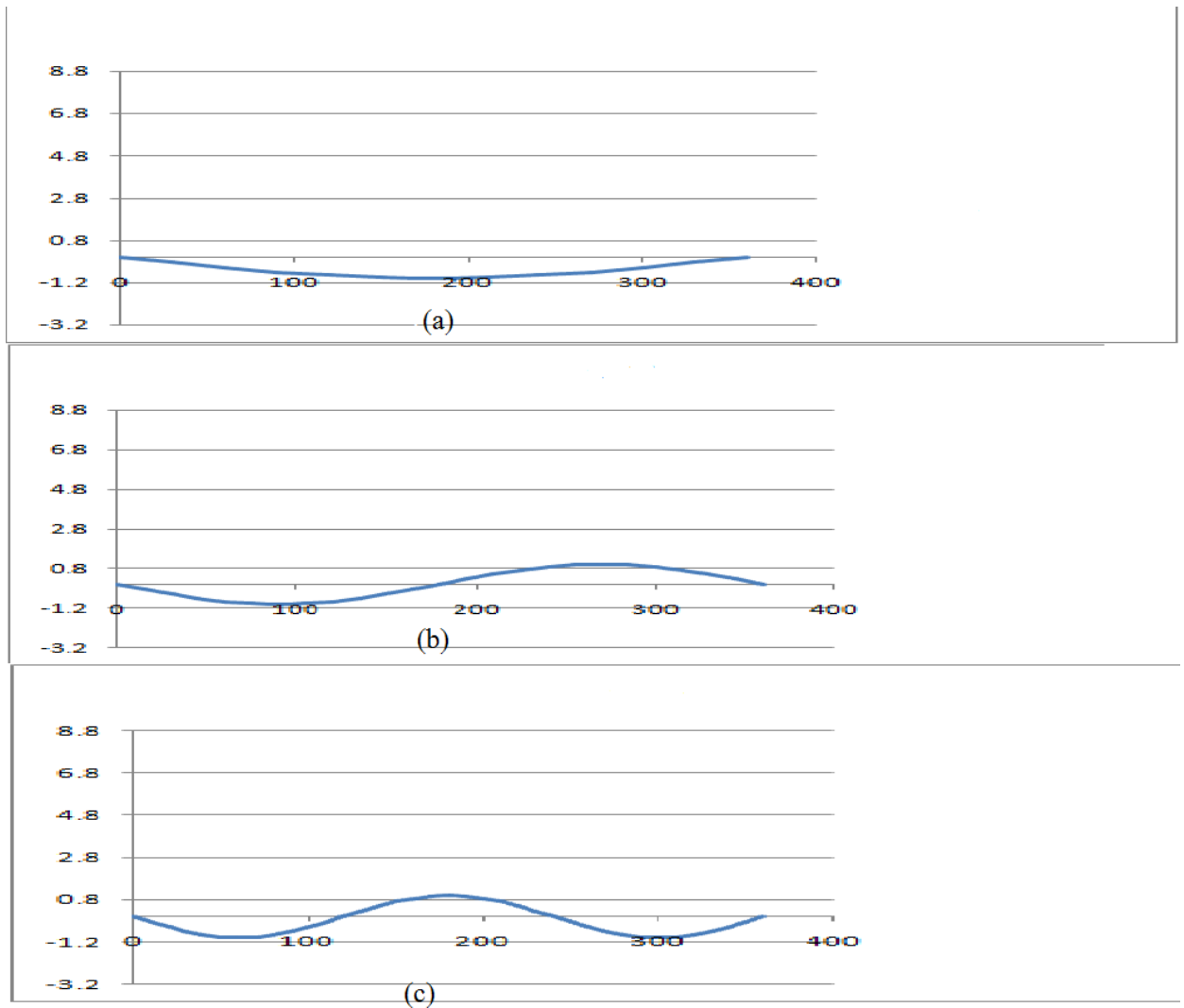


Figure 5.58 Mode shapes for aluminum specimen for simply supported simply supported configuration.

(a) Mode 1 (b) Mode 2 (c) Mode 3

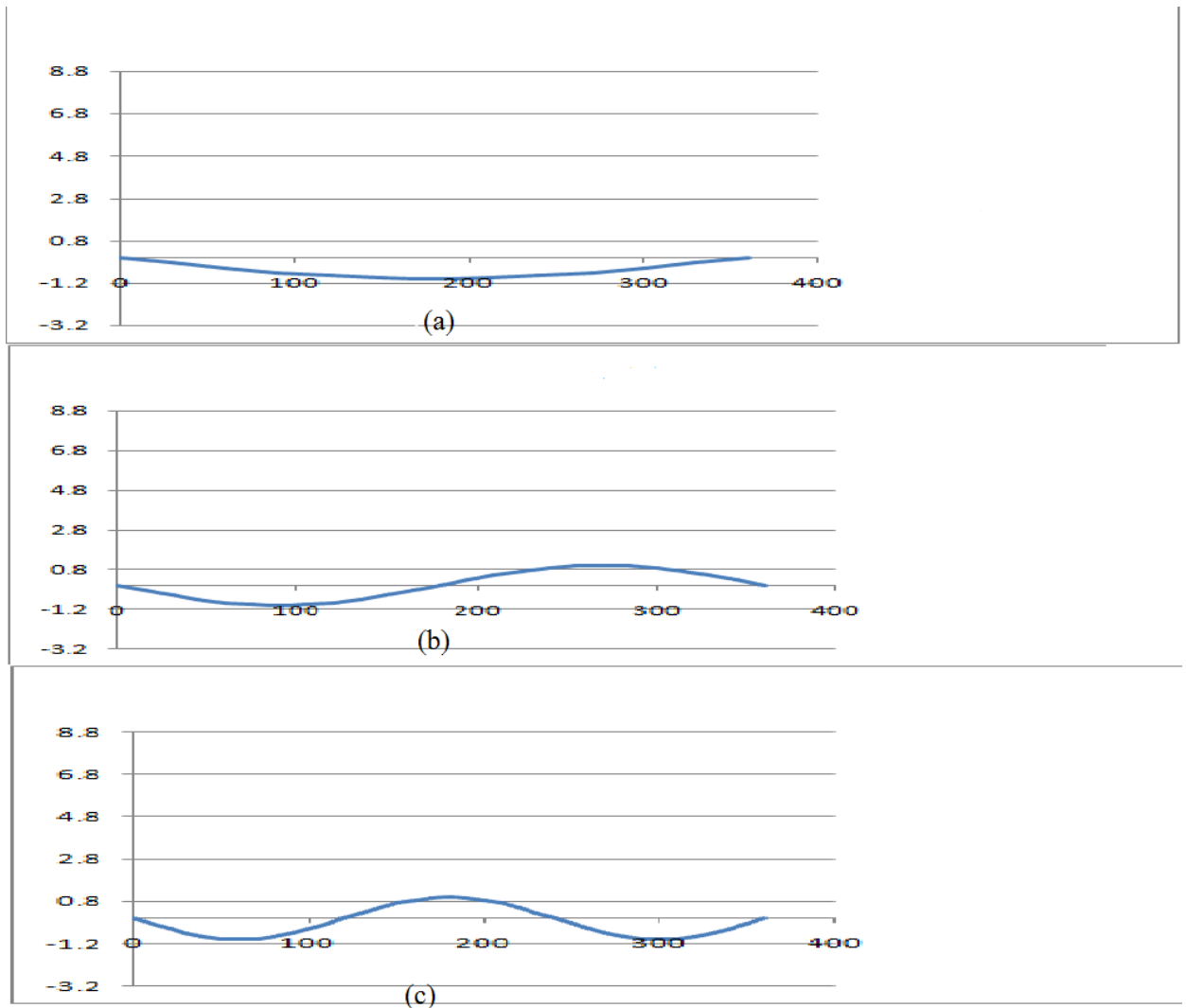


Figure 5.59 Mode shapes for mild steel specimen for simply supported simply supported configuration.

(a) Mode 1 (b) Mode 2 (c) Mode 3

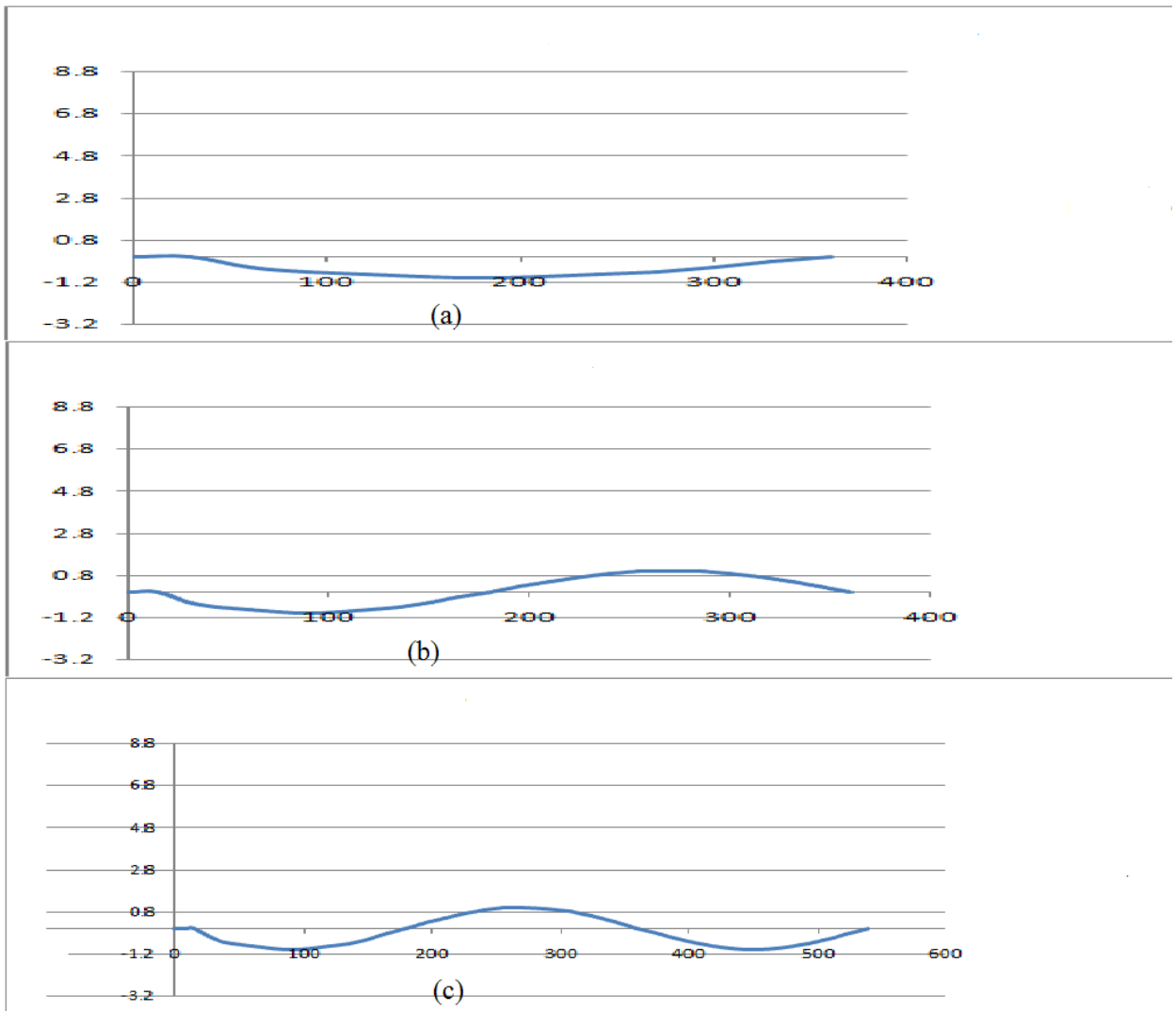


Figure 5.60 Mode shapes for aluminium specimen for fixed simply supported configuration.

(a) Mode 1 (b) Mode 2 (c) Mode 3

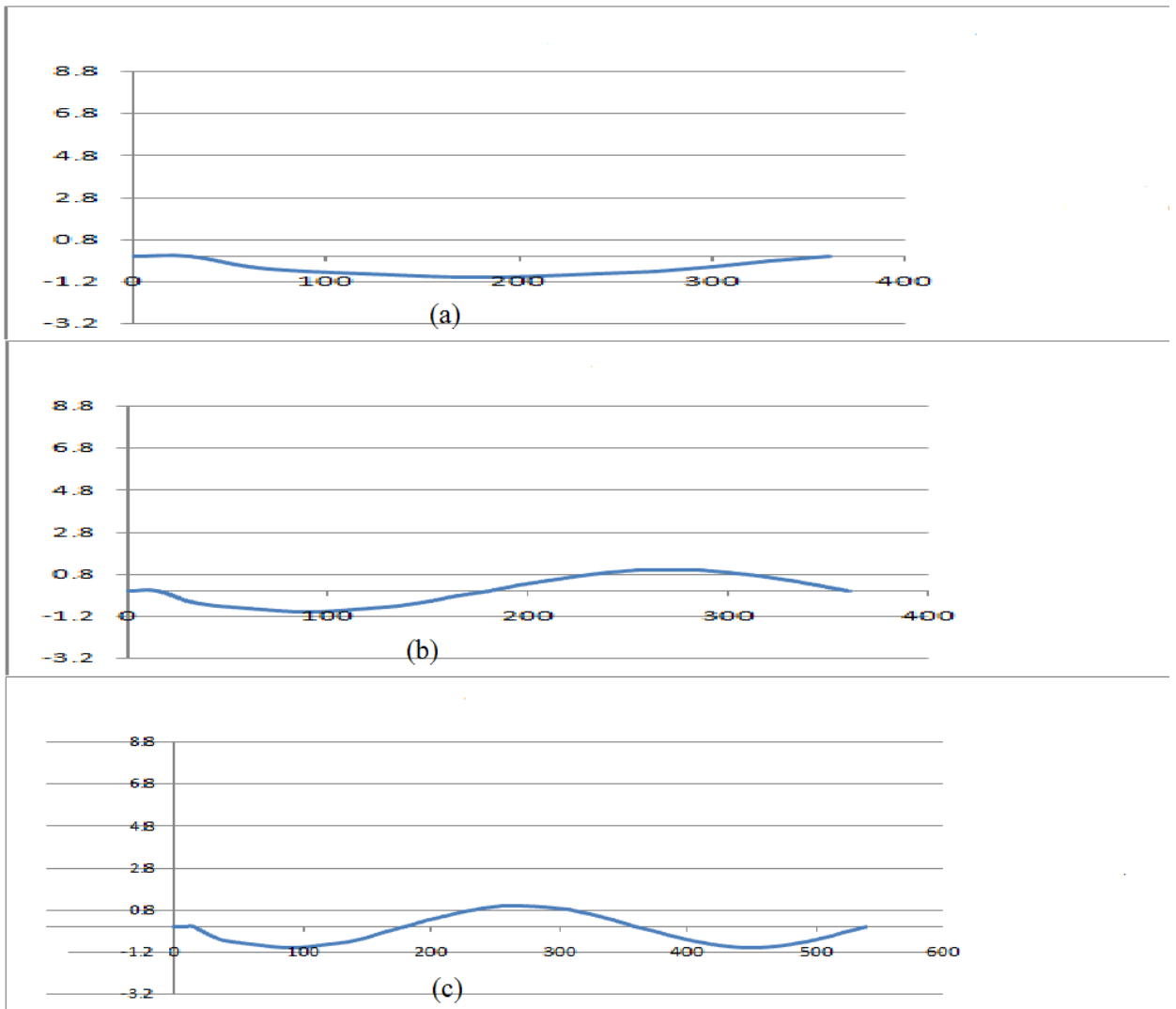


Figure 5.61 Mode shapes for mild steel specimen for fixed simply supported configuration.

(a) Mode 1 (b) Mode 2 (c) Mode 3

6. Results and discussion

A concerted effort has been made to analyze the rivet jointed composite beam problem both theoretically and experimentally. An exhaustive review of literature has been carried out to this effect in Chapter 2. The theoretical work was accomplished in two phases. The first phase of the work consisting of classical method and the second one using finite element method have been reported in chapters 3 and 4 respectively. Both, the methods have been demonstrated for evaluating dynamics and damping characteristics of beams with fixed-fixed, fixed-simply supported and simply supported-simply supported boundary conditions using Euler-Bernoulli hypothesis. The first method is based on an exact solution for the continuous system of the beam. Energy of dissipation and stored energy of the system per cycle of vibration have been derived for fixed fixed boundary condition. Logarithmic decrement and damping factor relations have been obtained considering the effect of the various parameters such as normal force on the rivet, kinematic coefficient of friction and relative interfacial micro slip. The process has been repeated for other beam configurations i.e. fixed-simply supported and simply supported-simply supported boundary conditions with suitable modification.

The second method i.e. the finite element method assumes discrete linear model for the beam under consideration. The solution for the fourth order governing equation of vibration of the beam has been obtained separately in terms of time and space variables. Shape functions relating intermediate displacement with nodal displacement for a beam element has been obtained using polynomial functions for space variable. Kinetic energy and strain energy have been determined in respect of nodal variables and element mass matrix and element stiffness matrix have been derived using Lagrange's equations. The global mass matrix and the global stiffness matrix for the whole beam and corresponding reduced matrices for a particular boundary condition have been determined. Assuming, harmonic solutions for the nodal displacements, natural frequencies and then modal displacement pattern of the beam have been computed using MATLAB. These results have been used to modify the expression of damping factor and its evaluation. In this connection, expression for dynamic slip, input strain energy and energy dissipation of the beam have been formulated in terms of stiffness matrix and displacement vector.

Both the methods, as discussed above are based on certain assumptions and there is a necessity to verify the validity of the results by performing experiments. To accomplish the experimental work a good number of test specimens were prepared from the same stock of mild steel and aluminums flats commercially available. The layout of the test set up instrumentation details, description of the used specimens are reported in chapter 5. The forced response curve has been plotted from the experimental observations and damping factor has been obtained by using band width method. This method is applicable to structures vibrating at low excitation level with a moderate frequency range.

The experimental results in respect of natural frequencies when compared with the same by classical and finite element methods show maximum variation within a range of 3.1% and 2.8% for mild steel and with a range of 3.8% and 2.4% for aluminum specimens for all considered boundary conditions. Experimental values of damping factor differ from classical and finite element analysis with a range of 3.6% and 2.7% for mild steel and 4.1% and 2.5% for aluminum specimen for all considered boundary conditions. Because of the closeness of the results the theory developed is considered to be validated.

The mechanism of damping in these structures is affected by interfacial pressure distribution, kinematic coefficient of frictions and micro slip under rivet head. These factors depend on thickness ratio of beam layers. The natural frequencies and mode shapes are affected by geometrical and material properties of the beam and its boundary conditions. The authentication of the analysis has been achieved by comparing the theoretical and experimental results of the specimens with all the influencing parameters. The following inferences have been drawn from the theoretical and experimental investigation related to present work.

1. Evaluation of damping capacity requires the value of interface pressure. This pressure depends on clamping action at the joints and has been reported to be non-uniform over the influencing zone under the rivet. Using Minakuchi et al [31] procedure, the pressure has been calculated using a polynomial function. Moreover, the influence zone depends on thickness ratio of beam layers. According to Minakuchi et al [31], the zone is of circular area concentric with rivet and has diameter 4.12, 5.0 and 5.6 times the diameter of rivet for thickness ratio of 1.0, 1.5 and 2.2 respectively. The pressure

distribution is parabolic being maximum at the rivet hole and gradually reducing to zero at the circumference. Because of variation of pressure from point to point, relative local motion or microslip occurs at the interface of the layers. The dissipation of energy and damping capacity depends on microslip.

2. The shearing action between the layers generates friction at the sliding surfaces. This action is dependent on preload on the rivet and friction coefficient. Due to transverse vibration, friction occurs as a result of the tendency of contacting layers to slide over each other and appears as a major source of energy dissipation. Coulomb's law of dry friction has been assumed to analyze the effect of friction at the contacting surfaces.

3. The joint is not absolutely rigid and causes relative motion to occur. The beam under transverse vibration gives rise to shear stresses to layers. Slipping which occurs at points where clamping force is low is known as microslip. Microslip takes place at lower level of excitation. Pressure diminishes at points away from the rivet causing more slippage at these points and higher dissipation of energy consequently more damping is produced due to uneven pressure distribution. With increase in the level of excitation, the whole layer slips resulting in macroslip. Macroslip is undesirable in jointed structures since it causes structural damage and is generally avoided.

4. The friction coefficient ' μ ' and dynamic slip ' α ' both influence energy loss. But these are dependent on each other and their estimation is quite complex. It is important to assume the product $\alpha \cdot \mu$ as a single variable and use the product to determine damping. Variation of the product $\alpha \cdot \mu$ with frequency and amplitude for mild steel and aluminum respectively has been determined using (156). These values are further used for getting damping factor of jointed beams with changing configuration. This concept also accounts for non linearity, modes of vibration and support effects.

5. By performing load deflection tests for the specimens, modulus of elasticity has been found for a number of observations and their average value has been taken for the analysis. Thus, considering material non-homogeneity and irregularity the value of E was calculated.

6. The factor 'K' i.e. the static bending stiffness is a major parameter influencing dynamics and damping of jointed structures. Higher the value of this factor, lower is

damping due to increase is stored energy of the system. On the contrary, natural frequency increases with increase in stiffness. It is seen that the use of joints decreases the stiffness. Ratio of stiffness of a jointed beam to that of a solid beam with identical combined thickness and other properties is less than one. This parameter has been evaluated by conducting static bending test for the specimens. There is a reduction of 5 to 10 % in flexural stiffness of layered mild steel and aluminum beams to that of identical solid beams. Moreover, the stiffness ratio of aluminum specimen is higher than that of steel specimen due to greater coefficient of friction of the former.

7. From the theoretical analysis it is noted that inclusion of the joints increases damping and reduces natural frequency of the structure. The same effect is also noticed from experimental analysis. At lower modes of vibrations the difference of frequency is reasonably low.

8. Surface roughness of contacting layers increases coefficient of friction ' μ ' but decreases the microslip factor ' α '. In the analysis, the product $\alpha \cdot \mu$ has been assumed to be a constant. Hence, surface roughness has no effect on damping of jointed structures and damping factor remains unaltered, even if there is variation of roughness at the interfaces.

9. From the graph showing pressure distribution against thickness ratio it is observed that pressure increases with decrease of thickness ratio. The spacing between consecutive joints is less in case of structures with low thickness ratio which results in higher normal force; frictional force and energy dissipation. All these effects cause maximum damping in structures with low thickness ratio.

10. A comparison of damping factor of a mild steel layered beam with that of a solid beam shows an increase of 50% in favor of layered beam. An increase of 50% is observed in case of aluminum composite beam compared to an identical solid beam. Damping factor is further increased by using more number of layers in a composite structure which happens for increased friction due to introduction of more number of friction surfaces and reduction in static stiffness.

11. It is seen that damping capacity of aluminum is more than that of steel. This is attributed to lower bending stiffness and higher coefficient of friction between contacting

layers of aluminum specimen compared to those of steel specimens. The lower input strain energy and higher energy dissipation results in higher damping of aluminum.

12. Manufacturing processes and accuracy influence the surface undulations, friction and microslip which are major parameters affecting damping and may vary from one joint to another. As a consequence, the joints and the jointed structure may exhibit non linear characteristics. However, the vibrations in the present case take place at lower amplitude and lower modes. Hence, linear vibration theory is applied.

The dynamics and damping of composite riveted structures has been analyzed considering length of specimen, diameter of rivet, beam thickness, vibration amplitude and boundary constraints. The effect of these factors on dynamic and damping behavior of these structures have been presented below.

a) Increase of length of specimen causes reduction in flexural stiffness and input strain energy and accommodates more number of rivets, resulting in higher overall dynamic slip and energy loss. The net effect of all these is to increase damping. Hence, the damping factor of longer specimen with considered boundary conditions increases.

b) As stated earlier, vibrations of the system with higher amplitudes leads to more input strain energy and increased value of the product $\alpha.\mu$. However, the damping of the system reduces due to increase of amplitude.

c) Use of larger diameter of rivets enhances the preload on rivets resulting in higher energy dissipation. Although, the flexural system decreases the increased diameter of rivets, damping factor of the structure increases.

d) The combined thickness of layered beam influences damping significantly. There is an increase of bending stiffness due to higher overall thickness leading to higher energy. The vibration energy loss is also increased due to increase in natural frequency and the product " $\alpha.\mu$ ". However, the rate of increase of input energy is more compared to energy loss which results in decrease of damping factor.

Finally, it is concluded that the use of joints in assembled structures generates significant damping due to micro slip along the frictional interface thereby compensating the low inherent material damping of the structure. The influence of various factors on dynamics

and damping of rivet jointed layered structures with different boundary conditions have been presented in this chapter. A brief summary of influencing factors and their affects are reported in chapter 6.

7 Conclusion and scope for further work

The present research work aims at evaluation and improvement of dynamic and damping characteristics of layered and rivets jointed structures with various boundary conditions. The background and prospective of work has been described in Chapter 1 and 2. To achieve the objective, conventional, numerical and experimental studies have been presented in Chapter 3, 4 and 5 respectively. In chapter 6, interpretation of theoretical and experimental results and discussion on the results has been reported. The ongoing chapter provides a brief summary of the conclusions derived from the different aspects of analysis discussed in earlier chapters. The chapter concludes with discussions on the scope for further work in this research area.

7.1 Conclusion

The effect of various material and geometrical factors on dynamics and damping of jointed structures has been studied extensively. The dynamics of these structures has been analyzed for various boundary constraints. The damping has been estimated considering the influence of the variables such as interfacial pressure distribution, dynamic slip ratio, surface asperities, kinematic coefficient of friction, thickness ratio of beam layers, diameter of rivet etc. both theoretically and experimentally.

1. Effect of boundary condition:

The specimens are analyzed for fixed-fixed, fixed- simply supported and simply supported-simply supported boundary conditions. From the graphical presentation of results, it is observed that there is close agreement between theoretical and experimental results. As expected, modal frequencies for a specimen are lowest for simply supported simply supported ends and largest for fixed fixed ends and lie in between these two values for fixed simply supported end conditions. Damping factor is found to be more for simply supported simply supported edges compared to fixed fixed edges and that for fixed simply supported edges lies within these two values.

2. Effect of Interface pressure:

Interface pressure distribution varies with thickness ratio. It is maximum for thickness ratio 1.0. As average pressure increases, the normal force and dissipated energy also increase. Therefore, damping is maximum for jointed structures with identical thickness of beam layers.

3. Effect of dynamic slip ratio:

The dynamic slip ratio is influenced by surface texture of the joint interface and is dependent on coefficient of friction. As its evaluation is complicated, it is important to consider the combined effect of dynamic slip ratio and coefficient of friction. It is observed that damping increases with the increase of the slip ratio.

4. Effect of coefficient of friction:

The shearing action between the layers gives rise to friction force that varies with preload on the rivet and coefficient of friction. It is shown that the energy is dissipated due to the frictional effect and is a function of both α and μ , which, are interdependent and show complex behavior under dynamic conditions. Hence, the product $\alpha \cdot \mu$ is assumed to be a constant single parameter and energy dissipation and damping increase with increase of the product of dynamic slip ratio and coefficient of friction.

5. Effect of specimen length and modal frequencies:

The flexural stiffness and modal frequencies of the specimen decrease with increase in its length. However, in longer specimens dynamic slip is higher as large number of rivets can be accommodated and energy dissipated is more. As a consequence, damping is more with increased length of specimens.

6. Influence of layer thickness ratio:

Energy dissipation is a complex process in jointed structures and is substantially influenced by interface pressure profile which in turn depends on thickness ratio. When thickness ratio is less, the width of beam and stiffness of beam are reduced. The strain energy stored in the system being less, damping in the system is increased. Hence,

maximum damping is achieved with structures having equal thickness of composite layers.

7. Effect of amplitude of vibration:

With increase of amplitude both the input strain energy and interfacial energy dissipation are increased. However, due to proportionately higher increase of strain energy the logarithmic decrement and damping factor are decreased.

8. Effect of rivet diameter:

The preload on the rivet increases with increase of rivet diameter. As a result, the normal force and energy dissipation are increased. On the other hand, the static flexural stiffness increases with increase of diameter of rivet which results in larger input of strain energy. Since, energy dissipation takes place at a higher rate compared to the strain energy, damping factor increases as a whole with increase in rivet diameter.

9. Effect of number of rivet:

More the number of rivets, larger the energy dissipated. This occurs due to increased number of friction interfaces. Hence, damping in the system is enhanced with more number of rivets.

10. Effect of number of layers:

With increase in number of layers the number of friction interfaces increase. This causes more dissipation of energy resulting in higher damping.

11. Effect of overall beam thickness:

Increase of overall thickness of beam causes increase in bending stiffness and input strain energy. However, the energy loss at the interfaces increases as the product $\alpha \cdot \mu$ increase due to greater natural frequency of vibration. As the input strain energy is increased at a higher rate compared to energy loss due to dissipation, there is net decrease in damping due to increase of overall structure thickness.

As stated above, damping effects occur at the interfaces of layers of jointed structures and are significantly affected by the boundary constraints. From the present investigation, it is observed that natural frequencies calculated theoretically differ by 30% at the most form

experimental results and damping factor is within 8.5% of the corresponding experimental value. This is true for all boundary conditions of the beam. It may be summarized from the experimentally validated theoretical results that the damping effectiveness of rivet jointed built-up structures of longer specimens, larger diameter of rivets, lower total beam thickness, equal thickness ratio, more number of layers and larger number of rivets with low amplitudes of vibration can be significantly enhanced.

The control of vibration of structures is an important basic requirement. The solid monolithic structures possess low inherent damping and are incapable of resisting vibrations. This leads to malfunctioning and reduction of life expectancy of structures. It is essential to maintain the vibration level low and increase life of structures by incorporating suitable damping mechanism. This has been a challenging task and subject of study for the designer, over the years. Considering these facts, it is of great importance to design structures which are not only robust and safe but also capable of preventing undesirable vibrations. The present study is primarily intended to determine dynamic and damping characteristic of jointed built-up structures, which have enormous application in machine tool and naval frame works, trusses, aircrafts, spacecrafts, bridges, machine components, robotic manipulators etc.

On the whole, it is of great importance to predict dynamics and damping of assembled structures and to have knowledge of estimation of damping capacity. For overcoming the unwanted and spurious effects of vibration and noise in composite beams with riveted connections and various boundary conditions, the following design criteria drawn from the present study are suggested:

- Increasing the diameter of rivets
- Increasing the length of beams
- Using equally thick layers of beam
- Decreasing overall thickness of beams
- Decreasing the initial amplitude of motion

7.2 Scope for further work

In the present investigation, the process and mechanism of damping has been demonstrated and the parameters affecting dynamics and damping of rivet jointed butting structures have been estimated and reported. However, sufficient scope exists for continuation and up gradation of present study. A host of work is to be carried out in the line of present study is envisaged as follows:

- Dynamic and damping of jointed beams with elastic supports
- Damping analysis of thick beams using Timoshenko beam theory
- The damping analysis of layered and jointed beams of dissimilar materials
- Beams with active damping
- Analysis of beams with non linear properties
- Elaborate analysis considering variation in boundary constraints

8. Bibliography

1. Nashif, A.D., Jones, D.I.G. and Henderson J.P., 1985 *Vibration Damping*, John Wiley and Sons, NY.
2. Chen, J.H., H Sich, S.C. and Lee A.C., 2005 The failure of Threaded fasteners due to vibration, *Proceedings of the I Mech E. Part C: Journal of Mechanical Engg. Science*, Vol. 219, No 3, pp 299-314.
3. Beards, C.F., 1986, The damping of structural vibration by controlled interfacial slip in joints, ASME publication 81-DET-86, pp1-5.
4. Ren, Y., 1988, *Damping in Structural Joints*, M.Sc. Thesis, Imperial College, London University.
5. Earles S.W., and Mansoori, F.S., 1974, Frictional Damping applied to a cantilever beam structure: A Theoretical and Experimental Response comparisons, *International Journal of Machine Tool Design and Research*, Vol. 14, No. 1, pp 111-124.
6. Beards C.F. and Imam, I.M.A., 1978, The damping of plate vibration by interfacial slip between layers, *International Journal of Machine Tool Design and Research*, Vol. 18, No. 3, pp 131-137.
7. Beards, C.F. and Williams, J.L., 1977, The damping of structural vibration by rotational slip in joints, *Journal of sound and vibration*, Vol. 53, No. 3, pp 333-340.
8. Beards, C.F. 1975, Some effects of interface preparation on frictional damping in joints, *Internal Journal of Machine Tool Design and Research*, Vol. 15, No. 1, pp 77-83.
9. Menq, C.H., Bielak. J., and Griffin, J.H., 1986, The influence of microslip on vibratory response, Part 1: A new microslip model, *Journal of Sound and Vibration*, Vol. 107, No. 2, pp 274-293.
10. Menq, C.H., Griffin, J.H. and Bielak J., 1986, The influence of microslip on vibratory response, part-II: A comparison with experimental results, *Journal of Sound and Vibration*, Vol. 107, No. 2, pp 295-307.
11. Hansen S.W. and Spies R.D., 1997, Structural damping in laminated beams due to interfacial slip, *Journal of sound and vibration*, Vol 204, No. 2, pp 183-202.

12. Ungar, E.E., 1973, The status of Engineering Knowledge concerning the damping of built-up structures, *Journal of Sound and Vibration*, Vol. 26, No. 1, pp 141-154.
13. Beards, C.F., 1992, Damping in Structural Joints, *The shock and vibration digest*, Vol 24, No. 7, pp 3-7.
14. Ibrahim, R.A., 1994, Friction induced vibration, chatter, squeal and chaos, part-II, *Dynamics and Modeling*, ASME, *Applied Mechanics Reviewers*, vol 47, No. 7, pp 227-253.
15. Gaul, L. and Nische, R., 2000, Friction control for vibration suppression, *Mechanical systems and signal processing*, Vol 14, No. 2, pp 139-150
16. Gaul, L., and Nische, R., 2001, The role of friction in mechanical joints, ASME, *Applied Mechanics Reviewers*, Vol. 54, No. 2, pp 93-106.
17. Donnely, Jr., R.P. and Heinrich Sln, R.L., 1988, The effect of energy dissipation due friction at the joint of a simple beam structure, *Mathematical compiler Modelling*, Vol-II, pp 1022-1027.
18. Asoor, A.A.A. and Pashaei, 2010, Experimental study on the effects of types of joints on damping, *World Applied Sciences Journal*, Vol-8, No. 5, pp 608-613.
19. Nayfeh, A.H. and Pai, P.F., 2004 *Linear and Non linear structural mechanics*, John Wiley & Sons, New York.
20. Beards, C.F., 1996, *Structural vibrations: Analysis and Damping*, Butter worth-Heinemann, Oxford.
21. Timoshenko, S.P., 1921, On the correction or shear of the differential equation for transverse vibrations of prismatic bars, *Philosophical Magazine*, Vol. 41, pp 744-746.
22. Timoshenko, S.P., 1922, On the transverse vibrations of bars of uniform cross-section, *Philosophical Magazine and Journal of Science*, Vol. 43, pp 125-131. Meriovitch, L., 1967, *Analytical Methods in vibrations*, Macmillan, New York.
24. Bert C.W., 1973, *Material Damping: An introductory review of mathematical models, measures and experimental techniques*, *Journal of Sound and vibration*, vol 29, No. 2, pp 129-153.
25. Cremer, L., Hackl, M. and Petersson, B.A.T., 2005, *Structure-Borne Sound: Structural vibrations and sound radiation at audio frequencies*, Springer Berlin Heidelberg

26. Clarence W. De Silva, 2007, *Vibration Damping, Control and Design*, CRC Press, Taylor and Francis Group LLC, Boca Raton.
27. Masuko, M., Ito, Y. and Yoshida, K., 1973, Theoretical Analysis for a damping ratio of a jointed cantilever, *Bulletin of JSME*, Vol 16, Nogg pp 1421-1432.
28. Nishiwaki, N., Masuko, M. Ito, Y. and Okumura, I,1978, A study on damping capacity of jointed cantilever beam, 1st Report: Experimental Results, *Bulletin of JSME* No. 153, pp 524-531.
29. Nishiwaki, N., Masuko, M., Ito, Y. and Okumura, I., 1978, A study on damping capacity of a jointed cantilever beam, 2nd report: Comparison between theoretical and experimental values, *Bulletin of JSME*, Vol. 23, No. 177, pp 469-475.
30. Nanda, B.K. and Behera A.K., 1999, Study of damping in layered and jointed structures with uniform pressure distribution at the interfaces, *Journal of Sound and Vibration*, Vol. 226, No. 4, pp 607-624.
31. Minakuchi, Y., Koizumi, T. and Shibuya, T., 1985, Contact pressure measurement by means of Ultrasonic waves using angle probes, *Bulletin of JSME*, Vol. 28 No. 243, pp 1859-1863.
32. Kelly, S.G., 2000, *Fundamentals of Mechanical vibrations*, McGraw-Hill International Edition, Singapore.
33. Ferri, A.A. and Hack, B.S., 1992, Analytical Investigation of Damping enhancement using active and passive structural joints, *Journal of guidance, control and dynamics*, Vol. 15, No 5, pp 1258-1264
34. Gandhi, R.V., 1990, Optimum design of space structures with active and passive damping, *Engineering with computers*, Vol. 6, No. 3, pp 177-183.
35. Park, Jin-Tack and Choi, Nak-Jam, 2004, Flexural vibration analysis of a sandwich beam specimen with a partially inserted viscoelastic layer, *KSME Journal of Mechanical Science and Technology*, Vol. 18, No. 3, pp 347-356.
36. Lazan, B.J., 1968, *Damping of materials, and member in structural mechanics*, London, Pergamon press.
37. Clarence W. Desilva, 2000, *Vibrations: Fundamentals and practice*, CRC press, LLC, Boca Raton.

38. Water house, R.B., 1981, Fretting Fatigue, Applied Science publishers, Essex, England.
39. Meirovitch, L., 2001, Fundamentals of vibrations, McGraw Hill International Editions, Mechanical Engineering Series, Singapore.
40. Thorby, D., 2008, Structural Dynamics and Vibration in practice, Butter worth Heinemann Publication, First Edition, Oxford, UK.
41. Ranky, M.F., and Clarkson B.L., 1983, Frequency average loss factor of plates and shells, Journal of Sound and Vibration, Vol. 89, No. 3, pp 309-323.
42. Bies, D.A. and Hamid, S., 1980, In situ determination of loss and coupling loss factors by the power injection method, Journal of Sound and Vibration, Vol. 70, No. 2, pp 187-204.
43. Lee, G.F., and Hartmann, B., 1998, Specific damping capacity for arbitrary loss angle, Journal of Sound and Vibration, Vol. 211, No. 2, pp 265-272.
44. Inman, D.J., 1994 Engineering Vibration, Prentice Hall, Englewood cliffs.
45. Sun, C. Tand Lu, Y.P., 1995, Vibration Damping of structural Elements, Prentice Hall PTR, Englewood cliffs, New Jersey.
46. Ross, D., Ungar, E.E. and Kerwin, E.M. Jr., 1959, Damping of plate flexural vibrations by means of viscoelastic laminate, ASME colloquium on Structural damping pp 49-87
47. Pearce, B.K. and Baumgarten, J.R., 1971, The damping effects of viscoelastic materials part 2: Transverse vibration of plates with viscoelastic coatings, Transactions of ASME, Journal of Engineering for Industry, Vol. 93, pp 645-655.
48. Reddy, C.V.R. and Narayanan, S., 1980, Response of plates with unconstrained layer damping treatment to random acoustic excitation, part I: Damping and frequency evaluations, Journal of Sound and Vibration, Vol. 69, No. 1, pp 35-43.
49. Parthasarathy, G., Reddy, C.V.R and Ganesan, N., 1985 Partial coverage of rectangular plates by unconstrained layer damping treatments, Journal of Sound and Vibration, Vol. 69, No. 1, pp 35-43.
50. Kerwin Jr., E.M., 1959, Damping of flexural waves by a constrained viscoelastic layer, Journal of the Acoustical Society of America, Vol. 31, pp 952-962.
51. Di Taranto, R.A. 1965, Theory of vibratory bending of elastic and viscoelastic layered finite length beams, ASME, Journal of Applied Mechanics, vol 32, pp 881-886.

52. Douglas, B.E. and Yang J.C.S., 1978 Transverse compressional damping in the vibratory response of elastic-viscoelastic-elastic beams, *AIAA Journal*, Vol. 16, pp 925-930.
53. Douglas, B.E., 1986, Compressional damping in three layer beams incorporating nearly incompressible viscoelastic core, *Journal of Sound and Vibration*, Vol. 104, No. 2 pp 343-347.
54. Sylwan, O., 1987, Shear and compressional damping effects of constrained layered beams, *Journal of Sound and Vibration*, Vol. 118, No. 1, pp 35-45.
55. Lee, B.S and Kim, K.J., 1995, Consideration of both extensional and shear strain of core material in modal property estimation of sandwich plates, *ASME Design Engineering Technical Conference 3*, pp 701-708.
56. Meed, D.J., and Markus, S., 1969, The forced vibration of a three layer, damped sandwich beam with arbitrary boundary conditions, *Journal of Sound and Vibration*, Vol. 10, No. 2, pp 163-175.
57. Mead, D.J. and Markus, S., 1970, Loss factors and resonant frequencies of encastre damped sandwich beams, *Journal of Sound and Vibration*, Vol. 12, No. 1, pp. 99-112.
58. Mead, D.J., 1982, A comparison of some equations for the flexural vibration of damped sandwich beams, *Journal of Sound and Vibrations*, Vol. 83, No. 3, pp 363-377.
59. Faruk Sen and Mural Pakdil, 2008, Experimental failure analysis of mechanically fastened joints with clearance, in composite laminates, *Materials and Design* No. 29, pp 1159-1169.
60. Malik, A.K. and Ghosh, A., 1973, Improvement of damping characteristics of structural members with high damping elastic inserts, *Journal of Sound & Vibration*, Vol. 27, No. 1, pp. 25-36.
61. Malik, A.K. and Ghosh, A., 1970, Improvement of damping capacity with introduced stress concentration, *Indian Journal of Technology*, Vol. 8, pp 113-119.
62. Malik, A.K and Ghosh, A., 1971, Improvement of dynamic rigidity of structural members with introduced stress concentration, *Journal of Technology*, Vol. 13, pp 19-26.
63. Rshmatollah, R. and Malik, A.K., 1979, Damping of cantilever strips with inserts, *Journal of Sound and vibration*, Vol. 66, No. 1, pp. 109-117

64. Sextro, W., 2002, Dynamical contact problems with friction: Models, methods, experiments and applications, Lecture notes in Applied Mechanics, Vol. 3, Series Editor Feiffer, F., Springer.
65. Beards, C.F., 1982, Damping in structural joints, The shock and vibration digest, Vol. 14 pp 9-11.
66. Murty, A.S.R. and Padmanabhan, K.K., 1982 Effect of surface topography on damping in machine joints, Precision Engineering, Vol. 4, pp. 185-190.
67. Goodman L.E., 1959, A review of progress in analysis of interfacial slip damping, Edited by Ruzicka, J.E., Structural Damping, New York, ASME, pp 35-48.
68. Yoshimura, M., 1977, Measurement of dynamic rigidity and damping property for simplified joint models and simulation by computer, Annals of the CIRP, Vol. 25, No. 1, pp. 193-198
69. Tsutsumi, M. and Ito, Y., 1979, Damping mechanism of a bolted joint in machine tools, proceedings of the 20th International Machine Tool Design and Research Conference, Birmingham, U.K., pp 443-448.
70. Padmanabham, K.K. and Murty, A.S.R., 1991, Damping in structural joints subjected to tangential loads, Journal of the structural division, proceedings of Institute of Mechanical Engineers, Vol. 25, pp 121-129.
71. Lenz, J. and Gaul, L., 1995, The influence of microslip on the dynamic behavior of bolted joints, 13th International Modal Analysis Conference, Nashville, Vol. 3, pp. 248-254.
72. Bhagat Singh, 2012, The study of damping in layered and welded beams, Ph.D. Thesis, NIT, Rourkela.
73. Cochardt, A.W., 1954, A method for determining the internal damping of machine members, ASME, Journal of Applied Mechanics, Vol. 76, No. 9, pp. 257-262.
74. Goodman, L.E. and Klumpp, J.H., 1956, Analysis of slip damping with reference to turbine blade vibration, ASME, Journal of Applied Mechanics, Vol. 23, pp. 421-429.
75. Groper, M., June 1985, Microslip and Macroslip in bolted joints, Experimental Mechanics, pp. 171-174.

76. Hartwigsen, C.J., Song, Y., Mefarland, D.M. Bergman, L.A. and Vakakis, A.F., 2004, Experimental study of nonlinear effects in a typical shear lap joint configuration, *Journal of Sound and Vibration*, Vol. 277, No. 1-2, pp 327-351.
77. Pratt, J.D. and Pardoen, G., 2002, Numerical modeling of bolted lap joint behavior, *Journal of Aerospace Engineering*, Vol. 15, No. 1, pp 20-31.
78. Fenny, B., Guran, A., Hinrichs, N. and Popp, K., 1998, A historical review on dry friction and stick-slip phenomena, *ASME, Applied Mechanics Reviews*, Vol. 55, No 5, pp 321-341.
79. Williams, E.J. and Earles, S.W.E., 1974, Optimization of the response of frictionally damped beam type structure with reference to gas turbine compressor blading, *ASME, Journal of Engineering for Industry*, Vol. 96, pp 471-476.
80. Beards, C.F. and Robb, D.A., July 1980, The use of frictional damping to control the vibration of the plates infrastructure, *International Conference on Recent Advances in Structural Dynamics*, South Hampton, England, pp 749-760.
81. Dowell, E.H and Schwartz, H.B., 1983, Forced response of a cantilever beam with a dry friction damper attached, Part 1: Theory, *Journal of Sound and Vibration*, Vol. 91, No. 2, pp 255-267.
82. Dowell, E.H. and Schwartz, H.B., 1983, Forced response of a cantilever beam with a dry friction damper attached, Part II : Experiment, *Journal of Sound and Vibration*, Vol. 91, No. 2, pp. 269-291.
83. Beards, C.F. and Woodwat, A., 1985, The control of frame vibration by friction damping in joints, *ASME, Journal of Vibration, Acoustics, Stress Analysis, Reliability and Design*, Vol, 107, pp. 27-32.
84. Menq, C.H. and Griffin, J.H., 1985, A compression of transient and steady state finite element analysis of the forced response of a frictionally damped beam, *ASME, Journal of Vibration, Acoustics, Stress and Reliability in Design*, Vol. 107, pp 27-32.
85. Chen, S. and Sinha, A, 1990, Probabilistic method to compute the optional slip load for a mistuned bladed disk assembly with friction dampers, *ASME, Journal of Vibration and Acoustic*, Vol. 112, No. 2, pp 214-221.

86. Wang, J.H. and Chen, W.K., 1993, Investigation of the vibration of a blade with friction damper by HBM, ASME, Journal of Engineering for Gas Turbines and Power, Vol. 115, No. 2, pp. 294-299.
87. Sanliturk, K.Y., Ewins, D.J., Ellist, R and Green, J.S., 2001, Friction damper optimization: Simulation of rainbow tests, ASME, Journal of Engineering for Gas Turbines and Power, Vol. 123, No. 4, pp. 930-939.
88. Cigeroglu, E., 2002, Nonlinear vibration analysis of bladed disks with dry friction dampers, MS Thesis, Middle East Technical University, Ankara.
89. Cigeroglu, E., 2002, Lu, W. and Menq, C.H., 2006, One-dimensional dynamic microslip friction model, Journal of Sound and Vibration, Vol. 292, pp. 881-898.
90. Lu, W., 2001, Modeling of microslip friction and design of frictionally constrained turbine blade systems, Ph.D Thesis, The Ohio State University.
91. Csaba, G., 1998, Forced response analysis in time and frequency domains of a tuned bladed disk with friction dampers, Journal of Sound and Vibration, Vol. 214, No. 3, pp. 395-412.
92. Sanliturk, K.Y., Imregun, M. and Ewins, D.J. 1997, Harmonic balance vibration analysis of turbine blades with friction dampers, ASME, Journal of vibration and Acoustics, Vol. 119, No. 1, pp 96-103.
93. Olofsson, U. and Hagman, L., 1997, A model for microslip between flat surfaces based on deformation of ellipsoidal elastic bodies, Tribology International, Vol. 30, No. 8, pp 599-603.
94. Yang, R., 1992, The analysis and identification of friction joint parameters in the dynamic response of structures, Ph.D. Thesis, Imperial College, University of London, U.K.
95. Thomson, W.T. 1993, Theory of vibration with applications, 2nd Edition, George Allen and Unwin, London.
96. Den Hartog, J.P., 1931, Forced vibration with combined coulomb and viscous friction, Transactions of ASME, Vol. 53, No. 9, pp 107-115.
97. Liang, J.W. and Fenny, B.F., 1998, Identifying Coulomb and viscous friction from vibration decrements, Nonlinear dynamics, Vol. 16. No. 4, pp. 337-347.

98. Ibrahim, R.A., 1994, Friction induced vibration, chatter, squeal and chaos; Part I – Mechanics of contact and friction, ASME, Applied Mechanics Reviews, Vol. 47, No. 7, pp 209-226.
99. Awrejcewicz, J. and Olejnik, p., 2007, Occurance of stick-slip phenomenon, Journal of Theoretical and Applied Mechanics, Vol. 45, No. 1, pp 30-40.
100. Motosh, N., 1975, Stress distribution in joints of bolted or riveted connections, ASME, Journal of Engineering for Industry, Vol. 97, No. 1, pp. 157-161.
101. Pian, T.H.H., 1957, Structural damping of simple built-up beam with riveted joints in bending, ASME, Journal of Applied Mechanics, Vol. 24, pp 35-38.
102. Sidorov, O.T., 1983, Change of damping of vibrations in the course of operation in dependence on the parameters of bolted joints, Strength of materials, Vol. 14, pp. 671-674.
103. El-Zahry, R.M., 1985, Investigation of vibration behavior of preloaded bolted joints, Dirasat Engineering College Vol. 12, pp. 201-223.
104. Marshall, M.B., Lewis, R. and Dwyer-Joyce, R.S., 2006, characterization of contact pressure distribution of bolted joints, Strain, Vol. 42, No. 1, pp. 31-43.
105. Kaboyashi, T. and Matsubayashi, T., 1986, consideration on the improvement of the stiffness of bolted joints in machine tools, Bulletin of JSME, Vol. 29, pp. 3934-3937.
106. Tsai, J.S. and Chou, Y.F., 1988, Modeling of dynamic characteristics of two bolted joints, Journal of Chinese Institute of Engineering, Vol. 11, pp 235-245.
107. Shin, Y.S., Inverson, J.C. and Kim K.S., 1991, Experimental studies on damping characteristics of bolted joints for plates and shells, ASME, Journal of Pressure Vessel Technology, Vol. 113, No. 3, pp 402-408.
108. Gould, H.H. and Mikic, B.B., 1972, Areas of contact and pressure distribution in bolted joints, ASME, Journal of Engineering for Industry, Vol. 94, No. 3, pp 864-870.
109. Ziada, H.H. and Abd, A.K., 1980, Load pressure distribution and contact areas in bolted joints, Institute of Engineers (India), Vol. 61, pp. 93-100.
110. Hisakado, T. and Tsukizoe, T., 1978, Measurement of the interface pressure distribution of metallic joints, Wear, Vol. 48, No. 1, pp 209-212.

111. Damisa, O., Olunloyo, V.O.S., Osheku, C.A. and Oyediran, A.A., 2007, Static analysis of slip damping with clamped laminated beams, *European Journal of Scientific Research*, Vol. 17, No. 4, pp. 455-476.
112. Damisa, O., Olunloyo, V.O.S., Osheku, C.A. and Oyediran, A.A., 2008, Dynamic analysis of slip damping with clamped layered beams with non uniform pressure distribution at the interface, *Journal of Sound and Vibration*, Vol. 309, No. 3-5, pp. 349-374.
113. Olunloyo, V.O.S., Damisa, O., Osheku, C.A., Oyediran, A.A., 2007, Further results on static analysis of slip damping with clamped laminated beams, *European Journal of Scientific Research*, Vol. 17, No. 4, pp. 491-508.
114. Minakuchi, Y., Yoshimine, K., Koizumis, T. and Hagiwara, T., 1985, Contact pressure measurement by means of ultrasonic waves: On a method of quantitative measurement, *Bulletin of JSME*, Vol. 38, No. 235, pp. 40-45.
115. Minakuchi, Y., 1985, Contact pressure measurement by ultrasonic waves: On a bolted joint with a solid metal flat gasket, *Bulletin of JSME*, Vol. 28, No. 239, pp. 792-798.
116. Earles, S.W.E., 1966, Theoretical estimation of frictional energy dissipation in a simple lap joint, *Institute of Mechanical Engineers, Part C : Journal of Mechanical Engineering Science*, Vol. 8, No. 2, pp 207-214.
117. Masuko, M. , Ito, Y. and Koizumi, T., 1974, Horizontal stiffness and microslip on a bolted joint subjected to repeated tangential static loads, *Bulletin of JSME*, Vol. 17, No. 113, pp. 1494-1501.
118. Richardson, R.J.H. and Nolle, H., 1977, Energy dissipation in rotary structural joints, *Journal of Sound and Vibration* Vol. 54, No. 4, pp 577-588.
119. Jezequel, L., 1983, Structural damping by slip in joints, *ASME, Journal of Sound and Vibration, Acoustics, Stress, Reliability and Design*, Vol. 105, No. 2, pp. 497-504.
120. Hanks, B.R. and Stephens, D.G., 1967, Mechanism and Scaling of damping in a practical structural joints, *Shock and Vibration Bulletin*, Vol. 36, pp. 1-8.
121. Brown, C.B., 1968, Factors affecting the damping in a lap joint, *ASCE, Journal of Structural Division*, Vol. 94, pp. 1197-1217.

122. Beards, C.F., 1983, The damping of structural vibration by controlled interface slip in joints, ASME, Journal of Vibration, Acoustics, Stress & Reliability in Design, Vol. 105, No. 3, pp 369373.
123. Hertz, T.J. and Crawley, E.F., 1985, Displacement dependent frictions in space structure joints, AIAA Journal, Vol. 24, pp 1998-2000.
124. Ferri, A.A., 1988, Modeling and analysis of nonlinear sleeve joints of large space structures, AIAA Journal of Spacecraft and Rockets, Vol. 25, No 5, pp 354-360.
125. Ferri, A.A. and Bindemann, A.C., 1992, Damping and vibration of beams with various types of frictional support condition ASME, Journal of vibration and Acoustics, Vol. 114, No. 3, pp. 284-296.
126. Folkman, S.L. and Redd, F.J., 1990, Gravity effects on damping of a space structure with pinned joints, AIAA Journal of Guidance and Control Dynamics, Vol. 13, No 2, pp 228-233.
127. Folkman, S.L., Roswell, E.A. and Ferney, G.D., 1995, Influence of pinned joints on damping and dynamic behavior of a truss, AIAA Journal of Guidance and Control Dynamics, Vol. 18, No. 6, pp 1398-14031.
128. Beards, C.F., 1985, Damping in structural Joints, Shock and Vibration Digest, Vol. 17, No. 11, pp 17-20
129. Beards, C.F., 1989, Damping in structural joints, shock and vibration Digest, Vol. 21, No. 4, pp 3-5.
130. Gregory, D.L., Small wood, D.O., Coleman, R.G. and Nusser, M.A., 1999, Experimental studies to investigate damping in frictional shear joints, Proceedings of the 70th Shock and Vibration Symposium, NM.
131. Smallwood, D.O., Gregory, D.L and Coleman, R.G., 2000, Damping investigations of a simplified frictional shear joint, proceedings of the 71st Shock and Vibration Symposium, Alexandria, Virginia.
132. Heller, L., Follete, E. and Piranda, J, 2009, Experimental identification of nonlinear dynamic properties of built-up structures, Journal of Sound and Vibration, Vol. 327, No. 1-2, pp. 183-196.
133. Walker, S.J.I., Aglietti, G.S. and Cunningham, P, 2009, A study of Joint damping in metal plates, Acta Astroonautica, Vol. 65, No. 1-2, pp 184-191.

134. Ferri, A.A., 1995, Friction damping and isolation systems, ASME, Journal of vibration and acoustics, Vol. 117, pp 196-206.
135. Ibrahim, R.A. and Pettit, C.L., 2005, Uncertainties and dynamic problems of bolted joints and other fasteners, Journal of Sound and Vibration, Vol. 279, No. 3-5, pp 857-936.
136. Gaul, L. and Lenz, J., 1997, Nonlinear dynamics of structures assembled by bolted joints, Acta Mechanica, Vol. 125, No. 1-4, pp. 169-181.
137. Song, Y., Hartwigsen, C.J., McFarland, D.M., Vakakis, A.F. and Bergman, L.A., 2004, Simulation of dynamics of beam structures with bolted joints using Adjusted Iwan Beam Elements, Journal of Sound and Vibration, Vol. 273, No. 1-4, pp. 249-276.
138. Miller, J.D. and Quinn, D.D., 2009, A two sided interface model for dissipation in structural systems with frictional Joints, Journal of Sound and Vibration, Vol. 321, pp. 201-219.
139. Khattak, A.R., Garvey, S. and Popo V, A., 2010, Proper orthogonal decomposition of the dynamics in bolted joints, Journal of Sound and Vibration, Vol. 329, No. 9, pp. 1480-1498.
140. Olunloyo, V.O.S., Osheku, C.A. and Damisa, O., 2008, Vibration damping in structures with layered viscoelastic beam-plate, ASME, Journal of Vibration and Acoustics, Vol. 130, No. 6, pp 061002-(1-26).
141. Wang, J.H. and Chuang, S.C., 2004, Reducing errors in the identification of structural joint parameters using error functions, Journal of Sound and Vibration, Vol. 273, No. 1-2, pp. 295-316.
142. Ulf Arne Grahmar, et al. 1993, Dynamic analysis of composite members with interlayer slip, International Journal of Solids and structures, Vol. 130, No. 6, pp 797-823.
143. Tsai, J.S. and Chou Y.F., 1988, The identification of dynamic characteristics of a single bolt joint, Journal of Sound and Vibration, Vol. 125, No. 3, pp. 487-502.
144. Yin, H.P., Duhamel, D. and Argoul, P., 2004, Natural frequencies and damping estimation using wavelet transform of a frequency response function, Journal of Sound and Vibration, Vol. 271, No. 3-5, pp 999-1014.
145. Hwang, H.Y., 1998, Identification techniques of structure connection parameters using frequency response functions, Journal of Sound and Vibration, Vol. 212, No. 3, pp. 469-479.

146. Ahmadian, H. and Jalali, H., 2007, Identification of bolted lap joints parameters in assembled structures, *Mechanical Systems and Signal Processing*, Vol. 21, No. 2, pp. 1041-1050.
147. Sainsbury, M.G. and Zhang, Q.J., 1999, The Galerkin element method applied to take vibration of damped sandwich beams, *Computers and Structures*, Vol. 71, No. 3 pp. 239-256.
148. Lee, S.Y., Ko, K.H. and Lee, J.M., 2000, Analysis of dynamic characteristics of structural joints using stiffness influence coefficients, *KSME International Journal*, Vol. 14, No. 12, pp. 1319-1327.
149. Chen, W. and Deng, X., 2005 Structural damping caused by micro slip along frictional interfaces, *International Journal of Mechanical Sciences*, Vol. 47, No. 8, pp 1191-1211.
150. Oldfield, M., Ouyang, H. and Mottorshead, J.E., 2005, Simplified models of bolted joints under harmonic loading, *Computers and Structures*, Vol. 84, No. 1-2 pp. 25-33.
151. Pian, T.H.H. and Hallo Well, F.C., 1950, Investigation of structural damping in simple built up beams, Technical Report, Aeroelastic and Structures Laboratory, Massachusetts Institute of Technology, Cambridge, Massachusetts.
152. Nanda, B.K., 2006, Study of the effect of bolt diameter and washer on damping in layered and jointed structures, *Journal of Sound and Vibration*, Vol. 290, No. 3-5, pp. 1290-1314.
153. Shigley, J.E. Mischke, R. and Brown, Jr., T.H., 2004, *Standard Handbook of Machine Design*, 3rd edition, McGraw Hill Book Company, pp 246.
154. Maitra, G.M. and Prasad, L.V., 1995, *Handbook of Mechanical Design*, 2nd edition, Tata Mc-Graw Hill publication, pp 579-580.
155. Mohanty, R.C., 2010, Damping of layered and jointed beams with riveted joints, PhD dissertation NIT Raurkela
156. Clough, R.W. and Penzien, J., 2003, *Dynamics of Structures*, 3rd edition, Computers and structures, Inc., Berkeley, U.S.A.

Curriculum Vitae

Name : Binit Kavi

Email : binit.kavi@gmail.com

Date of birth : 7th July 1980

Nationality : Indian

Permanent address : Kakuriapara
P.O. Benirampur
District : Cuttack
PIN- 754134

Education : 1. B. Tech. (Metallurgy and materials technology) 2004,
N. I. T., Rourkela
2. M. Tech. (Mechanical engineering) 2009, N. I. T.
Rourkela

Publication : Generalised formulation of laminate theory using beam FE for delaminated composite beams with piezo actuators and piezo sensors, B Kavi¹, B K Nanda², 2012, Vol. 02, No. 1, International Journal of Composite Materials and Manufacturing